Global changes in *Brassica napus* gene activity in response to *Sclerotinia sclerotiorum* and the biocontrol agent *Pseudomonas chlororaphis* PA23

By

Kelly Duke

A Thesis submitted to the Faculty of Graduate Studies of

The University of Manitoba

In partial fulfillment of the requirements of the degree of

MASTER OF SCIENCE

Department of Microbiology

University of Manitoba

Winnipeg

ABSTRACT

The biological control agent *Pseudomonas chlororaphis* PA23 is effective at protecting *Brassica napus* (canola) from the necrotrophic fungus *Sclerotinia sclerotiorum* via direct antagonism. Despite the growing importance of biocontrol bacteria in protecting crop plants from fungal pathogens, little is known about how the host plant responds to bacterial priming on the leaf surface and certainly nothing about global changes in gene activity in the presence and absence of *S. sclerotiorum*. PA23 priming of mature canola plants reduced the number of lesion-forming petals by 90%. Global RNA sequencing of canola tissue at the host-pathogen interface showed a 16-fold reduction in the number of genes uniquely upregulated in response to *S. sclerotiorum* when pretreated with PA23. Upstream defense-related gene patterns suggest MAMP-triggered immunity via surface receptors detecting PA23 flagellin and peptidoglycans. Although systemic acquired resistance (SAR) was induced in all treatment groups, a response centered around a glycerol-3-phosphate (G3P)-mediated pathway was exclusively observed in canola plants treated with PA23 alone. Activation of these defense mechanisms by PA23 involved production of reactive oxygen species as well as pronounced thylakoid membrane structures and plastoglobule formation in leaf chloroplasts. PA23 therefore primes defense responses in the plant through the induction of unique local and systemic regulatory networks.

ACKNOWLEDGEMENTS

I would like to first and foremost thank my advisor, Dr. Teri de Kievit, for giving me the opportunity to work in her lab and for supporting me throughout my academic career. Her guidance and encouragement have motivated me to strive for greatness while working on this project. The work ethic that she instills in her lab members has and will continue to be an inspiration to me moving forward in my career as a scientist.

I would like to thank Dr. Mark Belmonte and his lab members for welcoming me into their lab and for their invaluable guidance throughout my project. As a committee member and second mentor, Dr. Belmonte has been instrumental in the success of my project and his insight has been invaluable to me. The Belmonte lab members past and present, in particular Ian, Mike and Sherry, have shared their time and knowledge on plant RNA extraction and library synthesis which has been the core of this project. I would also like to thank Jenna for her transmission electron microscopy work, which contributed greatly to my project.

To Dr. Dilantha Fernando and his lab, I wish to express my deepest gratitude for allowing me to space to work with my plants. Dr. Fernando has been a valued committee member and his vast knowledge of plant biocontrol interactions has been an asset to my success. A special thank you to the Fernando lab's senior research technician, Paula Parks, for teaching me how to grow and care for my plants and for giving me a much needed background on plant physiology.

Finally, I would like to thank my labmates past and present from the de Kievit and Loewen labs: to Jack and Jacelyn for helping and teaching me how to work with proteins, and to Munmun, Nidhi, Akrm, Amanda, Sanjay, and the other members of the de Kievit lab. Your friendship and support over the years has made working in the lab an absolute joy.

TABLE OF CONTENTS

LIST OF FIGURES

LIST OF TABLES

LIST OF ABBREVIATIONS

Aza – azelaic acid
BCA – biocontrol agent
bp – base pair
cDNA – complementary DNA
cfu – colony-forming units
DAMP – damage-associated molecular pattern
DEGs – differentially-expressed genes
DP – dominant pattern (of expression)
ET – ethylene
ETI – effector-triggered immunity
ETS – effector-triggered susceptibility
FPKM – fragments per kilobase of transcript per million mapped reads
GO term – gene ontology term
G3P – glycerol-3-phosphate
H_2O_2 – hydrogen peroxide
HCN – hydrogen cyanide
HR – hypersensitive response
ISR – induced systemic resistance
JA – jasmonic acid
MAMP – microbe-associated molecular pattern
MeSA – methyl salicylate
mRNA – messenger RNA
MTI – MAMP-triggered immunity
O_2^- – superoxide radical
ORF – open reading frame
PAMP – pathogen-associated molecular pattern
PGPR – plant growth promoting rhizobacteria
Pip – pipecolic acid
PR protein – pathogenesis-related protein
PRR – pattern recognition receptor
PTI – PAMP-triggered immunity
RNA-seq – RNA sequencing
ROS – reactive oxygen species
SA – salicylic acid
SAR – systemic acquired resistance
TEM – transmission electron miroscopy

1. INTRODUCTION

1.1. *Brassica napus*

Oilseed rape (*Brassica napus* L.) is an economically important crop of global significance that has been grown around the world for food, oil and animal fodder (Allender and King 2010). *B. napus* has major agricultural and economical significance in the form of canola, contributing an average of 19.3 billion dollars annually to the Canadian economy alone (LMC International 2013). The term "canola" (Canadian Oil Low Acid) was coined by Canadian scientists in the 1970s to describe emerging "double low" lines of oilseed rape. These lines were deemed to be excellent sources of vegetable oil due to their low erucic acid content in the oil (<2%) and low glucosinolate content in the meal (<30mg/g) (Iniguez-luy and Federico 2011). Today, the major products of canola are oil and meal. Oil is obtained from the seeds of the plant, and is primarily used as a cooking oil. The extraction of oil from canola seeds creates canola meal as a by-product, which is a high protein feed source for animals. In 2015, over 20 million acres of canola were harvested in Canada alone (Statistics Canada 2016).

B. napus is an allotetraploid (n=19, AACC) and a relatively recent hybridization (7,500 - 12,500 years) between *B. oleracea* (n=9, CC) and *B. rapa* (n=10, AA) followed by chromosome doubling (Parkin et al. 1995; Chalhoub et al. 2014). This plant species is thought to have multiple origins from numerous independent and spontaneous hybridization events. However as *B. napus* and its relatives are rarely found in the wild, phylogenetic analysis of its origin is difficult (Iniguez-luy and Federico 2011). The *B. napus* genome is comprised of an estimated 101,040 genes from a C subgenome of 525.8 Mb and an A subgenome of 314.2 Mb. Orthologous genes in *B. rapa* and *B. oleracea* coexist as homologous gene pairs in *B. napus*, and significant cross-talk and homologous exchange between subgenomes has been confirmed (Chalhoub et al.

2014). Comparisons between the *B. napus* genome and that of the plant model organism *Arabidopsis thaliana* (hereon: Arabidopsis) have identified extensive synteny between the two genomes, indicating a common ancestor (Parkin et al. 2005; Cai et al. 2014). This allows for the exploitation of many tools designed for Arabidopsis in *B. napus* research.

1.2. Disease management in canola

A significant portion of the Canadian economy depends on revenue generated from canola products; therefore, management of disease to ensure optimal growth and yield is essential. Commercial crops like canola are particularly susceptible to disease because they are grown in monoculture conditions, encouraging pathogen spread. Current strategies being employed to prevent the spread of pathogens include crop rotation, pesticide application, and the use of pathogen-resistant cultivars. Crop rotation is effective at reducing disease because it discourages the establishment of populations of soil-borne pathogens such as biotrophs and those with low saprophytic survival capacity (Janvier et al. 2007). However, it is not effective against pathogens that can survive saprophytically or that can exist for long periods of time in the soil (Walters 2009). Because canola is grown globally in many different environmental conditions, a variety of cultivars are commercially available which optimize growth in certain climates and exhibit tolerance to potential pathogens. For example, resistance breeding has been successful in protecting canola crops against hemibiotrophic fungal pathogens like *Leptosphaeria maculans* (Delourme et al. 2006; Fitt et al. 2006; Zhang et al. 2015 Nov 27). However, despite attempts to breed cultivars with broad resistance traits, canola is still susceptible to a variety of pathogens. One example being *Sclerotinia sclerotiorum*, to which no immune or highly resistant germplasm in *B. napus* has been found (Wu et al. 2013). Chemical pesticides are commonly used to mitigate

crop damage by pathogens, but come with unwanted side effects to the surrounding environment, and concerns over their safety for consumption. Thus, a combination of these strategies is often employed to optimize crop protection.

1.3. *Sclerotinia sclerotiorum*

The necrotrophic fungus *Sclerotinia sclerotiorum* (Lib.) de Bary is a soil-borne ascomycete and an important pathogen of many plants. Disease caused by this fungus is referred to as white mold or stem rot, depending on the host organism. *S. sclerotiorum* can infect over 400 host organisms worldwide, including many commercially important crops such as sunflower, soybean, green bean, and canola (Boland and Hall 1994). Given its wide host range and ability to persevere in the soil, fungicides have proven to be the most effective means of controlling this pathogen. Despite this, Sclerotinia stem rot continues to be a major source of crop loss. Annual losses in the United States due to Sclerotinia disease have exceeded 2 million dollars (Bolton et al. 2006). In Manitoba, canola yield losses from stem rot can range from 5-100% in a growing season (Manitoba Agriculture 2011). Thus, crop rotation, resistance breeding and traditional pesticide use have not been able to adequately protect canola against infection. Limited efficacy is mainly due to the life cycle of *S. sclerotiorum*, as fungicides and crop rotation are only practical against specific disease stages (Bolton et al. 2006; Huang and Erickson 2008).

1.4. Life cycle of *S. sclerotiorum* in canola

S. sclerotiorum remains a significant threat to many crops because of its ability to overwinter and persevere in the soil for up to eight years as sclerotia bodies (Adams 1979; Huang and Erickson 2008). Sclerotia are bundles of hyphae with carbohydrate sources encased

in a black rind several cell layers thick (Bolton et al. 2006). It is thought that melanin in the rind is the major component protecting fungal propagules from environmental conditions as well as attack by lytic enzymes of other microorganisms (Butler et al. 2005).

Figure 1.1 depicts the life cycle of *S. sclerotiorum* using canola as a host. Once conditions are favourable, sclerotia will germinate and the life cycle will continue. Sclerotia can germinate either myceliogenically (producing hyphae) or carpogenically (producing apothecia), where carpogenic germination is the major contributor to stem rot disease in canola (Huang and Erickson 2008). Apothecia formation is optimal at temperatures between 10 and 20ºC and requires continuously high soil moisture levels (Clarkson et al. 2004; Wu and Subbarao 2008). Infection occurs when airborne ascospores released by the apothecia land on the senescing petals of flowering canola plants, which detach and fall on the plant leaves and stem. The senescing petal is required for infection to occur as these are a rich nutrient source for the fungus (Bolton et al. 2006; Bashi et al. 2012). Once established, hyphae form infection cushions on the leaf surface which can pierce the cuticles of leaves and stems via formations known as penetration pegs. Penetration occurs via hydrolytic enzymes including oxalic acid, which degrade the host cell wall (Bolton et al. 2006; Huang et al. 2008; Bashi et al. 2012). Hyphae will colonize host tissue and invade dying and dead cells, creating dark lesions which move from the leaf to the petiole towards the stem (Lumsden 1979; Bolton et al. 2006). Sclerotia bodies will then form once more inside of infected tissue.

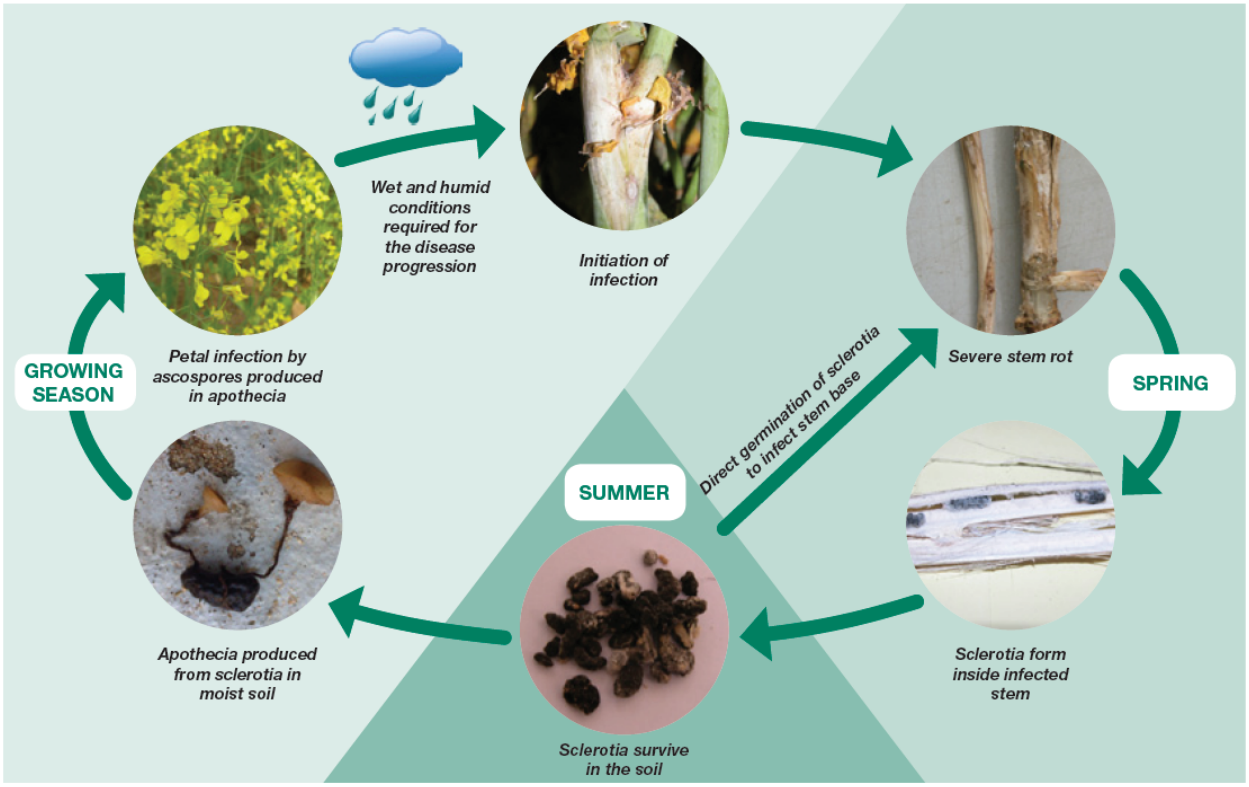

Figure 1.1. Life cycle of *Sclerotinia sclerotiorum* in *Brassica napus*. Reproduced from the Government of Western Australia Department of Agriculture and Food website, https://www.agric.wa.gov.au/canola/managing-sclerotinia-stem-rot-canola.

1.5. Biological control

To address growing concerns over the use of chemical pesticides, major advances have recently been made for developing biological control methods for a number of plant pathogens. The nature of the challenges faced in preventing the Sclerotinia stem rot infection process on canola makes the *B.napus*-*S. sclerotiorum* pathosystem an ideal model for employment of biological control.

Biological control, or biocontrol, is the management of pests using living organisms. The concept of using living organisms to control plant pathogens is not new, although the mechanisms behind these interactions remained unknown for a long time (Baker 1987). Initial identification of BCAs in an agricultural context often occurs with confirmation of significant antagonism against an important crop pathogen (Fravel 2005). The discovery of antibiotics released into the soil by some microorganisms as the driving force behind antibiosis fueled commercialization of biocontrol systems (Haas and Défago 2005). The global biocontrol market was worth 2.1 billion dollars in 2011, and is expected to rise to 3-4 billion dollars by 2017 (Velivelli et al. 2014). The first commercial biocontrol agent (BCA) for plant disease registered with the United States Environmental Protection Agency was *Agrobacterium radiobacter* strain K84 for use against crown gall disease in 1979. Currently, 11 bacterial and 10 fungal BCAs are registered in Canada for commercial use (Agriculture and Agri-Food Canada 2016). This number is expected to grow as BCAs become more recognized as a useful tool in plant disease control. Today, several common mechanisms of biocontrol have been revealed in the majority of effective BCAs. Mechanisms include the production of antibiotics such as phenazines and lipopeptides, competing for nutrients such as iron via siderophore production, and lytic enzyme production (Velivelli et al. 2014). As such, biocontrol represents an attractive alternative to

traditional pesticides, and the number of commercially available BCAs is steadily increasing (Fravel 2005; Pal and McSpadden Gardener 2006; Bhattacharyya and Jha 2012).

In addition to direct pathogen control, biocontrol agents (BCAs) on plants can have the added benefit of priming the hosts' defenses (Pieterse et al. 1996; Kurkcuoglu et al. 2006; Hase et al. 2008; Shoresh et al. 2010). These effects are dependent on host detection of specific bacterial determinants, where *Pseudomonas* spp. and *Bacillus* spp. comprise the majority of known inducers (Pal and McSpadden Gardener 2006). Successful implementation of BCAs in the field requires a broader understanding of the biocontrol interactions involved, including effects on the host plant.

1.6. *Pseudomonas chlororaphis* strain PA23

Pseudomonas chlororaphis PA23, which was first isolated from the root tips of soybean plants, is a candidate organism for biological control (Savchuk 2002). This bacterium is capable of preventing *S. sclerotiorum* growth both *in vitro* and *in planta* using susceptible *B. napus* cultivars (Savchuk and Fernando 2004; Fernando et al. 2007). PA23 directly antagonizes *S. sclerotiorum* through the excretion of antifungal metabolites including phenazines, pyrrolnitrin, proteases and lipases (Poritsanos et al. 2006; Zhang et al. 2006); pyrrolnitrin is the primary compound responsible for antagonistic activity (Selin et al. 2010). Phenazines function by inhibiting electron transport and are not specific, while pyrrolnitrin selectively inhibits fungal respiratory chains (Haas and Défago 2005). Siderophores are also produced by PA23, and may function not only by depriving potential pathogens of iron but also through direct antifungal activity (Haas and Défago 2005). Many fluorescent pseudomonads including PA23 produce hydrogen cyanide (HCN), which blocks the cytochrome oxidase pathway in aerobic

microorganisms and is thought to be effective against root pathogens (Pal and McSpadden Gardener 2006). Thus, PA23 has an arsenal of secondary metabolites at its disposal which all contribute to its biocontrol capabilities. Despite our growing understanding of the molecular genetics of PA23 antifungal activity, we have yet to learn how the presence of PA23 affects the host organism.

1.7. Plant defense responses

1.7.1. Structural resistance in plants

Unlike animals, plants lack mobile cells differentiated for defense and must depend on the innate immunity mechanisms of each cell (Jones and Dangl 2006). As sessile organisms which cannot escape changing environmental conditions, plants must face abiotic and biotic stressors without wasting energy (Atkinson and Urwin 2012). These organisms have thus evolved sophisticated defense responses that can be highly specific. The first line of defense is comprised of passive physical barriers that protect plants from many external threats. Morphological and structural barriers such as a waxy cuticle and tough cell wall are part of an innate immune response against living organisms as well as abiotic forces, such as cold and drought (Atkinson and Urwin 2012; Muthamilarasan and Prasad 2013). Because the hydrophobic waxy cuticle prevents undesired water loss and leaching of metabolites, the plant phyllosphere does not encourage the growth of microorganisms. Nonetheless, it should be noted that many microbial communities have adapted to life under these conditions and thrive in the phyllosphere of plants (Vorholt 2012). The cuticle also serves as a physical barrier to pathogen entry and has been found to play an important role in systemic defense signaling (Xia et al. 2009).

Underneath the cuticle lies the cell wall, comprised mainly of the polysaccharides

cellulose, hemicellulose and pectin. Although a seemingly rigid structure, the cell wall is constantly being remodeled in response to environmental cues and throughout plant development (Hématy et al. 2009). How a pathogen bypasses these tough outer layers of protection depends mainly on its lifestyle. Necrotrophs such as *S. sclerotiorum* will destroy plant tissues by releasing hydrolytic enzymes that degrade cell wall polymers (Laluk and Mengiste 2010). Hemibiotrophs and biotrophs, however, require living tissue and thus their strategies for infection are different. Such fungal pathogens penetrate the cuticle and cell wall mechanically using haustoria, while bacteria and rusts must rely on preformed openings such as stomata or surface wounds (Underwood 2012; McLachlan et al. 2014). Stomata are pores on the leaf surface that function in gas exchange, and are formed by two guard cells. The size of the pore changes in response to certain environmental conditions. Signaling networks to the guard cells controlling stomatal aperture are complex and can involve abscisic acid and other plant hormones (McLachlan et al. 2014). Some bacteria, such as *Pseudomonas syringae* pv. *tomato* DC3000, can hijack these signaling pathways to force stomata open enabling entry (Boureau et al. 2002; A.S. Kumar et al. 2012). Thus, pathogens have different strategies of infection which the host plant must be able to adapt to and defend against.

1.7.2 PAMP-triggered immunity

In addition to passive physical barriers, invading organisms are concurrently challenged by an inducible type of broad spectrum defense. Transmembrane pattern recognition receptors (PRRs) will detect microbe- or pathogen-associated molecular patterns (MAMPs or PAMPs) present on the cell surface. Recognition of a MAMP or PAMP common to many pathogen types, such as bacterial flagellin, will elicit PAMP-triggered immunity (PTI, also referred to as MAMP-triggered immunity, MTI) (Jones and Dangl 2006; Muthamilarasan and Prasad 2013).

Necrotrophs such as *S. sclerotiorum* generate PAMPs including cutin, chitin fragments and oligogalaturonides which trigger this type of immunity (Mengiste 2012). Induction of PTI results in changes to the local cell surface environment as well as broader systemic responses involving hormone biosynthesis. All of these defense responses are induced by a signal transduction cascade beginning with PAMP/MAMP detection. Structural changes include reinforcement of the cell wall via formation of papillae at the site of PAMP or MAMP recognition. These papillae commonly contain callose, lignin, cell wall polymers and structural proteins, antimicrobial proteins, reactive oxygen species (ROS) and peroxidases, although composition varies depending on the plant species (Hématy et al. 2009; Underwood 2012). Stomatal closure also occurs in PTI to limit pathogen entry into the cell (Melotto et al. 2006). In addition to these physical changes, the plant will release toxic reactive oxygen species (ROS) such as superoxide radicals and hydrogen peroxide to the cell surface. Here, ROS are thought to serve several functions including antimicrobial activity against pathogens and induction of other immune signaling pathways (Muthamilarasan and Prasad 2013). Therefore, basal resistance mechanisms in plants involve both passive and active immune responses.

1.7.3. Effector-triggered immunity and effector-triggered susceptibility

In the early stages of infection, plant pathogens produce molecules which facilitate colonization of host tissue or which disrupt the host defense response (Gururani et al. 2012). These molecules are known as effectors and they are the basis for a second layer of defense known as effector-triggered immunity (ETI). Where PTI is induced in response to the detection of MAMPS/PAMPS common to many organisms, effector-triggered immunity (ETI) involves detection of molecules specific to certain pathogens. For example, *P. syringae* is a phytopathogen that injects effector proteins into the host cell and disrupts defense pathways via a

type III secretion system (Block and Alfano 2011). Both PAMPs/MAMPs and effectors are detected on the cell surface by PRRs, but only effectors, also known as Avr proteins, are also detected by intracellular receptors (Muthamilarasan and Prasad 2013). These intracellular receptors are encoded by disease resistance (*R*) genes in the plant genome. This gene-for-gene resistance is the basis for ETI, also known as R-gene mediated pathogen resistance (Gururani et al. 2012). PTI and ETI elicit many of the same immune responses in the host plant, including systemic resistance (Mishina and Zeier 2007). However, ETI is a stronger and more effective defense response that often results in localized cell death, known as the hypersensitive response (HR) (Jones and Dangl 2006). HR is a localized defense strategy involving programmed cell death to prevent disease. Induction of HR involves the production of ROS in plant chloroplasts, which are involved in signaling and the execution of HR (Liu et al. 2007).

Gene-for-gene resistance is rare in necrotrophs, and only a handful of *avr* genes have been identified (Wang et al. 2014). As such, ETI is only effective against biotrophic and hemibiotrophic pathogens, who depend on living tissue for some or all of their life cycle. Where these pathogens will attempt to suppress HR in the host, necrotrophs will try to promote host cell death. Necrotrophs able to produce host-selective toxins can exploit the gene-for-gene relationship with the host resistance protein to cause disease, known as effector-triggered susceptibility (ETS). It is not known if R proteins are targeted directly by these effectors, but they are required for susceptibility to the pathogen (Mengiste 2012). ETS has also more broadly been described as a pathogen's ability to shut down PTI through the use of effectors (Jones and Dangl 2006; Derksen et al. 2013). Necrotrophs with broad host ranges such as *S. sclerotiorum* use a combination of toxins, which shut down host defenses, and crude pro-death strategies involving cell wall-degrading enzymes (Mengiste 2012). Because such pathogens have a wide

array of virulence factors at their disposal, developing resistance against them is exceedingly difficult.

1.7.4 Reactive oxygen species and the oxidative burst

Reactive oxygen species (ROS) are created by plants as a normal part of aerobic metabolism. The reduction of O_2 to form ROS such as superoxide radicals (O_2^-) and hydrogen peroxide (H_2O_2) occurs as a byproduct of electron transport and metabolic pathways of the cell. Due to the universal toxicity of ROS, concentrations of these molecules are kept low in the cell via antioxidant systems which scavenge these molecules (Noctor and Foyer 1998). An increase in ROS production occurs when cellular homeostasis is disrupted due to pathogen attack or subjection to certain environmental stressors.

ROS can take on a variety of roles in plant defense responses. In low concentrations, ROS function as important second messengers in multiple hormone-mediated pathways, including stomatal closure, lignin biosynthesis, programmed cell death and the HR (Sharma et al. 2012). Oxidative burst is one of the earliest detectable defense responses in plants, and involves rapid production of high levels of ROS in response to a biotic or abiotic stimuli (Wojtaszek 1997). ROS produced as part of the oxidative burst induce localized HR resulting in cell death and act as signals for the induction of protective genes in neighboring cells (Levine et al. 1994). *S. sclerotiorum* is able to manipulate ROS-mediated defense responses via oxalic acid, its key pathogenicity factor. ROS production is initially inhibited to avoid oxidative burst, but once the necrotroph is established it will promote ROS production to elicit programmed cell death (Williams et al. 2011). Oxidative bursts and ROS signaling are also required for the induction of systemic resistance (Durrant and Dong 2004; Kotchoni and Gachomo 2006).

1.7.5. Plant systemic resistance

The activation of local defense mechanisms in response to an inducing agent can also result in a systemic resistance response (Cameron et al. 1994). Systemic resistance bestows an enhanced defense capacity to the plant upon subsequent challenge by a broad spectrum of pathogens (Ramamoorthy et al. 2001). Two broad categories of systemic resistance have been defined: systemic acquired resistance (SAR) and induced systemic resistance (ISR). While ISR is activated in response to colonization of plant roots by nonpathogenic rhizobacteria and fungi, SAR is caused by pathogen attack and other elicitors of PTI/ETI (van Loon et al. 1998; Ramamoorthy et al. 2001; Pieterse et al. 2014). As such, these two forms of systemic resistance are unique, involving mostly different plant hormones and signaling pathways resulting in distinct resistance mechanisms induced.

1.7.5.1. Systemic acquired resistance (SAR)

SAR is classically characterized by systemic accumulation of the plant hormone salicylic acid (SA) followed by expression of pathogenesis-related (PR) proteins (Ryals et al. 1996). Although it was once thought that tissue necrosis was required for SAR onset, it is now known that PAMP detection is sufficient for SAR induction (Mishina and Zeier 2007). Besides biotic inducers, SAR can also be stimulated by application of SA, ethylene, dichloro-isonicotinic acid or benzothiadiazole (Ramamoorthy et al. 2001). The strength of SAR depends on the nature of the elicitor, which affects the intensity of oxidative burst and SA accumulation (Pastor et al. 2013). In *B. napus*, the effectiveness of SAR has also been correlated to *PR-1* and *PR-2* transcript levels, making these genes good markers of SAR (Potlakayala et al. 2007).

A number of long-distance signaling metabolites have been identified in SAR which can

be induced in response to different stimuli. Figure 1.2 is a working model of the metabolites and genes involved in SAR. It was once thought that SA was the long-distance signal of SAR. It is now known that although SA must be present in distal tissues for SAR activation, it is not the long-distance signal (Malamy et al. 1990; Métraux et al. 1990; Vernooij et al. 1994; Pallas et al. 1996). Methyl salicylate (MeSA) and dehydroabietinal (DA) are translocated throughout the plant and induce SAR (Park et al. 2007; Chaturvedi et al. 2012). MeSA biosynthesis is catalyzed by the SA methyltransferase BSMT1 in local tissues and converted back to SA in distal tissues by the methyl esterase MES9 (Shah and Zeier 2013; Gao et al. 2015). It is not known whether MeSA serves any other function in the distal tissues besides SA accumulation. DA, an abietane diterpenoid, is a potent activator of SAR when applied to leaves where it causes accumulation of SA and *PR1* expression in distal tissues (Chaturvedi et al. 2012). Pipecolic acid (Pip) and azelaic acid (Aza) are mobile metabolites implicated in priming a stronger and faster accumulation of SA in response to a pathogen (Shah and Zeier 2013). Like DA, exogenous application of Pip also causes SA accumulation, however its role is in defense amplification rather than induction (Návarová et al. 2012). Pip is synthesized by the aminotransferase ALD1, and Pip-deficient *ald1* plants fail to accumulate SA in distal tissues (Návarová et al. 2012). Aza-induced SAR also requires ALD1, but unlike Pip, exogenous application does not cause SA accumulation (Shah and Zeier 2013). Glycerol-3-phosphate (G3P), a precursor for the biosynthesis of all plant glycerolipids, was also found to be required for SAR. Only about 7% of Aza is transported systemically, and it appears that its major function in inducing SAR is by increasing G3P levels in distal tissues via upregulation of the *SFD1* gene (Yu et al. 2013). SFD1 is a plastid-localized dihydroxyacetone phosphate reductase responsible for G3P biosynthesis, and required for chloroplast lipid metabolism and defense signaling

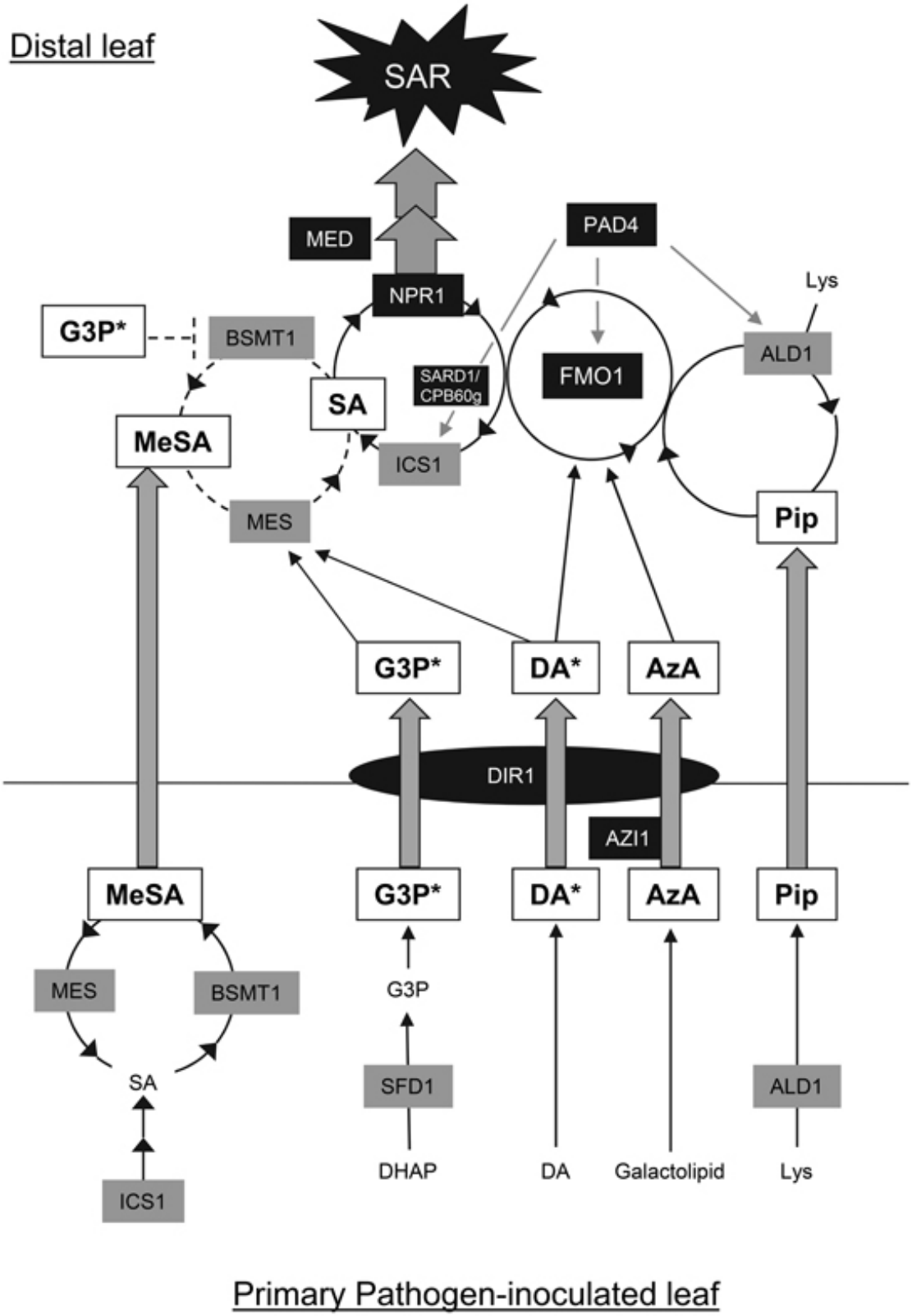

Figure 1.2. Working model of the signaling pathways involved in the systemic acquired response (SAR). Reproduced from Shah and Zeier, Front Plant Sci. 2013, doi: 10.3389/fpls.2013.00030 (open access).

(Nandi et al. 2004; Lorenc-Kukula et al. 2012). G3P derivative(s) functions as mobile signals, and interestingly, exogenous application of G3P induces SAR without inducing SA biosynthesis (Chanda et al. 2011). Other genes have been implicated in these networks which function to propagate SAR in distal tissues. FMO1 is a flavin-dependent monooxygenase required for systemic SA accumulation, and is critical for Aza-, Pip- and DA-induced SAR (Shah and Zeier 2013). ICS1 is an isochorismate synthase responsible for SA biosynthesis in distal tissues, and is regulated by the transcription factors CBP60g and SARD1 (Wildermuth et al. 2001; Zhang et al. 2010). These resistance pathways converge at PAD4, a central regulator with transcriptional control over *ALD1*, *FMO1* and *ICS1*, followed by NPR1, a transcriptional activator of SAR genes including *PR1* (Shah and Zeier 2013; Gao et al. 2015).

How are these metabolites transported from the site of infection to distal tissues? If the signals are soluble, they can move freely through the cytoplasm. However, the main biologically active fraction from SAR-inducing petiole exudates is apolar, indicating that transport proteins are being used to move hydrophobic molecules (Wittek et al. 2014; Cecchini et al. 2015). The lipid transfer proteins DIR1 and AZI1 (and its paralog, EARLI1) have been identified as essential, SAR-specific components (Maldonado et al. 2002; Jung et al. 2009). DIR1 is required for Aza-,

G3P-, and DA-mediated SAR, suggesting a convergent pathway (Yu et al. 2013). Mutation in either DIR1 or AZI1 results in the abolishment of SAR, and it is thought that they may form heteromers that function in systemic transport (Cecchini et al. 2015; Gao et al. 2015). The loss of DIR1 or AZI1 also results in a reduction of pathogen-induced G3P accumulation, while a lack of G3P results in less *DIR1* and *AZI1* transcripts (Yu et al. 2013). As DIR1 is required for the transport of a G3P derivative to distal tissues, it has been postulated that the DIR1/AZI1 complex

is responsible for transport of this signaling molecule (Chanda et al. 2011). AZI1 has been shown to localize to predicted sites of lipid exchange in the cell including the endoplasmic reticulum, plasmodesmata and chloroplast outer envelope (Cecchini et al. 2015). This evidence suggests that following synthesis of signaling metabolites in these organelles, a DIR/AZI1 complex facilitates transport to distal tissues in plants. Thus, the strength of the SAR response depends on differential signaling by several metabolites, indicating a response tailored to the plant stressor.

1.7.5.2. Induced systemic resistance (ISR)

Hundreds of studies have reported on the ability of plant growth-promoting rhizobacteria and fungi (PGPR and PGPF) to bestow induced resistance on plant hosts (Pieterse et al. 2014). Although initially thought to be mechanistically similar to SAR with different triggers, ISR and SAR involve unique priming strategies activated via different signaling pathways. Bacterial triggers of ISR include but are not limited to flagella, LPS, SA, and siderophores (Van Loon 2007). Where SAR involves the activation of SA-responsive genes, ISR utilizes the plant hormones ethylene (ET) and jasmonic acid (JA) to activate a different priming response (van Loon and Bakker 2005). Despite these differences, there are points of conversion between the two systemic responses. NPR1, a key regulator of SAR, is also required for ISR. Here, instead of activating SA-responsive genes in the nucleus, it has a cytoplasmic function in JA and ET signaling (Pieterse et al. 2014). The lipid transfer protein AZI1 (and its paralog EARLI1) which plays a role in SAR signal transport is induced in roots colonized by ISR-inducing bacteria (Zamioudis et al. 2014). AZI1 is also required for ISR activation, and may function in lipid-based signaling as well (Cecchini et al. 2015). Because JA and ET levels do not increase in ISR, no clear-cut markers of ISR activation have been identified and, compared to SAR, transcriptional changes are mild (Pieterse et al. 2014). Challenge with a pathogen may be the

only way to verify the existence of priming events by ISR.

1.7.6. Chloroplast roles in defense signaling

Chloroplasts have central roles in defense signaling and are targets for both host defense and pathogen disease signals. MAMP recognition reprograms the chloroplast transcriptome to elicit immune responses such as ROS oxidative burst. At the same time, some pathogen effectors can target the chloroplast to mute this response by destabilizing photosystem II (PSII) and electron transport (de Torres Zabala et al. 2015). *S. sclerotiorum* decreases photosynthetic activity in tobacco using its main effector, oxalic acid, but here it damages components of PSII which result in increased ROS accumulation (Yang et al. 2014). Manipulating the photosynthetic machinery to regulate oxidative burst may therefore be different depending on the pathogen lifestyle. In contrast, some nonpathogenic bacteria can enhance photosynthesis by increasing chlorophyll content or photosynthetic efficiency (Zhang et al. 2008; Baset Mia et al. 2010; Lenin and Jayanthi 2012; Kumar et al. 2016). Both host plant and PGPR benefit from this increase in energy production, as up to 30% of photosynthetic products are released in the soil as root exudates (Zhang et al. 2008).

Lipid metabolism in chloroplasts have been associated with defense signaling mechanisms. Chloroplasts are an important site of biosynthesis of Aza, G3P, ROS and SA, all vital components of SAR (Gao et al. 2015). The photosynthetic membrane system, which is organized into thylakoid structures, contains the galactolipids monogalactosyldiacylglycerol (MGDG) and digalatcosyldiacylglycerol (DGDG). These galactolipids are required for Aza biosynthesis, which is thought to occur via oxidation of C18 fatty acids on these lipids (Gao et al. 2014). While DGDG plays a role in SA accumulation and is required for SAR, MGDG regulates G3P and Aza biosynthesis, indicating that these lipids have non-redundant roles in SAR (Gao et

al. 2014). Thus, thylakoid membranes have a dual role in energy production via photosynthesis and systemic defense via signal production. At this time, changes in thylakoid membrane composition or structure have not been associated with defense activation by nonpathogenic organisms.

1.8. Priming of plant defenses

The major outcome of SAR and ISR in plants is a boosting of their defenses to react stronger and more quickly to future threats (Van Peer et al. 1991; Wei et al. 1991; van Loon et al. 1998; De Vleesschauwer and Höfte 2009; Shoresh et al. 2010; Pieterse et al. 2014). This "priming" of plant defenses involves short- and long-term cellular changes (Pastor et al. 2013). The earliest priming responses involve rapid ROS accumulation followed by the formation of papillae and stomatal closure occurring as part of PTI (Melotto et al. 2006; Luna et al. 2011). This immediate response is a potent but short-lived form of priming that protects the plants against pathogenic attack. The subsequent establishment of SAR or ISR results in transcriptomic, proteomic and epigenetic enhancements which poise the plant to react more quickly to future pathogen attack. ISR activation has been associated with upregulation of the AP2/ERF family of transcription factors which regulate JA- and ET-dependent defense genes. The *MYC2* gene, encoding a transcription factor co-regulating the expression of JA-induced genes, was also weakly upregulated (Van der Ent et al. 2009). A SAR-inducing analog of SA caused accumulation of MPK3 and MPK6 transcripts and inactive proteins, which are mitogen-associated protein kinases (MAPKs) involved in defense signaling (Beckers et al. 2009). Epigenetic changes have also been demonstrated in response to SAR. A reduction in cytosine methylation of genomic DNA attributed to SAR activators results in powdery mildew resistance

in barley (Kraska and Schönbeck 1993). Chromatin modifications in the promoter region of WRKY transcription factor genes, which facilitate transcriptional activation, have also been observed (Conrath 2011; Pieterse et al. 2014). These transcription factors are known to be key regulators of SA-dependent defense genes (Eulgem and Somssich 2007). Epigenetic changes involving priming are also heritable, meaning that future generations of organisms benefit from systemic resistance (Pastor et al. 2013). At this time, epigenetic and MAPK-related priming has not yet been demonstrated in ISR (Pieterse et al. 2014). Additionally, there is very little knowledge of the potential for pathogen-antagonizing BCA priming of the host organism and, in particular, how priming affects global changes of the host transcriptome.

1.9. Biocontrol agents and systemic resistance

Systemic resistance induced by plant growth-promoting microorganisms has commonly been shown (van Loon et al. 1998; Pieterse et al. 2014). However, examples of ISR or SAR caused by microorganisms which also protect plants via direct antibiosis towards pathogens are relatively rare. *Trichoderma* spp. exhibit mycoparasitism against other soil-borne fungi including plant pathogens such as *Rhizoctonia solani*, and secrete antibiotics and cell wall-degrading enzymes (Harman et al. 2004). These fungi are avirulent towards plants and reduce disease instances caused by a variety of pathogens by activation of ISR (Vinale et al. 2008). The majority of bacterial species that exhibit these dual roles are ISR-inducing *Pseudomonas* spp. or *Bacillus* spp. (Pal and McSpadden Gardener 2006). For example, *Pseudomonas putida* WCS358 suppresses soil-borne pathogens through siderophore-mediated competition for iron, but can also induce ISR in Arabidopsis via host detection of flagellin, pseudobactin and lipopolysaccharides (Meziane et al. 2005). *P. fluorescens* CHA0 is a biocontrol agent that protects the roots of

various plants from several phytopathogens by excreting compounds including pyluteorin, pyrrolnitrin and HCN (Jousset et al. 2006). When present in the soil, CHA0 confers resistance in leaves against tobacco necrosis virus, and leaves accumulate SA and PR proteins indicative of a SAR response (Maurhofer et al. 1994). Maurhofer *et al.* (1994) also found that the siderophore pyoverdine had no role in protecting plant roots from pathogens but was involved in SAR induction. *P. chlororaphis* O6 produces phenazines and pyrrolnitrin, similar to our organism of interest, *P. chlororaphis* PA23 (Park et al. 2011). Strain O6 elicits ISR in the tobacco rhizosphere through production of the volatile 2R, 3R-butanediol, protecting it against leaf pathogens (Han et al. 2006).

Even fewer examples exist of systemic resistance induced by a biocontrol agent in the phyllosphere. *P. fluorescens* Bk3 has antagonistic activity against *Venturia inaequalis*, the causative agent of apple scab on *Malus domestica* (apple). When applied to the phyllosphere, it induces the expression of PR proteins, indicative of SAR (Kürkcüoglu et al. 2004). *P. chlororaphis* PA23 induces low levels of systemic resistance against *L. maculans* when applied to *B. napus* cotyledons, although direct antibiosis was most effective (Ramarathnam et al. 2010). The mechanisms behind this systemic resistance have not been elucidated, and it is unknown whether PA23 confers similar resistance in the *B. napus* - S. *sclerotiorum* pathosystem.

1.10. Thesis Objectives

Knowledge of PA23 biocontrol activity in the *B. napus – S. sclerotiorum* pathosystem is limited to antibiosis of this necrotrophic fungus, but nothing is known about the effects of PA23 on the host plant. Therefore, the objectives of this thesis are:

1. To identify global transcriptomic changes occurring in *B. napus* in response to PA23 and/or *S. sclerotiorum*.
2. To identify shared and unique defense responses and cellular mechanisms induced in *B. napus* in response to these organisms.
3. To characterize defense responses including systemic resistance and priming induced by PA23.

2. MATERIALS AND METHODS

2.1. Plant and bacterial growth conditions

Brassica napus cv. Westar plants were grown in Sunshine Mix #1 soil in growth chambers at 21ºC with a light/dark photoperiod of 16h/8h and 0% humidity. *Pseudomonas chlororaphis* PA23 was grown overnight in Luria-Bertani broth at 28ºC in a shaking incubator.

2.2. Greenhouse infection assays

One day prior to fungal pathogen exposure, *B. napus* plants at the 30% flowering stage were sprayed until dripping with a $2x10^8$ cfu/mL solution of PA23 resuspended in sterile water supplemented with 0.02% Tween 20 as a surfactant. Plants not receiving biocontrol treatment (water control and Ss only groups) were sprayed with sterile water (0.02% Tween 20). Plants were sealed in clear bags to preserve relative humidity and returned to the growth chamber for 24 hours. The following day, bags were removed and plants receiving the pathogen treatment were sprayed with an $8x10^4$ spores/mL solution of *S. sclerotiorum* ascospores resuspended in sterile water (0.02% Tween 20). Control plants and plants to be exposed only to PA23 were sprayed with sterile water (0.02% Tween 20). Plants were transferred to a humidity chamber with humidity levels of 70-90% for 72 hours. During this time, plants were gently shaken at the base twice to encourage petals to detach and fall into the plant canopy. Infection rates were quantified by calculating the ratio of petals causing lesions to total petals in the plant canopy. Counts from three plants were pooled for each treatment. This experiment was performed three times.

2.3. RNA extraction and sequencing

Infection assays were carried out as described above, and tissue from three biological replicates was collected for RNA extraction. Three leaves per plant and three plants per treatment group were used for each biological replicate. Leaves upon which petals had landed were used for collection, as these are sites of potential infection. The petal was removed from the leaf and approximately 1cm^2 area of leaf tissue surrounding the site was collected with a scalpel. For *S. sclerotiorum*-infected leaves, green tissue immediately surrounding the lesion was collected. Cuttings were flash frozen in liquid nitrogen, and stored at -80℃ for no more than 2 days before processing. Total RNA was extracted using PureLink® Plant RNA Reagent (Invitrogen). DNA contamination was removed using Turbo DNA-*free*™ kit (Ambion), following the manufacturer's instructions. RNA concentration was verified using a NanoVue spectrophotometer (GE Healthcare), and quality was measured using an Agilent 2100 Bioanalyzer with Agilent RNA 6000 Pico and Nano Chips (Agilent Technologies; Santa Clara, CA, USA). RNA-seq libraries were prepared according to the alternative HTR protocol (C2) described by Kumar (2012) with the exception of PCR enrichment of the libraries, where the number of cycles was adjusted to 11. Libraries were validated using the Agilent Bioanalyzer High Sensitivity DNA Assay with DNA chips (Agilent Technologies). The desired fragment sizes of sheared cDNA with ligated adapters were isolated using the E-Gel® electrophoresis system (Invitrogen). 100 bp single-end RNA sequencing was carried out at Génome Québec (Montreal, Canada) on the Illumina HiSeq 2000 platform.

2.4. Data analysis

Sequenced reads were analyzed to remove barcode adapters and low quality reads using the Trimmomatic tool (Bolger et al. 2014). The parameters for Trimmomatic which maximized mapping efficiency to the *B. napus* and *S. sclerotiorum* genomes [*B. napus*: v.4.1, Chalhoub *et al.* (2014); *S. sclerotiorum*: v1, Amselem et al., (2011)] were determined using FastQC reports for quality control (http://www.bioinformatics.babraham.ac.uk/projects/fastqc/) followed by alignment using Tophat2 v.2.1.0 (Trapnell et al. 2012). Reads mapped to the *B. napus* and *S. sclerotiorum* genomes as expected, with 81.42% of reads mapping to *B. napus* across samples (Table 2.1). Alignment of reads to these genomes was performed in high-sensitivity mode using *B. napus* reference annotation v5 from Chalhoub et al. (2014) and the *S. sclerotiorum* reference annotation from Amselem et al. (2011) as guides. The cufflinks and cuffmerge tools within the Cufflinks v.2.2.1 suite (Trapnell et al. 2012) were used construct a transcriptome from the reads and identify novel transcripts. Transdecoder (https://transdecoder.github.io) was used to identify open reading frames (ORFs) within transcript sequences. Genes were identified by aligning translated ORF sequences with proteins in the Arabidopsis TAIR10, NCBI and Uniprot databases using BLAST (Altschul et al. 1990). Read counts were normalized to Fragments Per Kilobase of transcript per Million mapped reads (FPKM) values using the cuffquant and cuffdiff tools in the Cufflinks package with default settings (Trapnell et al. 2012). Significantly differentially expressed genes were identified as those with a corrected p-value < 0.05 (false discovery rate = 0.05). This output was used for hierarchical clustering via the pvclust package (https://cran.r-project.org/web/packages/pvclust/pvclust.pdf) and Venn diagram generation via Venny v2.1 (http://bioinfogp.cnb.csic.es/tools/venny/index.html). Dominant patterns (DPs) of expression were identified using the cuffdiff output data via the Fuzzy K-means (FKM)

Table 2.1. RNA-seq library reads mapped to the *Brassica napus* and *Sclerotinia sclerotiorum* genomes.

Treatment (Replicate)	Total reads	Reads mapped to *B. napus* genome	*B. napus* mapping %	Reads mapped to *S. sclerotiorum* genome	*S. sclerotiorum* mapping %
H_2O (1)	53,994,750	39,109,273	78.14%	46,038	0.09%
H_2O (2)	46,151,214	33,249,878	77.65%	33,761	0.08%
H_2O (3)	33,188,701	26,792,764	83.31%	24,608	0.08%
PA23 (1)	13,165,652	10,600,591	84.09%	14,545	0.12%
PA23(2)	28,819,289	23,359,660	83.80%	21,184	0.08%
PA23 (3)	23,310,938	18,915,639	83.78%	17,072	0.08%
PA23+Ss (1)	42,652,467	30,549,663	77.39%	34,130	0.09%
PA23+Ss (2)	29,392,010	23,728,001	83.48%	53,276	0.19%
PA23+Ss (3)	37,445,373	28,861,605	82.50%	358,553	1.02%
Ss (1)	28,442,683	22,522,734	82.03%	654,286	2.38%
Ss (2)	46,092,745	32,405,839	80.93%	1,143,800	2.86%
Ss (3)	23,707,533	18,188,028	79.97%	676,368	2.97%

implementation FANNY (https://cran.r- project.org/web/packages/cluster/cluster.pdf) using a K value of 10. Transcripts with a Pearson's correlation of 0.85 or above were assigned to DPs. Principal component analysis was performed on raw counts using the DESeq2 package (Love et al. 2014).

2.5. Staining for reactive oxygen species

B. napus leaves were stained for hydrogen peroxide (H_2O_2) and superoxide radical (O_2^-) accumulation as per the methods of Kumar et al. (2014). Briefly, leaves were severed with petioles intact and immersed in staining solution overnight in the dark, while avoiding contact between the solution and the severed petiole to reduce staining of the vein conduits. For H_2O_2 detection a 1mg/mL solution of 3,3′-diaminobenzidine was used. A 0.2% solution of nitrotetrazolium blue chloride in 50mM sodium phosphate buffer at pH 7.5 was used to identify O_2^-. The following day, chlorophyll was removed from the leaves by submersion in 95% ethanol and heating in a boiling water bath.

2.6. Chlorophyll quantification

Concentrations of chlorophyll *a* and *b* were determined based on methods described by Arnon (1949) and Porra (2002). Briefly, tissue from two leaves per plant was combined as one biological replicate and ground in liquid nitrogen. Approximately 200mg of powder was used for extraction in 80% acetone buffered to pH 7.8. All steps of the extraction were performed in the dark. Concentrations were calculated as described by Porra (2002). Three biological replicates were collected and this experiment was repeated twice.

2.7. Transmission electron microscopy

Leaf tissue was collected as above and processed following the methods of Chan and Belmonte (2013). Tissue was fixed overnight in 3% glutaraldehyde in 0.025 M cacodylate buffer supplemented with 5mM calcium chloride (pH 7.0). Plant material was rinsed with cacodylate buffer and post-fixed with 2% osmium tetroxide in 0.8% $KFe(CN)_6$ in cacodylate buffer. After post-fixation, seeds were rinsed with distilled water and stained overnight with a 0.5% aqueous uranyl acetate solution. Plant material was rinsed in distilled water and dehydrated in a graded ethanol series. The leaf tissue was then further dehydrated in 1:1 absolute ethanol to propylene oxide (*v:v*) and then in 100% propylene oxide. Finally, tissue was gradually infiltrated and embedded in Spurr's epoxy resin at 70ºC. All methods prior to embedding were performed at 4°C. Using a Reichert–Jung Ultracut ultramicrotome, sections were cut (90nm thickness) with a Diatome diamond knife and mounted on copper grids. The sections were visualized with a Hitachi H-7000 transmission electron microscope at 75 kV and pictures were taken using AMT Image Capture Engine version 601.384.

2.8. Differential gene expression verification using qRT-PCR

RNA collected for RNA sequencing was also used to synthesize cDNA for qRT-PCR. Primers for qRT-PCR are listed in Table 2.2. Following integrity checks employing the Agilent 2100 Bioanalyzer with Agilent RNA 6000 Pico and Nano Chips (Agilent Technologies; Santa Clara, CA, USA), cDNA was synthesized using the Maxima First Strand cDNA Synthesis Kit (Thermo Fisher Scientific, Inc.), following the manufacturer's instructions. qRT-PCR was conducted using the Bio-Rad CFX Connect™ Real-Time System with SsoFast™ EvaGreen® Supermix (Bio-Rad, USA). Reactions were conducted using the following cycling conditions:

Table 2.2. qRT-PCR primers used in this study.

Primer name	Oligonucleotide sequence	Gene name
ALD1both-F	5′- CCGAAGCAGATCACCTCAGA -3′	ALD1
ALD1both-R	5′- CTTGTCACCTTGTTCCAGGC -3′	ALD1
BnaA05g03420D-F	5′- GCTCAAGACCAGGTTCTTGC -3′	CHI
BnaA05g03420D-R	5′- CCTTGATTGTCGGGCCAAAG -3′	CHI
BnaA06g13830D-F	5′- GCGAGGCTTGATCCTTTGC -3′	CLH1
BnaA06g13830D-R	5′- AGCTTCCCTGAGGATACCAA -3′	CLH1
BnaA05g33880D-F	5′- ACGAGTGTCCCTTAAGCTCC -3′	DOX1
BnaA05g33880D-R	5′- GGGTGTACGGGAATTAAGCG -3′	DOX1
FMO1-F	5′- AAGAAAGTCGCGGTCATTGG -3′	FMO1
FMO1-R	5′- TCCACCTTCTCCTTGATTTGC -3′	FMO1
BnaC03g45470D-F	5′- TCTTGCAACTATGATCCTCGGG -3′	PR1
BnaC03g45470D-R	5′- ACGTCCTATATGCACGTGTT -3′	PR1
PR4-1-F	5′- GCGGTAGATGCTTAAGAGTGAC -3′	PR4
PR4-1-R	5′- CCCGTTACTGCACTGATCCA -3′	PR4
PR4-2-F	5′- AGTGCTTAAGGGTGAGGAACA -3′	PR4
PR4-2-R	5′- ACATTGCAACGTCCAAATCCA -3′	PR4

95°C for 30 s, followed by 45 cycles of 95°C for 2 s and 60°C for 5 s. Melt curves (0.5°C increments in a 68-90°C range) for each gene were performed to assess the sample for non-specific targets, splice

variants and primer dimers. CFX Manager v3.1 (Bio-Rad, USA) was used to calculate relative mRNA abundance using the $\Delta\Delta$Ct method. ATGP4 was used as an endogenous control and water-treated tissue was used as a reference sample.

3. RESULTS

3.1. *P. chlororaphis* PA23 reduces *S. sclerotiorum* infection rates in *B. napus*.

To understand how *B. napus* responds to PA23 and how PA23 protects the host plant from *S. sclerotiorum* infection, we compared infection rates at the 30-50% flowering stage in the presence or absence of PA23. When comparing the rate of infection as the proportion of lesion-forming petals to total petals fallen onto the plant canopy, application of PA23 reduced the number of lesions by more than 91% (Figure 3.1A). Using this infection model, leaf necrosis was visible under lesion-forming petals as soon as 24 hours post *S. sclerotiorum* infection in plants receiving the pathogen only treatment (Figure 3.1B).

3.2. Global patterns of gene expression in *B. napus* treated with combinations of PA23 and *S. sclerotiorum*.

Next, we studied global patterns of gene activity using RNA sequencing (RNA-seq) to better understand how *B. napus* responds to PA23 in the presence or absence of *S. sclerotiorum*. Principal component analysis (PCA) identified global relationships between transcriptomes of plants receiving combinations of PA23 and *S. sclerotiorum*. Biological replicates for each treatment grouped together, with PA23-only treatments grouping closely to the water controls (Figure 3.2A). Replicates representing treatment with *S. sclerotiorum* only (Ss) or PA23+Ss clustered into distinct groups, with Ss clustering farthest from the water control. This trend was also observed with hierarchical clustering analysis (Figure 3.2B).

Figure 3.2C summarizes mRNA detection in treatment groups and distribution of transcript abundance. A total of 48,454 genes with Fragments Per Kilobase of transcript per Million mapped reads (FPKM) ≥ 1 were detected across all samples, representing 48% of the

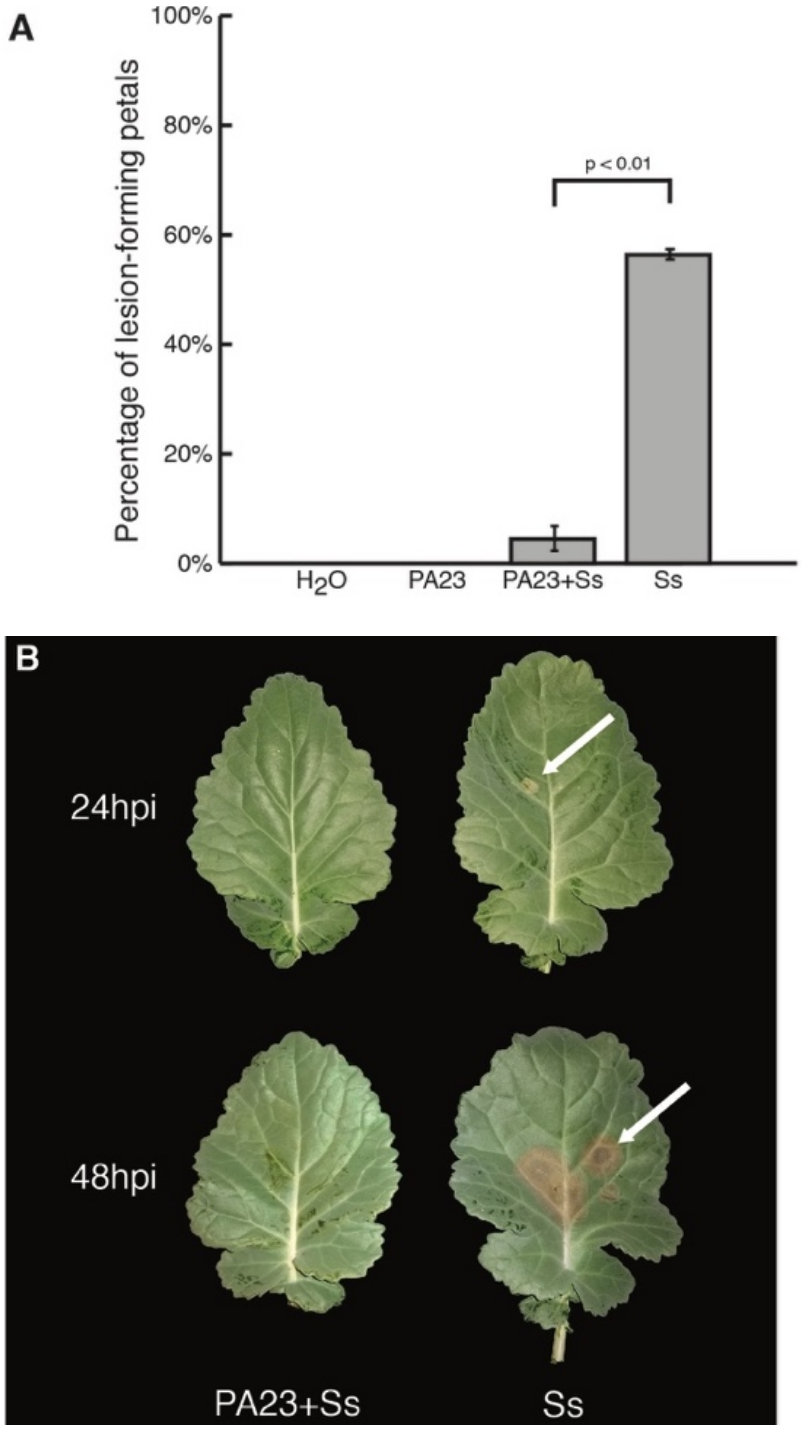

Figure 3.1. *B. napus in planta* infection rates in the presence of combinations of PA23 and *S. sclerotiorum* A. Lesion-forming petals as a percentage of total petals which fell onto plant leaves in greenhouse assays. B. *S. sclerotiorum* disease progression on canola leaves at 24 hours or 48 hours after petal application. PA23+Ss treatment petals were inoculated with PA23 24 hours prior to *S. sclerotiorum* inoculation, whereas Ss treatment petals were inoculated with sterile water. Both treatment groups (PA23+Ss and Ss) petals were then infected *in vitro* with *S. sclerotiorum* 48 hours prior to being placed on leaves.

predicted *B. napus* gene models (Chalhoub et al. 2014). The number of unique transcripts detected was similar across treatments at an average of 43,007 expressed genes. We divided expression levels into low (FPKM ≥ 1, < 5), moderate (FPKM 5-25), and high (FPKM > 25). The proportion of expressed genes falling into each category was similar across all treatment groups (39.0-43.5%, low; 35.3-44.3% moderate;11.5-13.2%, high), where plants treated with *S. sclerotiorum* alone resulted in the greatest number of highly accumulating transcripts and the lowest number of moderately accumulating transcripts when compared to other treatments (Figure 4C). In contrast, the PA23+Ss treatment group had the greatest number of moderately and lowly accumulating transcripts across treatments.

Because we had observed profound differences on the leaf surface when *S. sclerotiorum* was present with or without PA23, we compared differentially-expressed genes (DEGs) between treatments to identify similarities and differences at the RNA level. Figure 3.3A shows shared and unique upregulated DEGs in treatment groups compared to the water control. Plants treated with *S. sclerotiorum* alone had the greatest number of uniquely upregulated DEGs at 8,237 genes. This trend held for both up- and downregulated genes (Figure 3.3C). Plants treated with both PA23 and *S. sclerotiorum* had the fewest uniquely upregulated DEGs at 515 genes, a 16-fold reduction compared to the *S. sclerotiorum* treatment group. The majority of upregulated DEGs observed in the PA23+Ss group were shared with the pathogen only (Ss) group (3159 genes). While the number of upregulated DEGs in plants treated with PA23 alone was comparatively small (1,361 genes), 556 genes were unique to PA23 treatment alone (Figure 3.3A). DEGs of significance from the PA23 treated plants are listed in Table 3.1. Several markers of a systemic acquired response (SAR) including pathogenesis-related proteins *PR-1* (*BnaC03G45470D*) and *PR-2* (*BnaC08G28150D*), lipid transporter protein *D*

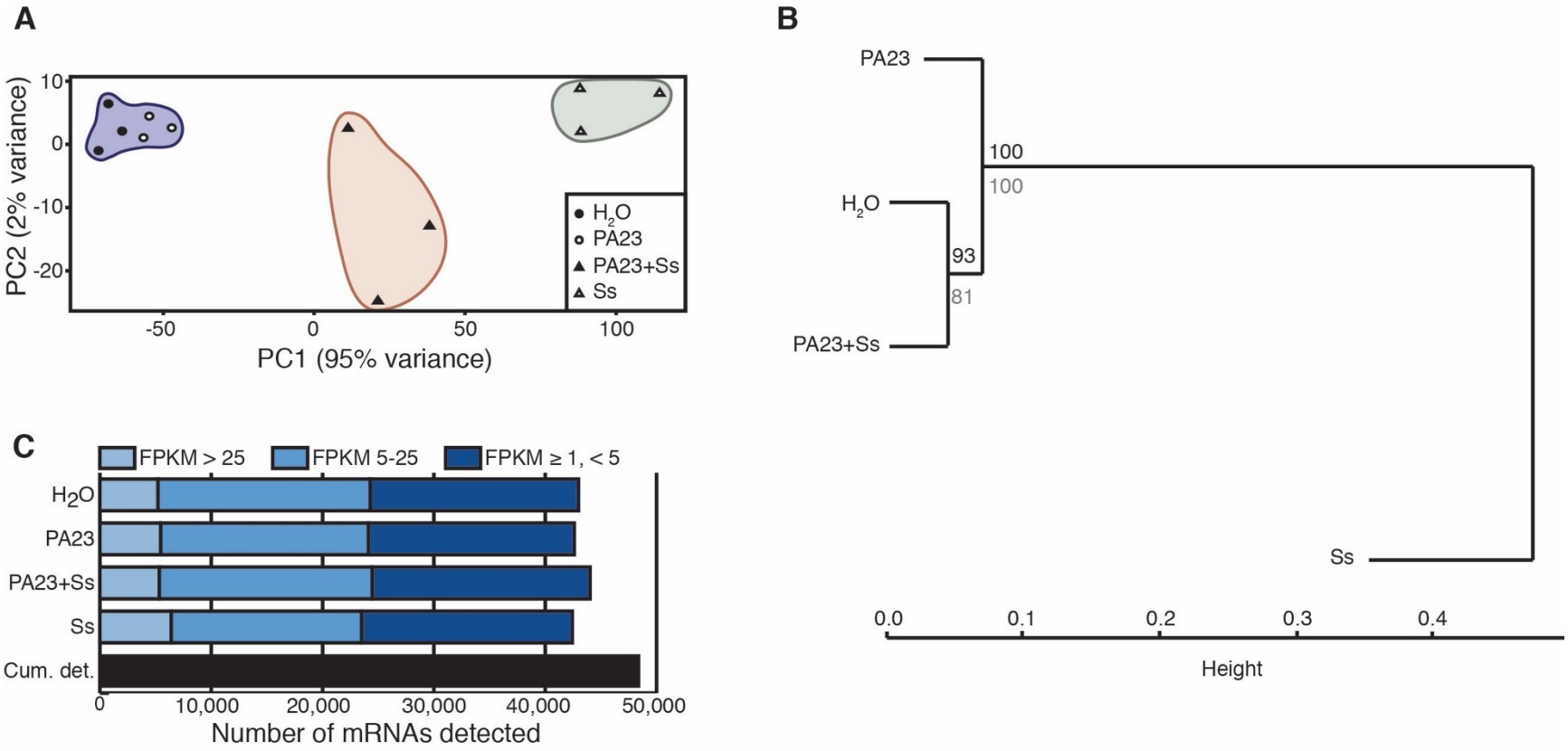

Figure 3.2. Global transcriptome changes in the presence of combinations of PA23 and *S. sclerotiorum*. A. Principal component analysis of mRNA sequences from the four treatment groups examined by RNA-seq. Variation between treatments is greater that variation between replicates, and phenotypically similar treatment groups are clustered more closely together. B. Hierarchical clustering of mRNAs from the four treatment groups. AU (approximately unbiased) and BP (bootstrap probability) values are shown in gray and black, respectively. C. Number of unique mRNAs present in treatment groups, as well as cumulative number of unique mRNA transcripts identified. Transcripts are categorized by frequency of occurrence in the library, as described by the number of fragments per kilobase of transcript per million mapped reads (FPKM) value.

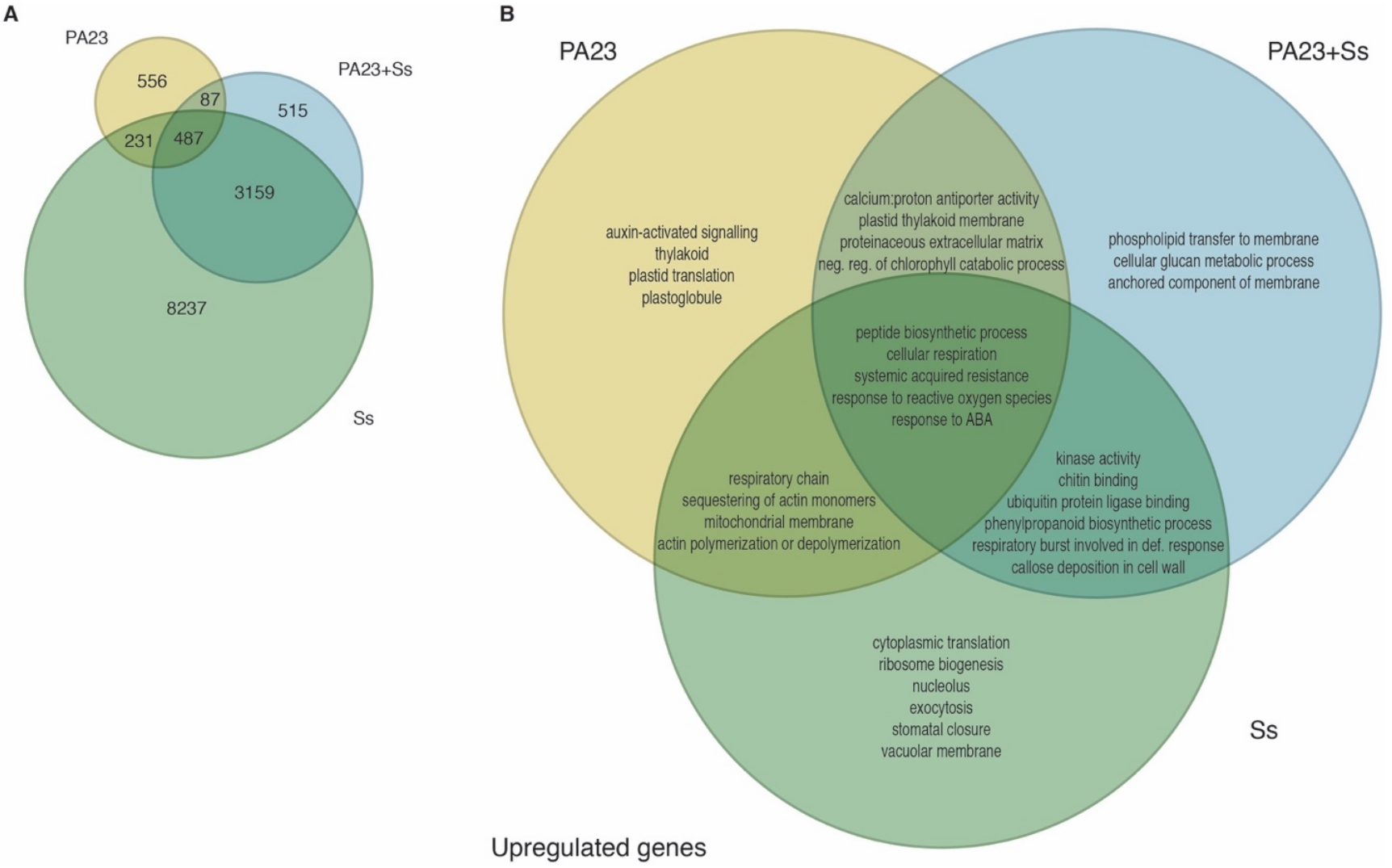
A
PA23
PA23+Ss
556
87
515
231
487
3159
8237
Ss
B
PA23
PA23+Ss
auxin-activated signalling
thylakoid
plastid translation
plastoglobule
calcium:proton antiporter activity
plastid thylakoid membrane
proteinaceous extracellular matrix
neg. reg. of chlorophyll catabolic process
phospholipid transfer to membrane
cellular glucan metabolic process
anchored component of membrane
peptide biosynthetic process
cellular respiration
systemic acquired resistance
response to reactive oxygen species
response to ABA
respiratory chain
sequestering of actin monomers
mitochondrial membrane
actin polymerization or depolymerization
kinase activity
chitin binding
ubiquitin protein ligase binding
phenylpropanoid biosynthetic process
respiratory burst involved in def. response
callose deposition in cell wall
cytoplasmic translation
ribosome biogenesis
nucleolus
exocytosis
stomatal closure
vacuolar membrane
Ss
Upregulated genes

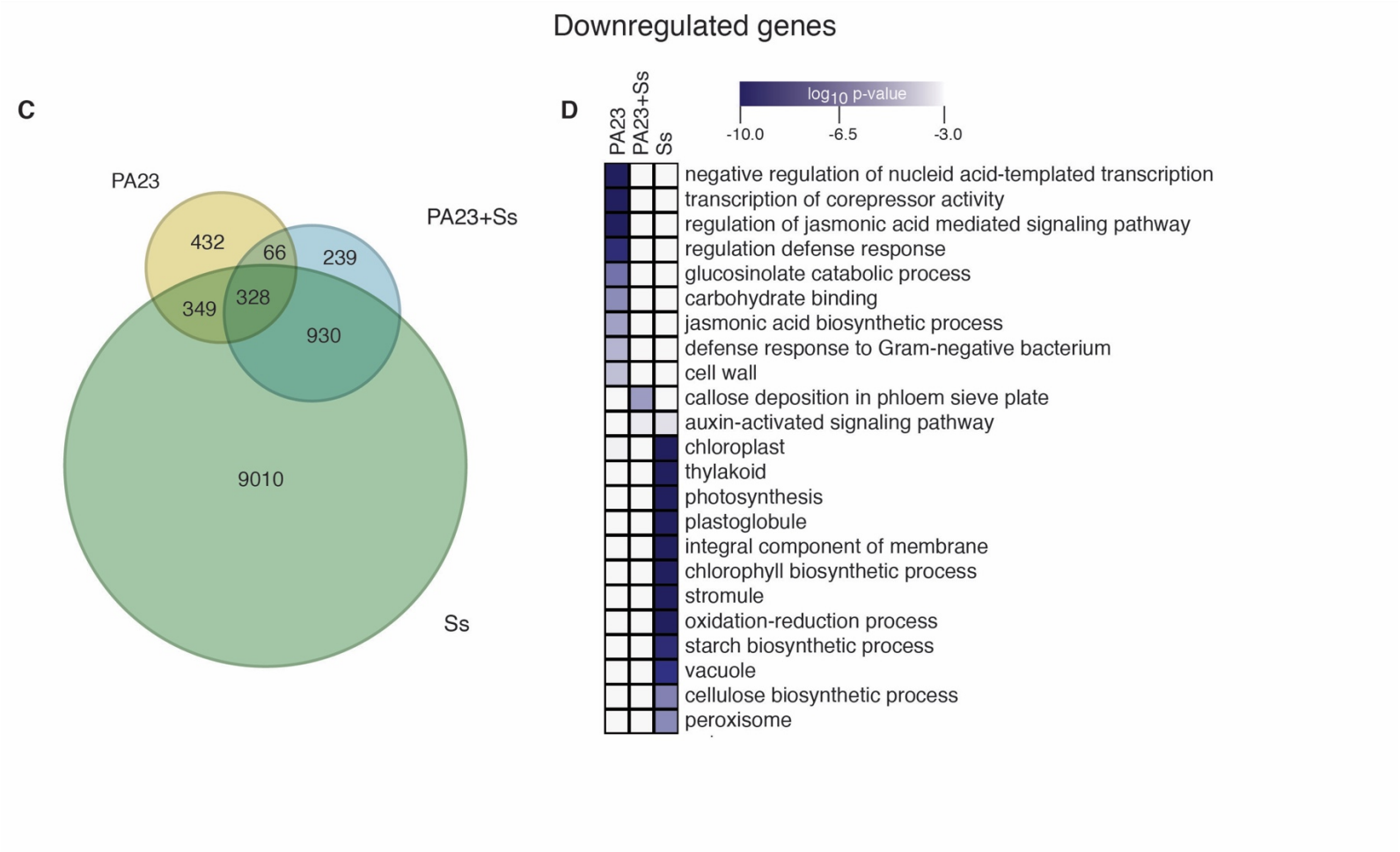

Figure 3.3. Gene expression changes unique to bacterial or fungal treatments of canola leaves. A. Venn diagram of *B. napus* gene counts for uniquely and significantly upregulated genes in treatment groups compared to the water control. B. Venn diagram of enriched GO terms selected from upregulated genes in A. C. Venn diagram of *B. napus* gene counts for uniquely and significantly downregulated genes in treatment groups compared to the water control. D. Heatmap of enriched GO terms selected from genes identified in A.

Table 3.1. Genes upregulated in response to PA23 treatment. *B*. *napus* identifiers used as per the Genome Genoscope Database (www.genoscope.cns.fr/brassicanapus). TAIR identifiers used as per The Arabidopsis Information Resource (TAIR, https://www.arabidopsis.org). Fold change in PA23 compared to the water control.

B. napus identifier	TAIR identifier	Gene name/function	Fold change
BnaC03g29580D	*AT4G12490.1*	EARLI1-like lipid transfer protein 2	53.07
BnaA09g20900D	*AT4G12490.1*	EARLI1-like lipid transfer protein 2	40.22
BnaC07g14090D	*AT1G22070.1*	TGA3 (Transcriptional activator)	35.95
BnaC06g37650D	*AT1G21310.1*	EXT3 (Extensin 3)	32.56
BnaC06g18380D	-	F-box/LRR-repeat protein 4-like	30.61
BnaC02g31910D	*AT5G45890.1*	SAG12 (Senescence-specific cysteine protease)	18.37
BnaC09g26890D	-	Possible nucleotide phosphorylase	17.43
BnaC08g46150D	-	Possible malonate decarboxylase	16.69
BnaC06g14700D	-	Photosystem II reaction center protein A	16.66
BnaA02g24130D	*AT5G45890.1*	SAG12 (Senescence-specific cysteine protease)	15.15
BnaC05g10350D	*AT1G14080.1*	FUT6 (Fucosyltransferase 6)	14.99
BnaCnng12890D	*ATMG00640.1*	ATP4 (ATP synthase subunit 4)	14.18
BnaA10g18480D	*AT5G15800.1*	SEP1 (SEPALLATA 1 transcription factor)	12.56
BnaCnng13130D	*ATMG00900.1*	CcmC (Cytochrome c assembly protein)	12.04
BnaC04g28910D	*AT5G24150.1*	Squalene monooxygenase 1-like	11.94
BnaAnng01030D	*AT5G04740.1*	ACR12 (ACT-domain containing protein)	11.88
BnaCnng24320D	*AT3G09190.1*	Concanavalin A-like lectin family protein	11.87
BnaA01g34180D	*ATCG00130.1*	AtpF (ATP synthase subunit b, chloroplastic)	11.79
BnaC09g29230D	-	Possible omega-6 fatty acid desaturase	11.24
BnaAnng35860D	*AT3G28700.1*	NADH dehydrogenase [ubiquinone] complex I, assembly factor 7-like	9.93
BnaA01g34980D	*AT4G19810.1*	ChiC (Class V chitinase)	9.74
BnaCnng12960D	*ATMG00070.1*	NAD9 (NADH dehydrogenase subunit 9)	9.64
BnaA01g33070D	*AT3G02310.1*	SEP2 (SEPALLATA 2 transcription factor)	9.39
BnaC05g38940D	*AT3G14610.1*	Cytochrome P450	8.93
BnaA03g38630D	*AT2G14580.1*	Basic PR-1	8.63

BnaC09g27530D	*ATCG00340.1*	PsaB (Photosystem I)	8.58
BnaC04g20930D	*AT3G30390.2*	Probable amino acid transporter	8.47
BnaA07g37560D	*AT5G38100.1*	S-adenosyl-L-methionine-dependent methyltransferases superfamily protein	8.02
BnaUnng03950D	*ATMG01170.1*	ATPase subunit 6	7.90
BnaC04g21290D	*ATMG01360.1*	COX1 (cytochrome c oxidase subunit 1)	7.87
BnaC09g32980D	*AT5G57220.1*	Cytochrome P450, family 81, subfamily F, polypeptide 2	7.77
BnaA08g22890D	*AT1G17860.1*	Kunitz family trypsin and protease inhibitor protein	7.73
BnaA07g21130D	-	Extensin-like protein	7.63
BnaA01g37280D	*AT4G11600.1*	GPX6 (Glutathione peroxidase, mitochondrial)	7.49

(*BnaA03G11410D*, *BnaC03G14230D*, *BnaA10G09640D*) and *EARLI1* (*BnaC03g29580D*, *BnaA09g20900D*) are upregulated in response to PA23.

To identify biological processes activated in response to the different treatments, we used the custom gene ontology (GO) term enrichment function of ChipEnrich with gene sets identified in Figure 3.3A (Belmonte et al. 2013). Figure 3.3B summarizes GO terms of interest from this analysis. Response to ROS ($\log_{10}$ *p*-value < -4) was significantly enriched in response to all treatments. Subsets of genes belonging to this category accumulated in PA23+Ss and Ss but not in plants treated with PA23 alone, while others were upregulated in all three treatment groups. In the latter, response to ROS involved upregulation of *FERRETIN 1* (*FER1, BnaC03G00160D*), *FERRETIN 3* (*FER3, BnaC06G15730D*), and two homologs of *HEAT SHOCK TRANSCRIPTION FACTOR A4A* (*HSFA4A, BnaC01G11370D, BnaC03G62890D*). In PA23+Ss and Ss treatment groups, four homologs of *ASCORBATE PEROXIDASE 1* (*APX1, BnaA06G04380D, BnaA09G49190D, BnaC05G05550D, BnaC08G43490D*), three homologs of *ETHYLENE RESPONSIVE ELEMENT BINDING FACTOR 6* (*ERF6, BnaA01G34910D, BnaA08G08300D, BnaC01G10080D*), two homologs of *XANTHINE DEHYDROGENASE 1* (*XDH1, BnaA09G00610D, BnaCNNG46690D*) and two additional homologs of *HEAT SHOCK TRANSCRIPTION FACTOR A4A* (*HSFA4A, BnaANNG31620D, BnaC07G35520D*) were identified. Similarly, all treatment groups were enriched for the SAR GO term, while the PA23+Ss and Ss treatment groups were enriched for respiratory burst involved in defense response.

The PA23+Ss group was uniquely enriched for GO terms involving cell wall remodeling (phospholipid transfer to membrane, $\log_{10}$ *p*-value < -6; anchored component of membrane, $\log_{10}$ *p*-value < -5; cellular glucan metabolic process, $\log_{10}$ *p*-value < -4). Here, overrepresented

transcripts of note included lipid transfer proteins and xyloglucan endotransglycosylases. Both PA23 only and PA23+Ss groups were also enriched for the proteinaceous extracellular matrix GO term ($\log_{10}$ *p*-value < -3).

In plants treated with PA23 only, the auxin-activated signaling GO term ($\log_{10}$ *p*-value < -4) was uniquely enriched. Upregulated genes included two homologs of *SKP1A* (*BnaA07G21520D*, *BnaC06G22030D*), *SKP2A* (*BnaA08G21350D*), two homologs of *NAC021* (*BnaA08G00130D* and *BnaC03G70990D*), *ARF16* (*BnaA03G49980D*) and two homologs of *IAA29* (*BnaA01G04710D* and *BnaC01G06240D*). Several *SMALL AUXIN UP RNA* genes were also upregulated (*SAUR23*, *BnaANNG37150D* and *BnaC03G08710D*; *SAUR20*-like genes *BnaA02G03930D* and *BnaC03G08750D*).

Several GO terms associated with the chloroplast were overrepresented in PA23-treated plants. Specifically, thylakoid ($\log_{10}$ *p*-value < -7), plastid translation ($\log_{10}$ *p*-value < -4) and plastoglobule ($\log_{10}$ *p*-value < -3) were enriched in the PA23 only treatment group, and plastid thylakoid membrane ($\log_{10}$ *p*-value < -3) as well as negative regulation of chlorophyll catabolic process ($\log_{10}$ *p*-value < -6) were enriched in both PA23 only and PA23+Ss treatment groups. Prominently accumulated transcripts among these groups included subunits of photosystems I and II, plastid-specific ribosomal subunits, and two homologs of the negative regulator of chlorophyll degradation *STAY-GREEN 2* (*SGR2*, *BnaA03G24900D* and *BnaC03G72930D*). A heatmap of relevant enriched GO terms for genes downregulated in these groups is available in Figure 3.3D.

3.3. PA23 prevents the accumulation of ROS in the leaf

We then validated the RNA-seq data revealing that both PA23-treated and Ss-treated plants were responding to ROS (Figures 5B and 6). We stained leaf tissues for detection of both hydrogen peroxide (H_2O_2) and (O_2^-) radicals. Whereas Ss-treated leaves retained both stains in the regions directly surrounding lesions indicative of H_2O_2 and O_2^- presence (Figure 3.4M-P), ROS production was greatly reduced when plants were treated with PA23 ahead of the fungal pathogen (Figure 3.4I-L). PA23-treated leaves had no regions containing large aggregations of these molecules, although H_2O_2 production appeared similar to the PA23+Ss treatment group (Figure 3.4G, H).

3.4. Treatment-specific effects are revealed through dominant patterns of expression

To identify more complex patterns of expression, we clustered gene activity from all treatment groups into dominant patterns (DPs) of co-expression using a modified Fuzzy K-means clustering algorithm. We identified six DPs from this analysis (Appendix A). To investigate how each treatment affected global gene activity, we focused our attention on three DPs where genes accumulated specifically in response to one of the treatments (Figure 3.5A). The number of genes clustering in these DPs ranges from 282 in DP5 to 11,340 in DP1. We identified genes associated with translation, response to fungus, plant-type hypersensitive response, and stomatal closure ($\log_{10}$ *p*-value < -8) when plants were infected with *S. sclerotiorum* without protection by PA23 (DP1). The chloroplast GO term is also significantly represented in DP1 ($\log_{10}$ *p*-value < -28), although no specific chloroplast-related processes were identified. In contrast, pre-treatment with PA23 (DP5) induced chloroplast-related components and processes, such as the chloroplast envelope, vitamin E biosynthesis, and starch metabolic processes ($\log_{10}$ *p*-value < -3). When

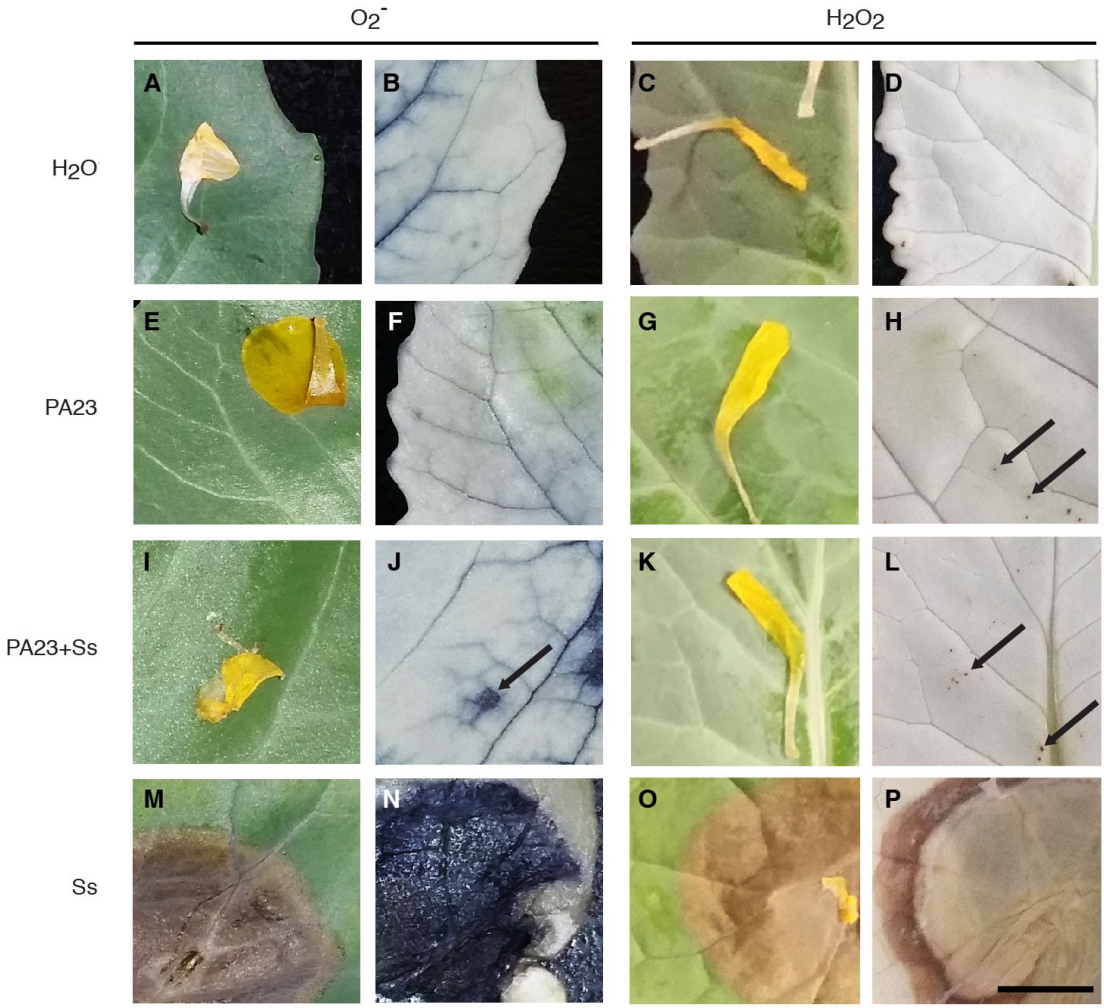

Figure 3.4. Detection of superoxide radicals (left) and hydrogen peroxide (right) in canola treatment groups. The leftmost column in each set depicts leaves after treatment and before staining. The rightmost column depicts the same area of tissue after petal removal, staining and treatment to remove leaf pigmentation. Scale bar in (P) = 5mm and is applicable to panels (A) - (P).

plants were treated with PA23 alone (DP3), genes associated with GO terms for cytoskeletal changes and auxin-activated signaling were upregulated ($\log_{10}$ *p*-value < -6), as well as several chloroplast-related terms including plastid translation, thylakoid and chloroplast envelope. Some GO terms were common to more than one DP; in particular, chloroplast (DP1 and DP3) and chloroplast envelope (DP3 and DP5), indicating differential expression of genes within these GO terms among treatments. GO terms prevalent amongst these patterns are presented in Figure 3.5B as a heatmap.

3.5. PA23 treatment results in structural and metabolic changes in the *B. napus* chloroplast

Since each DP identified a number of chloroplast component- and process-related GO terms, we decided to explore gene expression patterns within this organelle in more detail. The chloroplast GO term was significantly represented in more than one DP indicating differential expression of subsets of its associated genes. Accordingly, we compared relative expression levels of genes associated with chloroplast-related sub-regional and functional GO terms to reveal contrasting expression patterns (Figure 3.6A). For example, a comparison of relative abundance of genes associated with chlorophyll catabolite transmembrane transport reveals upregulation in the *S. sclerotiorum*-treated group. Although PA23+Ss treatment caused many of the same genes to be expressed, transcript abundance was higher in the absence of PA23. This trend was also observed for the chloroplast inner membrane and chloroplast stroma GO terms (Figure 3.6A, II and IV). The chloroplast photosystem I & II GO term as well as thylakoid-related GO terms were downregulated in *S. sclerotiorum* -treated plants and involved downregulation of genes encoding photosystem I subunits (*PSAN*, *BnaA06g23190D* and *BnaC03g50210D*; *PSAG*, *BnaC06g07480D*; *PSAP*, *BnaC04g51600D*), photosystem II subunits

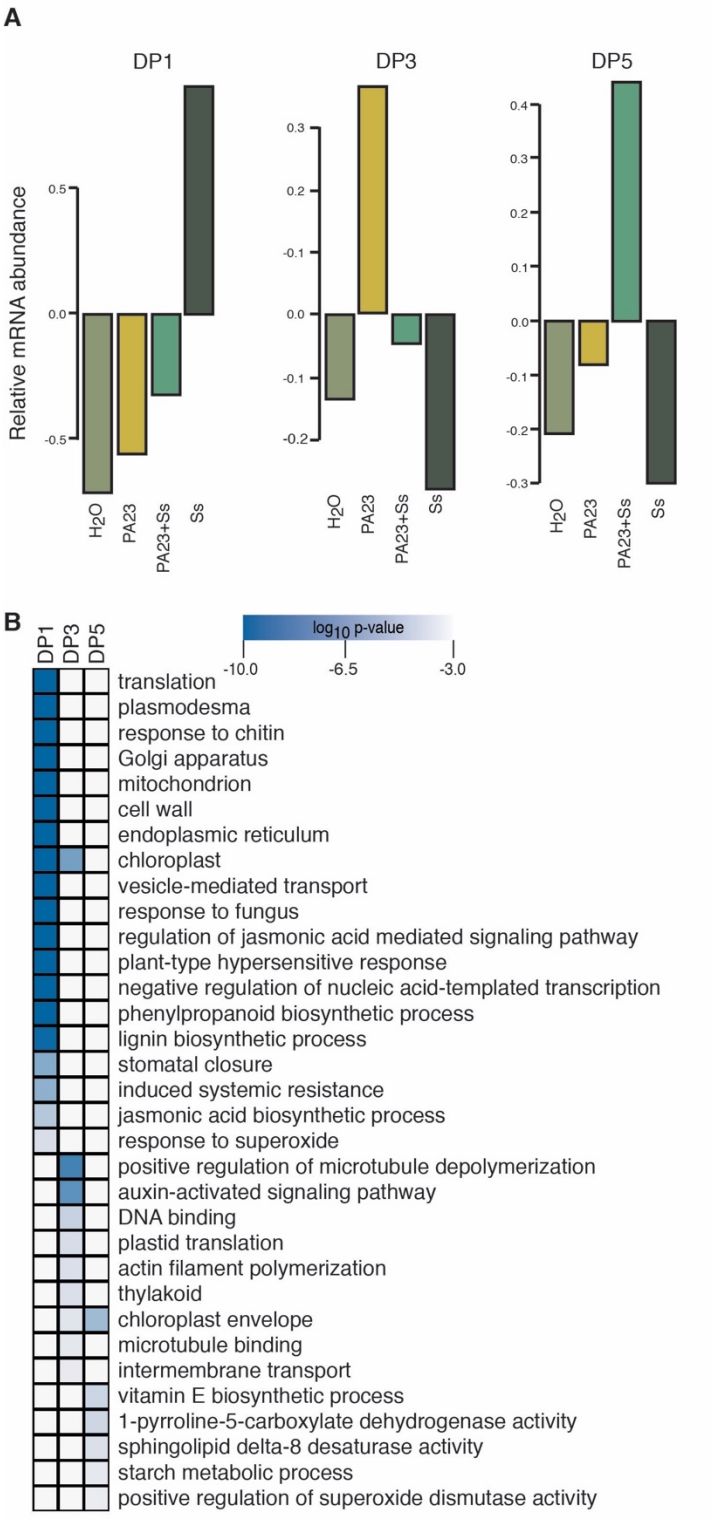

Figure 3.5. Dominant patterns of gene expression in canola treated with combinations of PA23 and *S. sclerotiorum*. A. Selection of three dominant patterns of gene expression depicting unique upregulation in one treatment group. b) Heatmap of enriched GO terms selected from genes identified in the dominant patterns from A.

and regulatory proteins (*PSBY*, *BnaA07g38700D* and *BnaC06g26560D*; *PSB27*, *BnaC08g46250D*; *PSBP-1*, *BnaC08g44890D*) and other photosynthesis-related proteins (*CRR23*, *BnaA07g28860D* and *BnaC06g31900D*; *PLASTOCYANIN 2*, *BnaA06g38550D*; *PNSL2*, *BnaA09g45770D*). Overall upregulation of the chloroplast thylakoid and plastoglobule GO terms (Figure 3.6A, V and VI) in the PA23 only group was also confirmed. A complete list of gene names and fold change values for genes in Figure 3.6A is available in Appendix B.

We then used transmission electron microscopy (TEM) to validate the global RNA sequencing data and identify changes in chloroplast membrane structure in response to PA23 (Figure 3.6B-F). Chloroplasts within the upper most layer of the palisade mesophyll from the water-treated control group contained large starch granules and reduced thylakoid membrane structure. When plants were treated with PA23, the area dedicated to thylakoid structures increased with a concomitant increase in granal stack organization and the accumulation of plastoglobuli 24 and 48 hours post inoculation (Figure 3.6C and D). While gene expression in plants treated with PA23 in combination with *S. sclerotiorum* indicated significant upregulation of starch metabolic processes (Figure 3.5B), these chloroplasts were similar in appearance to those of the biocontrol only-treated group with many grana stacks and plastoglobules (Figure 3.6E). When plants were inoculated with *S. sclerotiorum*, thylakoid structures of the chloroplast appeared diminished compared to other treatments (Figure 3.6F).

Since structural changes were observed in chloroplasts treated with PA23, we next wanted to determine whether plant chlorophyll was also affected. Chlorophyll content between treatment groups showed concentrations of total chlorophyll (chlorophyll *a* and *b)* significantly increased by 22.8% when plants were treated with PA23 while those treated with PA23 and *S. sclerotiorum* or *S. sclerotiorum* alone showed no difference when compared to the water control

(Figure 3.6G). To clarify whether these changes were due to increased chlorophyll production or decreased chlorophyll degradation, we examined expression of chlorophyllase genes. RNA-seq data of genes involved in chlorophyll degradation pathways revealed significant downregulation of *CHLOROPHYLLASE 1* (*CLH1*) in PA23-treated plants which was confirmed via qRT-PCR (Figure 3.6H). This was in contrast to *S. sclerotiorum*-treated plants, which showed significantly increased levels of *CLH1* and decreased activity in genes associated with several other chlorophyll-related pathways (Figure 3.6H, 5D).

3.6. PA23 activates unique innate immunity and SAR networks to prime plant defenses

To understand how PA23 triggers plant priming mechanisms, we compared the differential accumulation of transcripts known to be involved in innate immunity among treatment groups. The interactions of significantly up- or down-regulated genes encoding products known to function in triggered immunity were placed in a network (Figure 3.7A). Treatment-specific expression levels were expressed as a heatmap for each gene and homolog, from left to right: PA23 only, PA23+Ss, and Ss only. As expected, many of these genes were upregulated in response to the pathogen, *S. sclerotiorum*. In response to PA23, two prokaryote-specific surface receptors were downregulated. These included *FLS2* (*BnaA09g17950D*), encoding a receptor kinase which binds bacterial flagellin, and *LYM3* (*BnaCnng11350D*), encoding a receptor required for detection of peptidoglycan.

Systemic resistance and defense priming are often the results of activation of these innate immunity networks. As such, we investigated downstream responses to see how PA23 primes the host plant on a systemic level. The SAR GO term was enriched in all treatment groups, including treatment with PA23 alone (Figure 3.3B). Analysis of RNA-seq data for genes

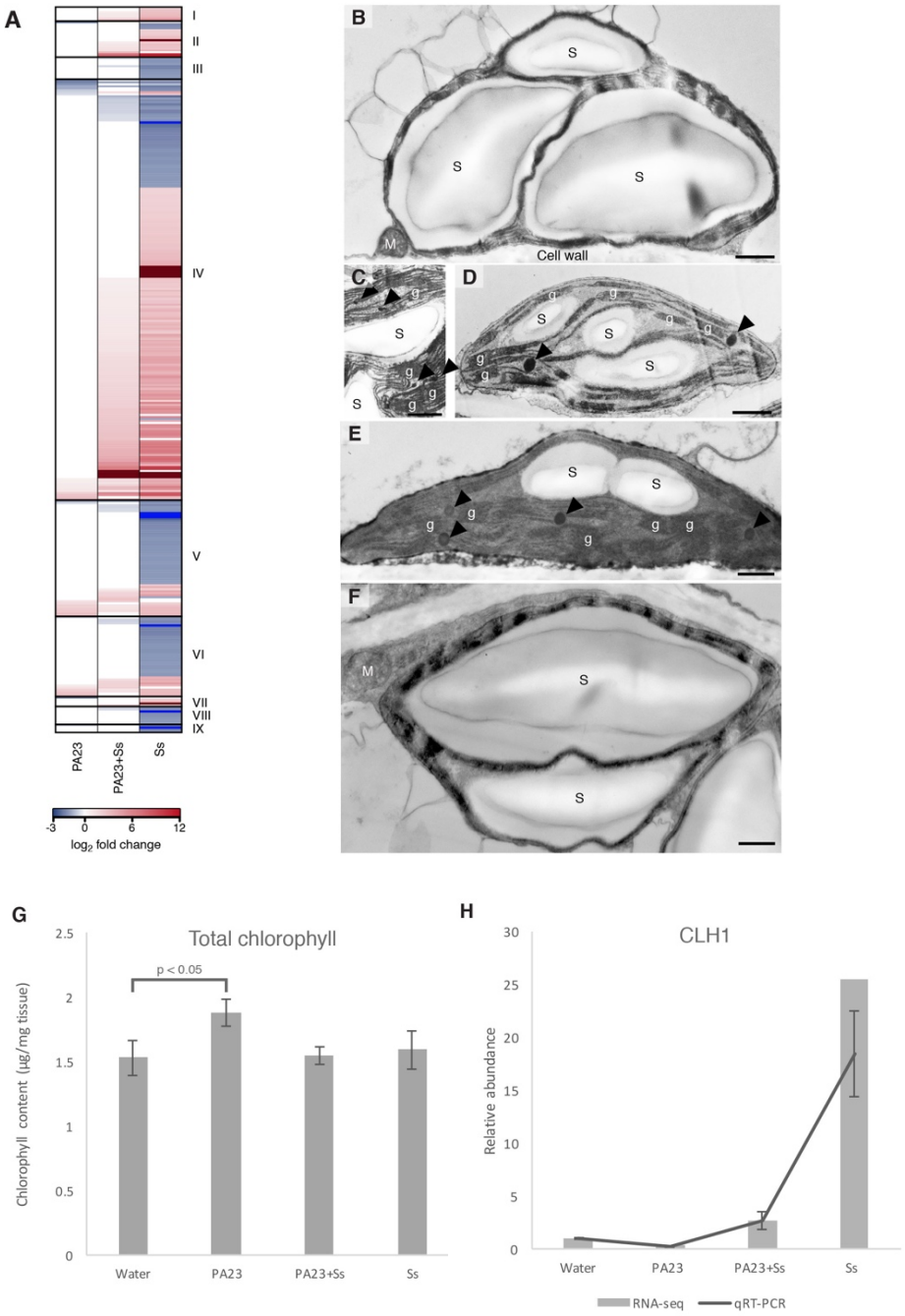

Figure 3.6. A. Differential expression of genes associated with chloroplast-related GO terms, compared to the water control. Only genes with a $\log_2$ fold change greater than 2 in at least one treatment group are shown. I, chlorophyll catabolite transmembrane transport; II, chloroplast inner membrane; III, chloroplast photosystem I & II; IV, chloroplast stroma; V, chloroplast thylakoid; VI, plastoglobule; VII, protein import into chloroplast stroma; VIII, thylakoid lumen; IX, thylakoid membrane. B-F. Transmission electron micrographs of leaf chloroplasts. B. Water control, 48hrs. C. PA23, 24 hrs. D. PA23, 48 hrs. E. PA23+Ss, 24 hrs. F. Ss, 48 hrs. S=starch granule; g=grana stack; M=mitochondria. Arrows indicate plastoglobules. Scale bar for panels A-E = 500nm. G. Chlorophyll b content of treated leaves. H. Relative abundance of the chlorophyllase 1 transcript as determined by RNA-seq (grey bars) and qRT-PCR (black line).

associated with this GO term revealed genes upregulated in the PA23 only group but downregulated in PA23+Ss and Ss groups (Figure 3.7B subgroup 1). We also observed genes induced only by *S. sclerotiorum* (Figure 3.7B subgroup 2), and genes whose expression was altered in all treatment groups compared to the water control (Figure 3.7B subgroup 3). Subgroup 1 consists of *DIR1*, *CPR5* and *ACP4*, indicating that these genes are involved in PA23-induced SAR. *S. sclerotiorum* but not PA23 was associated with the expression of many SAR genes including *ALD1*, *GLIP1*, *PR4* and *DOX1*. The genes *MES9*, *PR1*, *PR2* and *CHI* were upregulated in all treatment groups, although expression was higher in plants where *S. sclerotiorum* was present. The same trend could be observed for the downregulation of *CPN60B1*. Expression levels for several of the genes discussed (*ALD1*, *CHI*, *DOX1*, *FMO1*, *PR1*, and *PR4*) were confirmed using qRT-PCR (Figure 3.8).

4. DISCUSSION

Many nonpathogenic rhizobacteria are able to prime plants systemically for an enhanced defense response against pathogens via ISR or SAR (see van Loon *et al*., 1998; Van Wees *et al*., 2008; Pieterse *et al*., 2014 for reviews). However, only a few of these nonpathogenic microorganisms have been shown to directly antagonize pathogens, especially when applied to the plant phyllosphere (Kurkcuoglu et al. 2006). We demonstrate that in addition to direct antagonism of *S. sclerotiorum* modulating disease progression, PA23 protects *B. napus* through priming of host defense systems.

Patterns of gene expression revealed by RNA-seq showed only mild changes in plants treated with PA23 alone, in contrast to those treated with *S. sclerotiorum*. This was reflected in both clustering analysis and in the number of DEGs among groups (Figures 4A, 5A, 5C). Given the majority of DEGs in the PA23+Ss group were shared with the Ss group, we hypothesize that *S. sclerotiorum* triggers many of the same defense mechanisms in *B. napus* regardless of PA23. This could be due to antibiosis by PA23 occurring on the leaf surface, resulting in decreased *S. sclerotiorum* infection. PA23 may also attenuate defense responses to *S. sclerotiorum* via host detection of PA23 effectors as well as *S. sclerotiorum* virulence factors.

The first plant response to environmental stressors is the induction of innate immune responses. Genes associated with PAMP/MAMP- and DAMP-triggered immunity networks were activated in response to *S. sclerotiorum*, but not PA23 (Figure 3.7A). In the PA23-only group, *FLS2* downregulation is consistent with studies showing that FLS2 is degraded after initial ligand binding to prevent continuous stimulation (Smith et al. 2014). Therefore, it is logical to conclude that detection of PA23 flagellin by the FLS2 receptor complex contributes to downstream induced defense mechanisms. A similar mechanism may be responsible for the

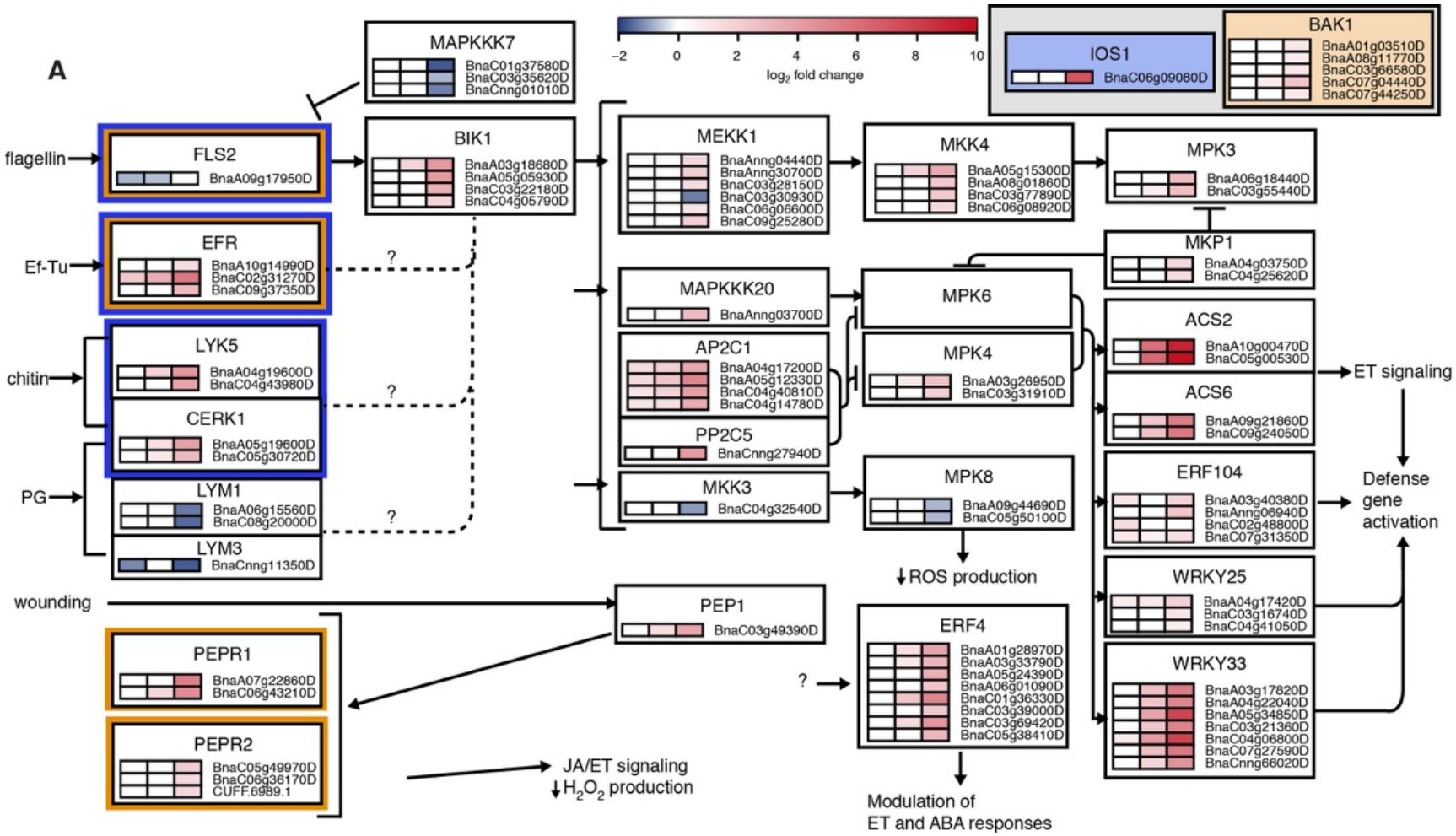
A
MAPKKK7
BnaC01g37580D
BnaC03g35620D
BnaCnng01010D
−2 0 2 4 6 8 10
log2 fold change
IOS1
BnaC06g09080D
BAK1
BnaA01g03510D
BnaA08g11770D
BnaC03g66580D
BnaC07g04440D
BnaC07g44250D
flagellin
FLS2
BnaA09g17950D
BIK1
BnaA03g18680D
BnaA05g05930D
BnaC03g22180D
BnaC04g05790D
MEKK1
BnaAnng04440D
BnaAnng30700D
BnaC03g28150D
BnaC03g30930D
BnaC06g06600D
BnaC09g25280D
MKK4
BnaA05g15300D
BnaA08g01860D
BnaC03g77890D
BnaC06g08920D
MPK3
BnaA06g18440D
BnaC03g55440D
MKP1
BnaA04g03750D
BnaC04g25620D
Ef-Tu
EFR
BnaA10g14990D
BnaC02g31270D
BnaC09g37350D
?
MAPKKK20
BnaAnng03700D
MPK6
chitin
LYK5
BnaA04g19600D
BnaC04g43980D
CERK1
BnaA05g19600D
BnaC05g30720D
?
AP2C1
BnaA04g17200D
BnaA05g12330D
BnaC04g40810D
BnaC04g14780D
MPK4
BnaA03g26950D
BnaC03g31910D
PP2C5
BnaCnng27940D
ACS2
BnaA10g00470D
BnaC05g00530D
ACS6
BnaA09g21860D
BnaC09g24050D
ET signaling
PG
LYM1
BnaA06g15560D
BnaC08g20000D
LYM3
BnaCnng11350D
?
MKK3
BnaC04g32540D
MPK8
BnaA09g44690D
BnaC05g50100D
ERF104
BnaA03g40380D
BnaAnng06940D
BnaC02g48800D
BnaC07g31350D
Defense gene activation
↓ROS production
WRKY25
BnaA04g17420D
BnaC03g16740D
BnaC04g41050D
wounding
PEP1
BnaC03g49390D
ERF4
BnaA01g28970D
BnaA03g33790D
BnaA05g24390D
BnaA06g01090D
BnaC01g36330D
BnaC03g39000D
BnaC03g69420D
BnaC05g38410D
?
WRKY33
BnaA03g17820D
BnaA04g22040D
BnaA05g34850D
BnaC03g21360D
BnaC04g06800D
BnaC07g27590D
BnaCnng66020D
PEPR1
BnaA07g22860D
BnaC06g43210D
PEPR2
BnaC05g49970D
BnaC06g36170D
CUFF.6989.1
JA/ET signaling
↓H2O2 production
Modulation of
ET and ABA responses

B

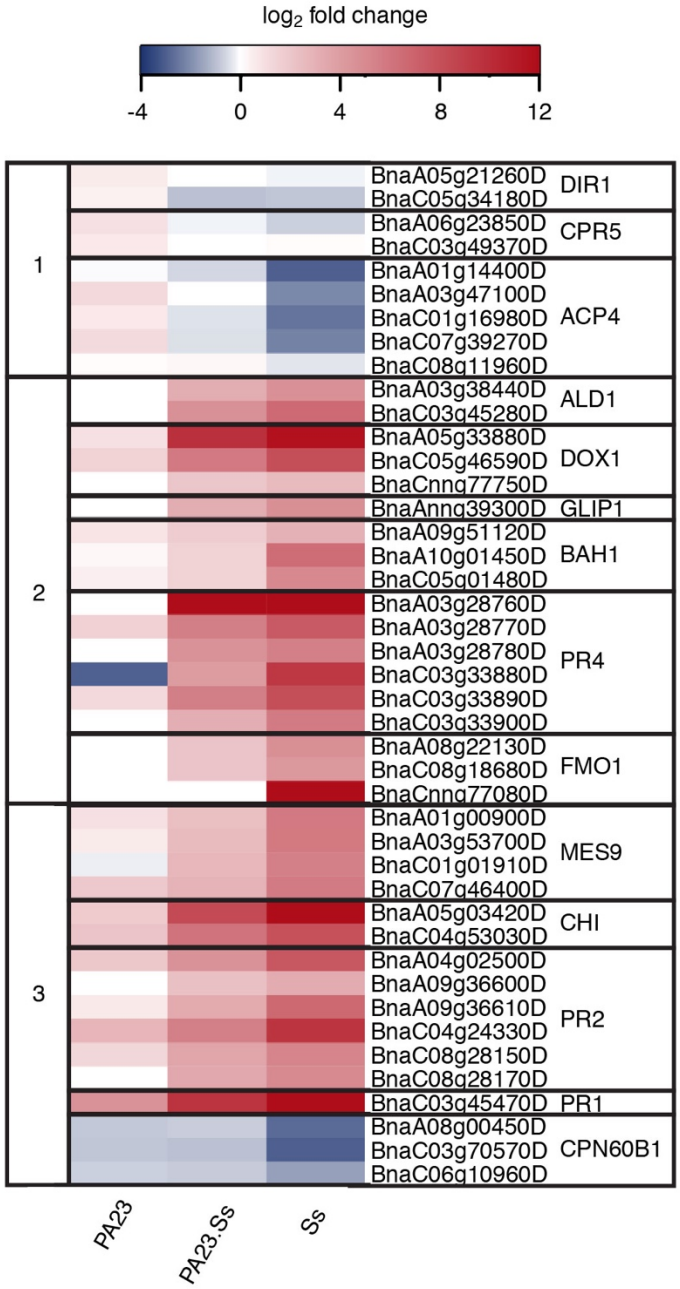

Figure 3.7. A. Differentially expressed genes involved in innate immunity mapped to known interactions. Expression for each homolog is represented as a heatmap value for each treatment group, from left to right: PA23, PA23+Ss, Ss. Transcript abundance is measured in log2 fold change. Orange and blue borders represent receptors which bind to BAK1 and IOS1 when activated, respectfully. B. Comparison of transcript abundance of select SAR-associated genes as determined by RNA-seq. Transcript abundance is measured in log2 fold change. The leftmost column groups genes by expression pattern.

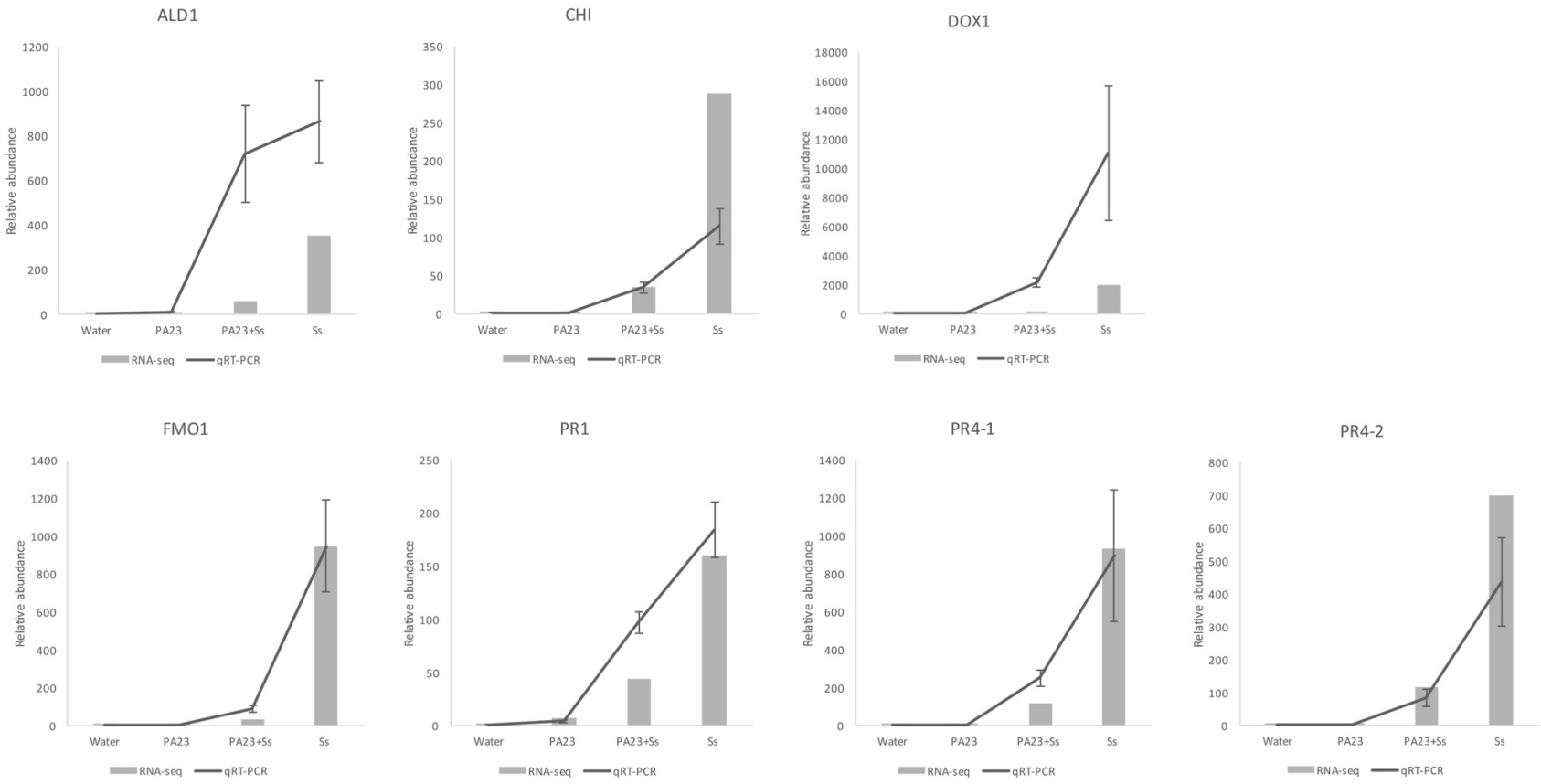

Figure 3.8. Relative abundance of select SAR-related gene transcripts as determined by RNA-seq (grey bars) and qRT-PCR (black line).

downregulation of *LYM3*. Willmann *et al*. (2011) found that in Arabidopsis, infection with virulent *P. syringae* pv. *tomato* DC3000 lead to strong downregulation of *LYM3* and *FLS2* (~0.1-fold expression) and milder downregulation of *LYM1* (~0.4-fold expression). *LYM1* expression is unchanged in response to PA23. Differences in *LYM1* and *LYM3* expression may indicate receptor specificity, as these two proteins are not functionally redundant (Willmann et al. 2011). The role that these receptors play in the activation of systemic resistance appears to be quite variable. Application of enteric bacteria to the leaves of Arabidopsis induced systemic defense responses, and flagellin was determined to play a significant role (Seo and Matthews 2012). In the rhizosphere, purified flagellin from nonpathogenic *Pseudomonas putida* WCS358 induced ISR in Arabidopsis but not in bean or tomato (Meziane et al. 2005). *Pseudomonas fluorescens* SS101 induced systemic resistance in Arabidopsis *fls2* mutants, indicating that this receptor was not required for priming (van de Mortel et al. 2012). Thus, further work is required to determine the roles of these receptors in defense priming in response to PA23. In Ss plants, the enrichment of GO terms such as response to fungus, plant-type hypersensitive response, and stomatal closure support strong activation of PAMP- and effector-triggered immunity (Figure 3.5B, DP1). PA23 thus induced a comparatively mild innate immune response, likely via detection of flagellin and peptidoglycan by receptor complexes at the plant cell surface.

As a downstream marker of innate immune responses, ROS can function as part of a localized hypersensitive-type response to invading pathogens, and also as signaling molecules for the onset of a systemic response (Sewelam et al. 2013). Thus, we were interested to see if the presence of PA23 on the leaf surface could cause production of ROS, or whether it could modulate ROS levels in response to the pathogen. In plants treated with PA23 alone, ROS production involving low levels of H_2O_2 only was observed (Figure 3.4). This is significant in a

priming context, as vitamin-dependent defense induction is associated with H_2O_2-dependent priming of defense genes and callose deposition as well as H_2O_2 accumulation (Pastor et al. 2013). In contrast, low levels of both H_2O_2 and O_2^- were present in PA23+Ss leaves, indicating that *S. sclerotiorum* induces an oxidative stress response involving both of these ROS types.

All plants treated with combinations of PA23 and *S. sclerotiorum* overexpressed ferretins *FER1* and *FER3*, which have been shown to be upregulated in response to viral and fungal attacks as well as bacterial infection (Deák et al. 1999; Dellagi et al. 2005). The main virulence factor of *S. sclerotiorum*, oxalic acid, induces ferretin expression in soybean (Calla et al. 2014). Ferretins buffer iron, as high levels of free iron not only increase ROS production, but also encourage the growth of potentially threatening microorganisms (Briat et al. 2010). In Arabidopsis, infection by the pathogenic bacterium *Erwinia chrysanthemi* caused plant ferretins to accumulate as a basal defense mechanism and occurred mainly in response to bacterial siderophores (Dellagi et al. 2005). It is therefore reasonable to hypothesize that ferretin synthesis in *B. napus* is induced by PA23 siderophores, which initiate an oxidative stress response followed by lower levels of free iron and ROS once ferretins are produced. This, in turn, functions to prime plant basal defenses which reduces ROS production upon subsequent *S. sclerotiorum* challenge.

We identified several other genes associated with the response to ROS GO term which are upregulated either in all treatment groups (PA23, PA23+Ss, Ss), or only in those treated with *S. sclerotiorum* (Ss and PA23+Ss). *HSFA4A* is thought to both regulate plant responses to oxidative stress and function as an antiapoptotic factor (Pérez-Salamó et al. 2014). Upregulation in PA23 groups suggests that PA23 treatment alone can induce an oxidative stress response in the plant resulting in ROS production. However, this response is likely mild in nature, as only two of the

four upregulated HSFA4A homologs accumulated in response to PA23, and only mild H_2O_2 production was observed in the PA23 treatment group. In addition, HSFA4A-induced *ASCORBATE PEROXIDASE 1* (*APX1*) was only upregulated in *S. sclerotiorum*-treated plants, and is required for H_2O_2 scavenging and the prevention of protein oxidation during oxidative stress (Davletova et al. 2005). It is likely, therefore, that H_2O_2 production is occurring in these two groups at levels that disrupt the normal balance of ROS metabolism. Similarly, expression of *ETHYLENE RESPONSE FACTOR 6* (*ERF6*) and *XANTHINE DEHYDROGENASE 1* (*XDH1*) were upregulated in these groups only. ERF6 modulates the expression of antioxidant enzymes to control ROS production and XDH1 is thought to be a source of O_2^- production (Zarepour et al. 2010; Sewelam et al. 2013). This correlates with O_2^- staining patterns seen in plants treated with PA23+Ss but not seen in the PA23 only treatment group (Figure 3.4F and J). An important difference in PA23+Ss and Ss groups is enrichment of the positive regulation of superoxide dismutase activity GO term in DP5, which suggests enhanced management of O_2^- molecules in PA23+Ss (Figure 3.5A and B). Taken together, this data indicates ROS production in PA23-treated leaves was limited to mild oxidative stress and ferretin synthesis, a likely outcome of a mild induction of innate immunity upstream. This mild response also supports a role for ROS in the priming of plant basal defenses and initiation of long-distance signaling consistent with downstream SAR gene induction in response to PA23. Pretreatment with PA23 limits ROS production in response to *S. sclerotiorum*, and is likely due to a combination of direct antagonism of the fungus by PA23 and increased capacity to maintain ROS homeostasis during oxidative stress.

Enrichment of GO terms related to cell wall development in the PA23+Ss group included the overexpression of thirteen xyloglucan endotransglycosylases which function to build up the

cell wall during cell growth (Xu et al. 1996). Three homologs of *LIPID TRANSFER PROTEIN 2* (*LTP2*) were also upregulated. Although these may be involved in the deposition of cutin or wax in the extracellular matrix, LTP2 overexpression conferred increased tolerance to bacterial pathogens in tobacco (Molina and Garcia-Olmedo 1997). As these genes were only upregulated in PA23+Ss, we hypothesize them to be the result of a heightened defense response to *S. sclerotiorum* primed by PA23 pretreatment.

Unlike the innate immune response networks, we identified genes involved in SAR which were upregulated in the PA23 group but downregulated in the Ss groups. Expression of *DIR1*, *CPR5*, and *ACP4* was increased, which indicates a strong connection to SAR induction via glycerol-3-phosphate (G3P). G3P is one of several inducer molecules of SAR, and also a precursor for the synthesis of membrane and storage lipids (Venugopal et al. 2009; Shah and Zeier 2013). DIR1 is a lipid transfer protein required for G3P accumulation and G3P-induced SAR (Yu et al. 2013). DIR1 binds to EARLI1, a paralog of AZI1 which is required for SAR and is also upregulated in PA23-treated plants (Table 3.1) (Cecchini et al. 2015). *ACP4* expression patterns also support this hypothesis, as ACP4 knockout plants have impaired 3GP biosynthesis, and ACP4 is required for chloroplast photosynthetic membrane development (Branen et al. 2003; Xia et al. 2009). While CPR5 is thought to have a role in inducing SAR, its exact function has not been defined. Notwithstanding, CPR5 has been linked to a regulatory role in cell death and proliferation, which supports the hypothesis that PA23 promotes plant growth, as it is known that *S. sclerotiorum* infection results in cell death (Bowling et al. 1997; Kirik et al. 2001). There appears to therefore be a strong link between increased lipid biosynthesis supporting plant growth and a priming of defenses using SAR via G3P molecules in PA23-treated plants.

We discovered that the genes induced in *S. sclerotiorum*-treated plants only participate in

SAR networks which use the signaling metabolites pipecolic acid (Pip) and azelaic acid (Aza), associated with amplification of SAR (Shah and Zeier 2013). ALD1 is required for Pip biosynthesis and Aza-induced SAR, while FMO1 is required for SAR and systemic salicylic acid (SA) accumulation, and is thought to be required for the Pip signal amplification pathway (Mishina and Zeier 2006; Návarová et al. 2012; Shah and Zeier 2013). DOX1 likely functions in the synthesis of Aza from fatty acids (Vicente et al. 2012; Shah and Zeier 2013). In addition to Pip and Aza-mediated amplification, the fungal growth inhibitor genes *PR4* and *GLIP1* were induced in *S. sclerotinia*-treated plants (Oh et al. 2005; Bertini et al. 2012), as well as a regulator of SA accumulation, BAH1, whose exact function in SAR is unknown (Yaeno and Iba 2008). We conclude that in response to *S. sclerotiorum*, and PA23, *B. napus* is able to tailor specific SAR-related defense responses. In particular, PA23 elicits defense priming and promotes lipid metabolism.

S. sclerotiorum caused tissue damage to chloroplasts and elicited an oxidative stress response. Reduction in photosynthetic activity is not due to changes in chloroplast physiology but fewer intact chloroplasts (Seay et al. 2009; Kabbage et al. 2013). Damage releasing chlorophylls from the thylakoid membranes induces *CHLOROPHYLLASE 1* (*CLH1*) expression for quick degradation of these photoactive molecules, a process shown to be induced by necrotrophic pathogens (Takamiya et al. 2000; Kariola et al. 2005). In contrast, we observed an increase in relative area dedicated to thylakoid structures in chloroplasts within PA23-treated plants coupled with an increase in total chlorophyll content and repression of *CLH1*. In other studies, BCA application has been associated with increased chlorophyll in the plant host (Solanki et al. 2015; Kumar et al. 2016; Zhang et al. 2016). Repression of *CLH1* in the PA23-only treatment group is also consistent with evidence showing that *CLH1* is exclusively induced

after cellular collapse, which is a defense response not elicited by nonpathogenic organisms (Hu et al. 2015). Detection of more plastoglobules in the chloroplasts of PA23-treated plants suggests increased lipid metabolism, likely for the synthesis of lipid signaling molecules and for the remodeling of thylakoid membranes (Rottet et al. 2015). These gene expression patterns together with observed morphological changes in the chloroplasts of PA23-treated leaves correlate to the activation of SAR- and auxin-modulated genes discussed.

In summary, we provide a global overview of changes in the *B. napus* transcriptome in response to a BCA, *P. chloropraphis* PA23, and a necrotrophic fungal pathogen, *S. sclerotiorum*. In the presence of PA23, a comparatively mild activation of plant innate-immune pathways involving ROS signaling molecules and induction of specific branches of SAR pathways is observed. The chloroplast plays a key role in all of these observed changes via influencing ROS production, increasing thylakoid membrane structures through lipid metabolic changes and the induction of a specific SAR response centered around a G3P-mediated pathway. Thus, application of PA23 protects canola from *S. sclerotiorum* infection not only through antibiosis-mediated pathogen suppression on the plant surface, but also by modulating host defense responses and activating defense priming mechanisms.

5. CONCLUSIONS AND FUTURE DIRECTIONS

The objective of the current study was to elucidate the effects of the biocontrol agent *P. chlororaphis* PA23 on *B. napus* in the presence and absence of the pathogen *S. sclerotiorum*. Global gene expression patterns revealed by RNA-seq supported a role for PA23 in the expression of host defense mechanisms and the promotion of plant growth. When present alongside *S. sclerotiorum*, the main mode of PA23-mediated disease mitigation occurred through direct antibiosis. However, PA23 treatment was also associated with reduced host activation of apoptosis-inducing defense pathways in response to *S. sclerotiorum,* and enhanced physiological responses such as reinforcement of the leaf cell wall. In response to PA23 alone, a comparatively mild activation of plant innate-immune pathways involving ROS signaling molecules and induction of specific branches of SAR pathways was observed. The chloroplast played a key role in these changes by influencing ROS production, increasing thylakoid membrane structures through lipid metabolic changes and by inducing a specific SAR response centered around a G3P-mediated pathway.

As a necrotrophic pathogen, *S. sclerotiorum* infection involves the release of a barrage of enzymes which aid in penetrating and killing host cells. The main pathogenicity factor, oxalic acid, plays a key role in manipulating host ROS production by suppressing plant defenses and encouraging cell death (Williams et al. 2011). Pretreatment with PA23 limited production of both H_2O_2 and O_2^- compared to leaves exposed to the fungus only. Although this could be due to PA23-mediated fungal antagonism, we also saw enrichment of the superoxide dismutase activity GO term in this group. These findings suggest that PA23 aids the host plant in maintaining ROS homeostasis during *S. sclerotiorum* attack. Furthermore, we observed increased expression of genes involved in cell wall remodeling. Thus, we can conclude that PA23 primes plant defenses

by quickening responses to both oxidative stress and the presence of lytic enzymes on the plant cell surface.

Defense signaling in plants is complex and includes innate immunity triggered by surface detection of MAMPs, PAMPs, DAMPs and effector molecules. This is often followed by systemic defense priming in the form of SAR and/or ISR. Defenses primed by PA23 are thought to occur via cell-surface receptors detecting PA23 MAMPs including flagellin and peptidoglycan. This conclusion was drawn based on the downregulation of receptors for these specific molecules, which is thought to occur to prevent overstimulation of the host defense response. However, because of the timing of tissue collection, we were unable to observe augmented expression among these gene networks. In the future, tissues should be collected at earlier time points, for example within the first few hours of exposure to PA23. Such samples should capture gene activity reflecting surface receptor recognition of bacterial molecules triggering innate immunity pathways. A time course experiment to monitor the expression patterns of key genes in this network may reveal the type of downstream defenses that are activated in response to PA23. Additionally, the use of PA23 mutants deficient in quorum sensing or secondary metabolite production may reveal compound-specific signaling patterns.

In this study, we have shown that both PA23 and *S. sclerotiorum* locally induce genes involved in the activation of systemic resistance pathways. In future studies directed at verifying the systemic nature of these responses, resistance induced by PA23 could be tracked by comparing gene expression in other areas of the plant. Distal induction of the marker gene PR1, a well-known indicator of SAR, would be an important validator of systemic resistance activation. This, again would benefit from a time course analysis of key genes involved in systemic resistance. A variety of messenger molecules can be used by the plant to signal SAR distally, and

PA23 appears to use a G3P-mediated pathway. We could further elucidate the specific networks activated via gene expression analyses or the detection of messenger molecules in the phloem exudates of distal tissues.

Foliar application of PA23 was used for the purposes of this study because this is the application method of choice to prevent *S. sclerotiorum* infection in the field. However, as a soil-borne organism, PA23 may affect the host plant differently when present in the rhizosphere. Plant growth-promoting rhizobacteria (PGPR) have been implicated in plant growth promotion, defense priming and soil pathogen antagonism (van Loon et al. 1998). Some of these PGPR are endophytic and live symbiotically within plant roots, while others live freely in soil surrounding the roots. Metabolites excreted by these PGPR can deter plant pathogens or encourage plant hormone production and micronutrient uptake (Van Loon 2007). Currently, preliminary studies are underway using PA23 to treat *B. napus* using seed and root dips or soil irrigation. While these methods are not expected to suppress *S. sclerotiorum* directly, they may be beneficial treatments to establish defense priming at early stages of plant life.

BCAs exist naturally as part of a larger microbial community, and some combinations of species function synergistically to antagonize pathogens. Such synergism results when the bacteria use different mechanisms of antagonism (Ramamoorthy et al. 2001). While the present study focused on biocontrol and defense priming by PA23 in isolation, it would be beneficial to try combinations of BCAs to prime plants. *Pseudomonas brassicacearum* strain DF41 is a rhizobacterium which also shows antagonistic activity towards *S. sclerotiorum* (Savchuk and Fernando 2004). PA23 and DF41 excrete some of the same antagonistic compounds, such as the volatile hydrogen cyanide and protease (Poritsanos et al. 2006; Berry et al. 2010). However, PA23 mainly inhibits *S. sclerotiorum* through pyrrolnitrin, whereas DF41 mediates pathogen

suppression through the novel lipopeptide sclerosin (Selin et al. 2010; Berry et al. 2012). In greenhouse assays, DF41 was also effective at protecting *B*. *napus* from *S*. *sclerotiorum* (Berry et al. 2010). The effects of DF41 on *B*. *napus* global gene expression patterns have not been elucidated, and in combination these bacteria may enhance the plant defense response over and above that of a single species application.

Transcriptomic analysis has provided us with global view of how gene expression patterns change in response to PA23 and *S*. *sclerotiorum*. These changes are not necessarily reflective of the cellular proteome, however. For example in Arabidopsis, the priming of plant defenses has been associated with the accumulation of mRNA encoding the mitogen-activated protein kinases 3 and 6 (Beckers et al. 2009). Because defense priming allows the host organism to respond more quickly to subsequent threats, the accumulation of defense-related transcripts is an excellent indicator of priming. A proteomic analysis following PA23 treatment may not elucidate priming mechanisms, but it could be a useful tool in the analysis of priming activation by subsequent pathogen exposure.

Another consequence of defense priming not examined in this study involves epigenetic changes. Chromatin remodeling and DNA methylation are a form of defense priming which can be transferred to future generations (Pastor et al. 2013). For example, SAR has been shown to be transferred between generations in Arabidopsis (Luna et al. 2012). This could be verified in our experimental model by checking levels of disease resistance in future generations of plants exposed to PA23.

With this study, we have gained a better understanding of how PA23 affects *B*. *napus* gene expression when applied to the phyllosphere. Future studies will shed more light on the precise local and systemic defense networks induced by this BCA. At this time, many of the

interactions and the crosstalk occurring between components of these networks are not known. The identification of key components of the plant immune response responding to PA23 will provide a more complete picture of this BCA's role in the *B. napus – S. sclerotiorum* pathosystem.

REFERENCES

Adams PB. 1979. Ecology of *Sclerotinia* species. Phytopathology 69(8):896.

Agriculture and Agri-Food Canada. 2016. Status report for biopesticide projects and submissions: Pesticide risk reduction program.

Allender CJ, King GJ. 2010. Origins of the amphiploid species *Brassica napus* L. investigated by chloroplast and nuclear molecular markers. BMC Plant Biol. 10:54.

Altschul SF, Gish W, Miller W, Myers EW, Lipman DJ. 1990. Basic local alignment search tool. J. Mol. Biol. 215(3):403–10.

Amselem J, Cuomo CA, van Kan JAL, Viaud M, Benito EP, Couloux A, Coutinho PM, de Vries RP, Dyer PS, Fillinger S, et al. 2011. Genomic analysis of the necrotrophic fungal pathogens *Sclerotinia sclerotiorum* and *Botrytis cinerea*. PLoS Genet. 7(8):e1002230.

Arnon DI. 1949. Copper enzymes in isolated chloroplasts. Polyphenoloxidase in *Beta vulgaris*. Plant Physiol. 24(1):1–15.

Atkinson NJ, Urwin PE. 2012. The interaction of plant biotic and abiotic stresses: from genes to the field. J. Exp. Bot. 63(10):3523–43.

Baker KF. 1987. Evolving concepts of biological control of plant pathogens. Annu. Rev. Phytopathol. 25(1):67–85.

Baset Mia MA, Shamsuddin ZH, Wahab Z, Marziah M. 2010. Effect of plant growth promoting rhizobacterial (PGPR) inoculation on growth and nitrogen incorporation of tissue-cultured Musa plantlets under nitrogen-free hydroponics condition. AJCS 4(2):85–90.

Bashi ZD, Rimmer SR, Khachatourians GG, Hegedus DD. 2012. Factors governing the regulation of *Sclerotinia sclerotiorum* cutinase A and polygalacturonase 1 during different stages of infection. Can. J. Microbiol. 58(5):605–16.

Beckers GJM, Jaskiewicz M, Liu Y, Underwood WR, He SY, Zhang S, Conrath U. 2009. Mitogen-activated protein kinases 3 and 6 are required for full priming of stress responses in *Arabidopsis thaliana*. Plant Cell 21(3):944–53.

Belmonte MF, Kirkbride RC, Stone SL, Pelletier JM, Bui AQ, Yeung EC, Hashimoto M, Fei J, Harada CM, Munoz MD, et al. 2013. Comprehensive developmental profiles of gene activity in regions and subregions of the Arabidopsis seed. Proc. Natl. Acad. Sci. U. S. A. 110(5):E435–44.

Berry C, Fernando WGD, Loewen PC, de Kievit TR. 2010. Lipopeptides are essential for *Pseudomonas* sp. DF41 biocontrol of *Sclerotinia sclerotiorum*. Biol. Control 55(3):211–218.

Berry CL, Brassinga AKC, Donald LJ, Fernando WGD, Loewen PC, de Kievit TR. 2012. Chemical and biological characterization of sclerosin, an antifungal lipopeptide. Can. J. Microbiol. 58(8):1027–34.

Bertini L, Proietti S, Aleandri MP, Mondello F, Sandini S, Caporale C, Caruso C. 2012. Modular structure of HEL protein from Arabidopsis reveals new potential functions for PR-4 proteins. Biol. Chem. 393(12):1533–46.

Bhattacharyya PN, Jha DK. 2012. Plant growth-promoting rhizobacteria (PGPR): emergence in agriculture. World J. Microbiol. Biotechnol. 28(4):1327–1350.

Block A, Alfano JR. 2011. Plant targets for *Pseudomonas syringae* type III effectors: virulence targets or guarded decoys? Curr. Opin. Microbiol. 14(1):39–46.

Boland GJ, Hall R. 1994. Index of plant hosts of *Sclerotinia sclerotiorum*. Can. J. Plant Pathol. 16(2):93–108.

Bolger AM, Lohse M, Usadel B. 2014. Trimmomatic: a flexible trimmer for Illumina sequence data. Bioinformatics 30(15):2114–20.

Bolton MD, Thomma BPHJ, Nelson BD. 2006. *Sclerotinia sclerotiorum* (Lib.) de Bary: biology and molecular traits of a cosmopolitan pathogen. Mol. Plant Pathol. 7(1):1–16.

Boureau T, Routtu J, Roine E, Taira S, Romantschuk M. 2002. Localization of hrpA-induced *Pseudomonas syringae* pv. tomato DC3000 in infected tomato leaves. Mol. Plant Pathol. 3(6):451–460.

Bowling SA, Clarke JD, Liu Y, Klessig DF, Dong X. 1997. The cpr5 mutant of Arabidopsis expresses both NPR1-dependent and NPR1-independent resistance. Plant Cell 9(9):1573–84.

Branen JK, Shintani DK, Engeseth NJ. 2003. Expression of antisense acyl carrier protein-4 reduces lipid content in Arabidopsis leaf tissue. Plant Physiol. 132(2):748–56.

Briat J-F, Ravet K, Arnaud N, Duc C, Boucherez J, Touraine B, Cellier F, Gaymard F. 2010. New insights into ferritin synthesis and function highlight a link between iron homeostasis and oxidative stress in plants. Ann. Bot. 105(5):811–22.

Butler MJ, Gardiner RB, Day AW. 2005. Degradation of melanin or inhibition of its synthesis: Are these a significant approach as a biological control of phytopathogenic fungi? Biol. Control 32(2):326–336.

Cai G, Yang Q, Yi B, Fan C, Edwards D, Batley J, Zhou Y, Adams K, Wendel J, Otto S, et al. 2014. A complex recombination pattern in the genome of allotetraploid *Brassica napus* as revealed by a high-density genetic map. Candela H, editor. PLoS One 9(10):e109910.

Calla B, Blahut-Beatty L, Koziol L, Simmonds DH, Clough SJ. 2014. Transcriptome analyses suggest a disturbance of iron homeostasis in soybean leaves during white mould disease establishment. Mol. Plant Pathol. 15(6):576–88.

Cameron RK, Dixon RA, Lamb CJ. 1994. Biologically induced systemic acquired resistance in *Arabidopsis thaliana*. Plant J. 5(5):715–725.

Cecchini NM, Steffes K, Schläppi MR, Gifford AN, Greenberg JT. 2015. Arabidopsis AZI1 family proteins mediate signal mobilization for systemic defence priming. Nat. Commun. 6:7658.

Chalhoub B, Denoeud F, Liu S, Parkin IAP, Tang H, Wang X, Chiquet J, Belcram H, Tong C, Samans B, et al. 2014. Plant genetics. Early allopolyploid evolution in the post-Neolithic *Brassica napus* oilseed genome. Science 345(6199):950–3.

Chan A, Belmonte MF. 2013. Histological and ultrastructural changes in canola (*Brassica napus*) funicular anatomy during the seed lifecycle. Botany 91(10):671–679.

Chanda B, Xia Y, Mandal MK, Yu K, Sekine K-T, Gao Q, Selote D, Hu Y, Stromberg A, Navarre D, et al. 2011. Glycerol-3-phosphate is a critical mobile inducer of systemic immunity in plants. Nat. Genet. 43(5):421–7.

Chaturvedi R, Venables B, Petros RA, Nalam V, Li M, Wang X, Takemoto LJ, Shah J. 2012. An abietane diterpenoid is a potent activator of systemic acquired resistance. Plant J. 71(1):161–72.

Clarkson JP, Phelps K, Whipps JM, Young CS, Smith J a, Watling M. 2004. Forecasting Sclerotinia disease on lettuce: toward developing a prediction model for carpogenic germination of sclerotia. Phytopathology 94(3):268–279.

Conrath U. 2011. Molecular aspects of defence priming. Trends Plant Sci. 16(10):524–531.
Davletova S, Rizhsky L, Liang H, Shengqiang Z, Oliver DJ, Coutu J, Shulaev V, Schlauch K, Mittler R. 2005. Cytosolic ascorbate peroxidase 1 is a central component of the reactive oxygen gene network of Arabidopsis. Plant Cell 17(1):268–81.

Deák M, Horváth G V, Davletova S, Török K, Sass L, Vass I, Barna B, Király Z, Dudits D. 1999. Plants ectopically expressing the iron-binding protein, ferritin, are tolerant to oxidative damage and pathogens. Nat. Biotechnol. 17(2):192–6.

Dellagi A, Rigault M, Segond D, Roux C, Kraepiel Y, Cellier F, Briat J-F, Gaymard F, Expert D. 2005. Siderophore-mediated upregulation of Arabidopsis ferritin expression in response to Erwinia chrysanthemi infection. Plant J. 43(2):262–72.

Delourme R, Chèvre AM, Brun H, Rouxel T, Balesdent MH, Dias JS, Salisbury P, Renard M, Rimmer SR. 2006. Major Gene and Polygenic Resistance to Leptosphaeria maculans in Oilseed Rape (*Brassica napus*). Eur. J. Plant Pathol. 114(1):41–52.

Derksen H, Rampitsch C, Daayf F. 2013. Signaling cross-talk in plant disease resistance. Plant Sci. 207:79–87.

Durrant WE, Dong X. 2004. Systemic acquired resistance. Annu. Rev. Phytopathol. 42:185–209.
Van der Ent S, Van Hulten M, Pozo MJ, Czechowski T, Udvardi MK, Pieterse CMJ, Ton J. 2009. Priming of plant innate immunity by rhizobacteria and β-aminobutyric acid: differences and similarities in regulation. New Phytol. 183(2):419–431.

Eulgem T, Somssich IE. 2007. Networks of WRKY transcription factors in defense signaling. Curr. Opin. Plant Biol. 10(4):366–371.

Fernando WGD, Nakkeeran S, Zhang Y, Savchuk S. 2007. Biological control of Sclerotinia sclerotiorum (Lib.) de Bary by *Pseudomonas* and *Bacillus* species on canola petals. Crop Prot. 26(2):100–107.

Fitt BDL, Brun H, Barbetti MJ, Rimmer SR. 2006. World-wide importance of phoma stem canker (*Leptosphaeria maculans* and *L. biglobosa*) on oilseed rape (*Brassica napus*). Eur. J. Plant Pathol. 114(1):3–15.

Fravel DR. 2005. Commercialization and implementation of biocontrol. Annu. Rev. Phytopathol. 43:337–59.

Gao Q, Yu K, Xia Y, Shine MB, Wang C, Navarre D, Kachroo A, Kachroo P. 2014. Mono- and digalactosyldiacylglycerol lipids function nonredundantly to regulate systemic acquired resistance in plants.

Gao Q-M, Zhu S, Kachroo P, Kachroo A. 2015. Signal regulators of systemic acquired resistance. Front. Plant Sci. 6(228).

Gururani MA, Venkatesh J, Upadhyaya CP, Nookaraju A, Pandey SK, Park SW. 2012. Plant disease resistance genes: Current status and future directions. Physiol. Mol. Plant Pathol. 78:51–65.

Haas D, Défago G. 2005. Biological control of soil-borne pathogens by fluorescent pseudomonads. Nat. Rev. Microbiol. 3(4):307–319.

Han SH, Lee SJ, Moon JH, Park KH, Yang KY, Cho BH, Kim KY, Kim YW, Lee MC, Anderson AJ, et al. 2006. GacS-dependent production of 2R, 3R-butanediol by *Pseudomonas chlororaphis* O6 is a major determinant for eliciting systemic resistance against *Erwinia carotovora* but not against *Pseudomonas syringae* pv. tabaci in tobacco. Mol. Plant-Microbe Interact. 19(8):924–930.

Harman GE, Howell CR, Viterbo A, Chet I, Lorito M. 2004. *Trichoderma* species — opportunistic, avirulent plant symbionts. Nat. Rev. Microbiol. 2(1):43–56.

Hase S, Takahashi S, Takenaka S, Nakaho K, Arie T, Seo S, Ohashi Y, Takahashi H. 2008. Involvement of jasmonic acid signalling in bacterial wilt disease resistance induced by biocontrol agent *Pythium oligandrum* in tomato. Plant Pathol. 57(5):870–876.

Hématy K, Cherk C, Somerville S. 2009. Host–pathogen warfare at the plant cell wall. Curr. Opin. Plant Biol. 12(4):406–413.

Hu X, Makita S, Schelbert S, Sano S, Ochiai M, Tsuchiya T, Hasegawa SF, Hörtensteiner S, Tanaka A, Tanaka R. 2015. Reexamination of chlorophyllase function implies its involvement in defense against chewing herbivores. Plant Physiol. 167(3):660–70.

Huang HC, Erickson RS. 2008. Factors affecting biological control of *Sclerotinia sclerotiorum* by fungal antagonists. J. Phytopathol. 156(10):628–634.

Huang L, Buchenauer H, Han Q, Zhang X, Kang Z. 2008. Ultrastructural and cytochemical studies on the infection process of *Sclerotinia sclerotiorum* in oilseed rape. J. Plant Dis. Prot. 115(1):9–16.

Iniguez-luy FL, Federico ML. 2011. The genetics of *Brassica napus*. Schmidt R, Bancroft I, editors. New York, NY: Springer New York.

Janvier C, Villeneuve F, Alabouvette C, Edel-Hermann V, Mateille T, Steinberg C. 2007. Soil health through soil disease suppression: Which strategy from descriptors to indicators? Soil Biol. Biochem. 39(1):1–23.

Jones JDG, Dangl JL. 2006. The plant immune system. Nature 444(7117):323–9.

Jousset A, Lara E, Wall LG, Valverde C. 2006. Secondary metabolites help biocontrol strain *Pseudomonas fluorescens* CHA0 to escape protozoan grazing. Appl. Environ. Microbiol. 72(11):7083–90.

Jung HW, Tschaplinski TJ, Wang L, Glazebrook J, Greenberg JT. 2009. Priming in systemic plant immunity. Science 324(5923):89–91.

Kabbage M, Williams B, Dickman MB. 2013. Cell death control: the interplay of apoptosis and autophagy in the pathogenicity of *Sclerotinia sclerotiorum*. PLoS Pathog. 9(4):e1003287.

Kariola T, Brader G, Li J, Palva ET. 2005. Chlorophyllase 1, a damage control enzyme, affects the balance between defense pathways in plants. Plant Cell 17(1):282–94.

Kirik V, Bouyer D, Schöbinger U, Bechtold N, Herzog M, Bonneville J-M, Hülskamp M. 2001. CPR5 is involved in cell proliferation and cell death control and encodes a novel transmembrane protein. Curr. Biol. 11(23):1891–1895.

Kotchoni SO, Gachomo EW. 2006. The reactive oxygen species network pathways: an essential prerequisite for perception of pathogen attack and the acquired disease resistance in plants. J. Biosci. 31(3):389–404.

Kraska T, Schönbeck F. 1993. About changes in the chromatin structure after resistance induction in *Hordeum vulgare* L. J. Phytopathol. 137(1):10–14.

Kumar AS, Lakshmanan V, Caplan JL, Powell D, Czymmek KJ, Levia DF, Bais HP. 2012. Rhizobacteria *Bacillus subtilis* restricts foliar pathogen entry through stomata. Plant J. 72(4):694–706.

Kumar R, Ichihashi Y, Kimura S, Chitwood DH, Headland LR, Peng J, Maloof JN, Sinha NR. 2012. A high-throughput method for Illumina RNA-Seq library preparation. Front. Plant Sci. 3:202.

Kumar S, Chauhan PS, Agrawal L, Raj R, Srivastava A, Gupta S, Mishra SK, Yadav S, Singh PC, Raj SK, et al. 2016. *Paenibacillus lentimorbus* inoculation enhances tobacco growth and extenuates the virulence of Cucumber mosaic virus. PLoS One 11(3):e0149980.

Kurkcuoglu S, Degenhardt J, Lensing J, Al-Masri AN, Gau AE. 2006. Identification of differentially expressed genes in *Malus domestica* after application of the non-pathogenic bacterium *Pseudomonas fluorescens* Bk3 to the phyllosphere. J. Exp. Bot. 58(3):733–741.

Kürkcüoglu S, Piotrowski M, Gau AE. 2004. Up-regulation of pathogenesis-related proteins in the apoplast of *Malus domestica* after application of a non-pathogenic bacterium. Z. Naturforsch. C. 59(11-12):843–848.

Laluk K, Mengiste T. 2010. Necrotroph attacks on plants: wanton destruction or covert extortion? Arabidopsis Book 8:e0136.

Lenin G, Jayanthi M. 2012. Efficiency of plant growth promoting rhizobacteria (PGPR) on enhancement of growth, yield and nutrient content of *Catharanthus roseus*. Int. J. Res. Pure Appl. Microbiol. 2(4):37–42.

Levine A, Tenhaken R, Dixon R, Lamb C. 1994. H_2O_2 from the oxidative burst orchestrates the plant hypersensitive disease resistance response. Cell 79(4):583–593.

Liu Y, Ren D, Pike S, Pallardy S, Gassmann W, Zhang S. 2007. Chloroplast-generated reactive oxygen species are involved in hypersensitive response-like cell death mediated by a mitogen-activated protein kinase cascade. Plant J. 51(6):941–954.

LMC International. 2013. The economic impact of canola on the Canadian economy.

Van Loon LC. 2007. Plant responses to plant growth-promoting rhizobacteria. Eur. J. Plant Pathol. 119(3):243–254.

van Loon LC, Bakker PAHM. 2005. Induced systemic resistance as a mechanism of disease suppression by rhizobacteria. In: Siddiqui ZA, editor. PGPR: Biocontrol and Biofertilization. Dordrecht. p. 39–66.

van Loon LC, Bakker PAHM, Pieterse CM. 1998. Systemic resistance induced by rhizosphere bacteria. Annu. Rev. Phytopathol. 36:453–83.

Lorenc-Kukula K, Chaturvedi R, Roth M, Welti R, Shah J. 2012. Biochemical and molecular-genetic characterization of SFD1's involvement in lipid metabolism and defense signaling. Front. Plant Sci. 3:26.

Love MI, Huber W, Anders S. 2014. Moderated estimation of fold change and dispersion for RNA-seq data with DESeq2. Genome Biol. 15(12):550.

Lumsden RD. 1979. Histology and physiology of pathogenesis in plant diseases caused by *Sclerotinia* species. Phytopathology 69(8):890.

Luna E, Bruce TJA, Roberts MR, Flors V, Ton J. 2012. Next-generation systemic acquired resistance. Plant Physiol. 158(2):844–53.

Luna E, Pastor V, Robert J, Flors V, Mauch-Mani B, Ton J. 2011. Callose deposition: a multifaceted plant defense response. Mol. Plant. Microbe. Interact. 24(2):183–193.

Malamy J, Carr JP, Klessig DF, Raskin I. 1990. Salicylic acid: a likely endogenous signal in the resistance response of tobacco to viral infection. Science 250(4983):1002–4.

Maldonado AM, Doerner P, Dixon RA, Lamb CJ, Cameron RK. 2002. A putative lipid transfer protein involved in systemic resistance signalling in Arabidopsis. Nature 419(6905):399–403.

Manitoba Agriculture. 2011. Crop Statistical Review: Canola Sector.

Maurhofer M, Hase C, Meuwly P, Métraux J-P, Défago G. 1994. Induction of systemic resistance of tobacco to Tobacco Necrosis Virus by the root-colonizing *Pseudomonas fluorescens* strain CHA0: Influence of the *gacA* gene and of pyoverdine production. Phytopathology 84:139–146.

McLachlan DH, Kopischke M, Robatzek S. 2014. Gate control: guard cell regulation by microbial stress. New Phytol. 203(4):1049–63.

Melotto M, Underwood W, Koczan J, Nomura K, He SY, Abramovitch RB, Martin GB, Alfano JR, Collmer A, Anderson JP, et al. 2006. Plant stomata function in innate immunity against bacterial invasion. Cell 126(5):969–980.

Mengiste T. 2012. Plant immunity to necrotrophs. Annu. Rev. Phytopathol. 50(1):267–294.

Métraux JP, Signer H, Ryals J, Ward E, Wyss-Benz M, Gaudin J, Raschdorf K, Schmid E, Blum W, Inverardi B. 1990. Increase in salicylic acid at the onset of systemic acquired resistance in cucumber. Science 250(4983):1004–6.

Meziane H, Van Der Sluis I, Van Loon LC, Hofte M, Bakker PAHM. 2005. Determinants of *Pseudomonas putida* WCS358 involved in inducing systemic resistance in plants. Mol. Plant Pathol. 6(2):177–185.

Mishina TE, Zeier J. 2006. The Arabidopsis flavin-dependent monooxygenase FMO1 is an essential component of biologically induced systemic acquired resistance. Plant Physiol. 141(4):1666–75.

Mishina TE, Zeier J. 2007. Pathogen-associated molecular pattern recognition rather than development of tissue necrosis contributes to bacterial induction of systemic acquired resistance in Arabidopsis. Plant J. 50(3):500–13.

Molina A, Garcia-Olmedo F. 1997. Enhanced tolerance to bacterial pathogens caused by the transgenic expression of barley lipid transfer protein LTP2. Plant J. 12(3):669–675.

van de Mortel JE, de Vos RCH, Dekkers E, Pineda A, Guillod L, Bouwmeester K, van Loon JJ a, Dicke M, Raaijmakers JM. 2012. Metabolic and transcriptomic changes induced in Arabidopsis by the rhizobacterium *Pseudomonas fluorescens* SS101. Plant Physiol. 160(4):2173–88.

Muthamilarasan M, Prasad M. 2013. Plant innate immunity: An updated insight into defense mechanism. J. Biosci. 38(2):433–449.

Nandi A, Welti R, Shah J. 2004. The Arabidopsis thaliana dihydroxyacetone phosphate reductase gene SUPPRESSSOR OF FATTY ACID DESATURASE DEFICIENCY1 is required for glycerolipid metabolism and for the activation of systemic acquired resistance. Plant Cell 16(2):465–77.

Návarová H, Bernsdorff F, Döring A-C, Zeier J. 2012. Pipecolic acid, an endogenous mediator of defense amplification and priming, is a critical regulator of inducible plant immunity. Plant Cell 24(12):5123–41.

Noctor G, Foyer CH. 1998. Ascorbate and glutathione: Keeping active oxygen under control. Annu. Rev. Plant Physiol. Plant Mol. Biol. 49:249–279.

Oh IS, Park AR, Bae MS, Kwon SJ, Kim YS, Lee JE, Kang NY, Lee S, Cheong H, Park OK. 2005. Secretome analysis reveals an Arabidopsis lipase involved in defense against *Alternaria brassicicola*. Plant Cell 17(10):2832–47.

Pal KK, McSpadden Gardener B. 2006. Biological control of plant pathogens. Plant Heal. Instr.

Pallas JA, Paiva NL, Lamb C, Dixon RA. 1996. Tobacco plants epigenetically suppressed in phenylalanine ammonia-lyase expression do not develop systemic acquired resistance in response to infection by tobacco mosaic virus. Plant J. 10(2):281–293.

Park JY, Oh SA, Anderson AJ, Neiswender J, Kim JC, Kim YC. 2011. Production of the antifungal compounds phenazine and pyrrolnitrin from *Pseudomonas chlororaphis* O6 is differentially regulated by glucose. Lett. Appl. Microbiol. 52(5):532–537.

Park S-W, Kaimoyo E, Kumar D, Mosher S, Klessig DF. 2007. Methyl salicylate is a critical mobile signal for plant systemic acquired resistance. Science 318(5847):113–6.

Parkin IAP, Gulden SM, Sharpe AG, Lukens L, Trick M, Osborn TC, Lydiate DJ. 2005. Segmental structure of the *Brassica napus* genome based on comparative analysis with *Arabidopsis thaliana*. Genetics 171(2):765–81.

Parkin IAP, Sharpe AG, Keith DJ, Lydiate DJ. 1995. Identification of the A and C genomes of amphidiploid *Brassica napus* (oilseed rape). Genome 38(6):1122–1131.

Pastor V, Luna E, Mauch-Mani B, Ton J, Flors V. 2013. Primed plants do not forget. Environ. Exp. Bot. 94:46–56.

Van Peer R, Niemann GJ, Schippers S. 1991. Induced resistance and phytoalexin accumulation in biological control of Fusarium wilt of carnation by *Pseudomonas* sp. Strain WCS417r. Phytopathology 81(7):728–734.

Pérez-Salamó I, Papdi C, Rigó G, Zsigmond L, Vilela B, Lumbreras V, Nagy I, Horváth B, Domoki M, Darula Z, et al. 2014. The heat shock factor A4A confers salt tolerance and is regulated by oxidative stress and the mitogen-activated protein kinases MPK3 and MPK6. Plant Physiol. 165(1):319–34.

Pieterse CM, van Wees SC, Hoffland E, van Pelt J a, van Loon LC. 1996. Systemic resistance in Arabidopsis induced by biocontrol bacteria is independent of salicylic acid accumulation and pathogenesis-related gene expression. Plant Cell 8(8):1225–37.

Pieterse CMJ, Zamioudis C, Berendsen RL, Weller DM, Van Wees SCM, Bakker PAHM. 2014. Induced systemic resistance by beneficial microbes. Annu. Rev. Phytopathol. 52:347–75.

Poritsanos N, Selin C, Fernando WGD, Nakkeeran S, de Kievit TR. 2006. A GacS deficiency does not affect *Pseudomonas chlororaphis* PA23 fitness when growing on canola, in aged batch culture or as a biofilm. Can. J. Microbiol. 52(12):1177–1188.

Porra RJ. 2002. The chequered history of the development and use of simultaneous equations for the accurate determination of chlorophylls a and b. Photosynth. Res. 73(1-3):149–56.

Potlakayala SD, Reed DW, Covello PS, Fobert PR. 2007. Systemic acquired resistance in canola is linked with pathogenesis-related gene expression and requires salicylic acid. Phytopathology 97(7):794–802.

Ramamoorthy V, Viswanathan R, Raguchander T, Prakasam V, Samiyappan R. 2001. Induction of systemic resistance by plant growth promoting rhizobacteria in crop plants against pests and diseases. Crop Prot. 20(1):1–11.

Ramarathnam R, Fernando WGD, Kievit T. 2010. The role of antibiosis and induced systemic resistance, mediated by strains of *Pseudomonas chlororaphis*, *Bacillus cereus* and *B. amyloliquefaciens*, in controlling blackleg disease of canola. BioControl 56(2):225–235.

Rottet S, Besagni C, Kessler F. 2015. The role of plastoglobules in thylakoid lipid remodeling during plant development. Biochim. Biophys. Acta 1847(9):889–99.

Ryals JA, Neuenschwander UH, Willits MG, Molina A, Steiner HY, Hunt MD. 1996. Systemic acquired resistance. Plant Cell 8(10):1809–1819.

Savchuk S. 2002. Evaluation of biological control of Sclerotinia sclerotiorum on canola (*Brassica napus*) in the laboratory, in the greenhouse, and in the field. University of Manitoba.

Savchuk S, Fernando WGD. 2004. Effect of timing of application and population dynamics on the degree of biological control of *Sclerotinia sclerotiorum* by bacterial antagonists. FEMS Microbiol. Ecol. 49(3):379–88.

Seay M, Hayward AP, Tsao J, Dinesh-Kumar SP. 2009. Something old, something new: plant innate immunity and autophagy. Curr. Top. Microbiol. Immunol. 335:287–306.

Selin C, Habibian R, Poritsanos N, Athukorala SNP, Fernando D, de Kievit TR. 2010. Phenazines are not essential for *Pseudomonas chlororaphis* PA23 biocontrol of *Sclerotinia sclerotiorum*, but do play a role in biofilm formation. FEMS Microbiol. Ecol. 71(1):73–83.

Seo S, Matthews KR. 2012. Influence of the plant defense response to *Escherichia coli* O157:H7 cell surface structures on survival of that enteric pathogen on plant surfaces. Appl. Environ. Microbiol. 78(16):5882–9.

Sewelam N, Kazan K, Thomas-Hall SR, Kidd BN, Manners JM, Schenk PM. 2013. Ethylene response factor 6 is a regulator of reactive oxygen species signaling in Arabidopsis. PLoS One 8(8):e70289.

Shah J, Zeier J. 2013. Long-distance communication and signal amplification in systemic acquired resistance. Front. Plant Sci. 4:30.

Sharma P, Jha AB, Dubey RS, Pessarakli M. 2012. Reactive oxygen species, oxidative damage, and antioxidative defense mechanism in plants under stressful conditions. J. Bot. 2012:1–26.

Shoresh M, Harman GE, Mastouri F. 2010. Induced systemic resistance and plant responses to fungal biocontrol agents. Annu. Rev. Phytopathol. 48:21–43.

Smith JM, Salamango DJ, Leslie ME, Collins CA, Heese A. 2014. Sensitivity to Flg22 is modulated by ligand-induced degradation and de novo synthesis of the endogenous flagellin-receptor FLAGELLIN-SENSING2. Plant Physiol. 164(1):440–54.

Solanki MK, Singh RK, Srivastava S, Kumar S, Kashyap PL, Srivastava AK. 2015. Characterization of antagonistic-potential of two *Bacillus* strains and their biocontrol activity against *Rhizoctonia solani* in tomato. J. Basic Microbiol. 55(1):82–90.

Statistics Canada. 2016. Table 001-0017 - Estimated areas, yield, production, average farm price and total farm value of principal field crops, in imperial units.

Takamiya K, Tsuchiya T, Ohta H. 2000. Degradation pathway(s) of chlorophyll: what has gene cloning revealed? Trends Plant Sci. 5(10):426–431.

de Torres Zabala M, Littlejohn G, Jayaraman S, Studholme D, Bailey T, Lawson T, Tillich M, Licht D, Bölter B, Delfino L, et al. 2015. Chloroplasts play a central role in plant defence and are targeted by pathogen effectors. Nat. Plants 1(6):15074.

Trapnell C, Roberts A, Goff L, Pertea G, Kim D, Kelley DR, Pimentel H, Salzberg SL, Rinn JL, Pachter L. 2012. Differential gene and transcript expression analysis of RNA-seq experiments with TopHat and Cufflinks. Nat. Protoc. 7(3):562–78.

Underwood W. 2012. The plant cell wall: a dynamic barrier against pathogen invasion. Front. Plant Sci. 3:85.

Velivelli SLS, De Vos P, Kromann P, Declerck S, Prestwich BD. 2014. Biological control agents: from field to market, problems, and challenges. Trends Biotechnol. 32(10):493–496.

Venugopal SC, Chanda B, Vaillancourt L, Kachroo A, Kachroo P. 2009. The common metabolite glycerol-3-phosphate is a novel regulator of plant defense signaling. Plant Signal. Behav. 4(8):746–9.

Vernooij B, Friedrich L, Morse A, Reist R, Kolditz-Jawhar R, Ward E, Uknes S, Kessmann H, Ryals J. 1994. Salicylic acid is not the translocated signal responsible for inducing systemic acquired resistance but is required in signal transduction. Plant Cell 6(7):959–965.

Vicente J, Cascón T, Vicedo B, García-Agustín P, Hamberg M, Castresana C. 2012. Role of 9-lipoxygenase and α-dioxygenase oxylipin pathways as modulators of local and systemic defense. Mol. Plant 5(4):914–28.

Vinale F, Sivasithamparam K, Ghisalberti EL, Marra R, Woo SL, Lorito M. 2008. Trichoderma–plant–pathogen interactions. Soil Biol. Biochem. 40(1):1–10.

De Vleesschauwer D, Höfte M. 2009. Chapter 6: Rhizobacteria-Induced Systemic Resistance. Adv. Bot. Res. 51:223–281.

Vorholt J. 2012. Microbial life in the phyllosphere. Nature 10:828–840.

Walters DR. 2009. Disease control in crops: Biological and environmentally-friendly approaches. 1st ed. Walters DR, editor. Blackwell Publishing Ltd.

Wang X, Jiang N, Liu J, Liu W, Wang G-L. 2014. The role of effectors and host immunity in plant-necrotrophic fungal interactions. Virulence 5(7):722–32.

Wei G, Kloepper JW, Tuzun S. 1991. Induction of systemic resistance of cucumber to *Colletotrichum orbiculare* by select strains of plant growth-promoting rhizobacteria. Phytopathology 81(12):1508–1512.

Wildermuth MC, Dewdney J, Wu G, Ausubel FM. 2001. Isochorismate synthase is required to synthesize salicylic acid for plant defence. Nature 414(6863):562–565.

Williams B, Kabbage M, Kim H-J, Britt R, Dickman MB. 2011. Tipping the balance: *Sclerotinia sclerotiorum* secreted oxalic acid suppresses host defenses by manipulating the host redox environment. Tyler B, editor. PLoS Pathog. 7(6):e1002107.

Willmann R, Lajunen HM, Erbs G, Newman M-A, Kolb D, Tsuda K, Katagiri F, Fliegmann J, Bono J-J, Cullimore J V, et al. 2011. Arabidopsis lysin-motif proteins LYM1 LYM3 CERK1 mediate bacterial peptidoglycan sensing and immunity to bacterial infection. Proc. Natl. Acad. Sci. U. S. A. 108(49):19824–9.

Wittek F, Hoffmann T, Kanawati B, Bichlmeier M, Knappe C, Wenig M, Schmitt-Kopplin P, Parker JE, Schwab W, Vlot AC. 2014. Arabidopsis ENHANCED DISEASE SUSCEPTIBILITY1 promotes systemic acquired resistance via azelaic acid and its precursor 9-oxo nonanoic acid. J. Exp. Bot. 65(20):5919–31.

Wojtaszek P. 1997. Oxidative burst: an early plant response to pathogen infection. Biochem. J. 322 (Pt 3:681–92.

Wu BM, Subbarao K V. 2008. Effects of soil temperature, moisture, and burial depths on carpogenic germination of *Sclerotinia sclerotiorum* and *S. minor*. Phytopathology 98(10):1144–1152.

Wu J, Cai G, Tu J, Li L, Liu S, Luo X, Zhou L, Fan C, Zhou Y. 2013. Identification of QTLs for resistance to Sclerotinia stem rot and BnaC.IGMT5.a as a candidate gene of the major resistant QTL SRC6 in Brassica napus. PLoS One 8(7):e67740.

Xia Y, Gao QM, Yu K, Lapchyk L, Navarre D, Hildebrand D, Kachroo A, Kachroo P. 2009. An intact cuticle in distal tissues is essential for the induction of systemic acquired resistance in plants. Cell Host Microbe 5(2):151–165.

Xu W, Campbell P, Vargheese AK, Braam J. 1996. The Arabidopsis XET-related gene family: environmental and hormonal regulation of expression. Plant J. 9(6):879–89.

Yaeno T, Iba K. 2008. BAH1/NLA, a RING-type ubiquitin E3 ligase, regulates the accumulation of salicylic acid and immune responses to *Pseudomonas syringae* DC3000. Plant Physiol. 148(2):1032–41.

Yang C, Zhang Z, Gao H, Liu M, Fan X. 2014. Mechanisms by which the infection of *Sclerotinia sclerotiorum* (Lib.) de Bary affects the photosynthetic performance in tobacco leaves. BMC Plant Biol. 14(1):240.

Yu K, Soares JM, Mandal MK, Wang C, Chanda B, Gifford AN, Fowler JS, Navarre D, Kachroo A, Kachroo P. 2013. A feedback regulatory loop between G3P and lipid transfer proteins DIR1 and AZI1 mediates azelaic-acid-induced systemic immunity. Cell Rep. 3(4):1266–78.

Zamioudis C, Hanson J, Pieterse CMJ. 2014. β-Glucosidase BGLU42 is a MYB72-dependent key regulator of rhizobacteria-induced systemic resistance and modulates iron deficiency responses in Arabidopsis roots. New Phytol. 204(2):368–79.

Zarepour M, Kaspari K, Stagge S, Rethmeier R, Mendel RR, Bittner F. 2010. Xanthine dehydrogenase AtXDH1 from *Arabidopsis thaliana* is a potent producer of superoxide anions via its NADH oxidase activity. Plant Mol. Biol. 72(3):301–10.

Zhang F, Ge H, Zhang F, Guo N, Wang Y, Chen L, Ji X, Li C. 2016. Biocontrol potential of *Trichoderma harzianum* isolate T-aloe against *Sclerotinia sclerotiorum* in soybean. Plant Physiol. Biochem. PPB / Société Fr. Physiol. végétale 100:64–74.

Zhang H, Xie X, Kim M-S, Kornyeyev DA, Holaday S, Paré PW. 2008. Soil bacteria augment Arabidopsis photosynthesis by decreasing glucose sensing and abscisic acid levels *in planta*. Plant J. 56(2):264–273.

Zhang X, Peng G, Kutcher HR, Balesdent M-H, Delourme R, Fernando WGD. 2015 Nov 27. Breakdown of Rlm3 resistance in the *Brassica napus–Leptosphaeria maculans* pathosystem in western Canada. Eur. J. Plant Pathol.

Zhang Y, Fernando W, de Kievit TR, Berry C, Daayf F, Paulitz T. 2006. Detection of antibiotic-related genes from bacterial biocontrol agents with polymerase chain reaction. Can. J. Microbiol. 52(5):476–481.

Zhang Y, Xu S, Ding P, Wang D, Cheng YT, He J, Gao M, Xu F, Li Y, Zhu Z, et al. 2010. Control of salicylic acid synthesis and systemic acquired resistance by two members of a plant-specific family of transcription factors. Proc. Natl. Acad. Sci. 107(42):18220–18225.

APPENDIX A

Dominant patterns of expression generated from RNA-seq FPKM values using a Fuzzy K-means clustering algorithm.

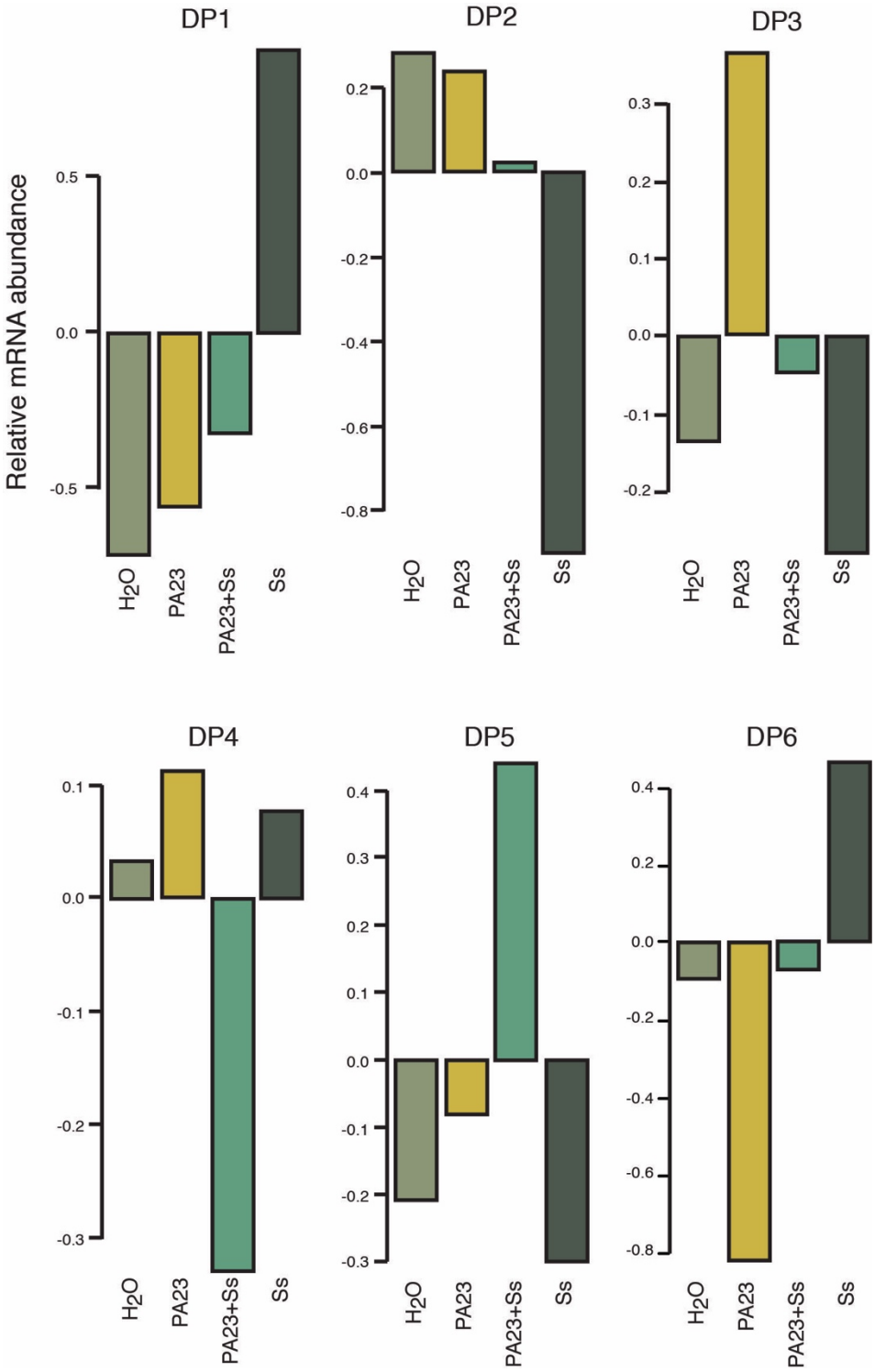

APPENDIX B

Gene names, log_2 fold change values and corresponding gene ontology (GO) term for select chloroplast-related GO terms.

BNA identifier	Gene Description	Gene name	Treatment log2 fold change			Gene Ontology (GO) term
			PA23	PA23+Ss	Ss	
BnaC01g37970D	multidrug resistance-associated protein 3	ATMRP3, MRP3, ABCC3	0	0	2.02886	chlorophyll catabolite transmembrane transport
BnaC01g38010D	multidrug resistance-associated protein 3	ATMRP3, MRP3, ABCC3	0	0	2.80703	
BnaC03g73610D	multidrug resistance-associated protein 3	ATMRP3, MRP3, ABCC3	0	0.679799	2.91333	
BnaC03g73620D	multidrug resistance-associated protein 3	ATMRP3, MRP3, ABCC3	0	0.852199	3.05066	
BnaCnng71820D	multidrug resistance-associated protein 3	ATMRP3, MRP3, ABCC3	0	0.853121	3.27561	
BnaA03g32690D	multidrug resistance-associated protein 3	ATMRP3, MRP3, ABCC3	0	1.40887	4.19548	
BnaA03g32640D	multidrug resistance-associated protein 3	ATMRP3, MRP3, ABCC3	0	3.65539	7.02952	
BnaA02g03640D	root cap 1 (RCP1)	RCP1, MEX1	-2.87334	0	0	chloroplast inner membrane
BnaA08g12800D	fatty acid desaturase 6	FAD6, FADC, SFD4	0	0	-2.49552	
BnaA03g04440D	magnesium-chelatase subunit chlH, chloroplast, putative / Mg-protoporphyrin IX chelatase, putative (CHLH)	GUN5, CCH, CHLH, CCH1, ABAR	0	0	-2.33801	
BnaAnng19090D	Pheophorbide a oxygenase family protein with Rieske [2Fe-2S] domain	CH1, ATCAO, CAO	0	0	-2.21313	
BnaA07g17240D	Transmembrane proteins 14C	0	0	0	2.0831	
BnaC08g33410D	Mitochondrial substrate carrier family protein	EMB104, SHS1, EMB42, ATBT1	0	0	2.24521	
BnaA10g13750D	reticulata-related 1	RER1	0	0	2.33591	
BnaA09g36620D	Transmembrane proteins 14C	0	0	0	2.68207	

BnaC09g36270D	reticulata-related 1	RER1	0	0	3.14704	
BnaCnng04000D	unknown protein; FUNCTIONS IN: molecular_function unknown; INVOLVED IN: biological_process unknown; LOCATED IN: chloroplast, chloroplast envelope; EXPRESSED IN: 22 plant structures; EXPRESSED DURING: 13 growth stages; Has 60 Blast hits to 59 proteins in 31 species: Archae - 0; Bacteria - 20; Metazoa - 1; Fungi - 2; Plants - 33; Viruses - 0; Other Eukaryotes - 4 (source: NCBI BLink).	0	0	0	10000	
BnaC03g58140D	autoinhibited Ca2+-ATPase 1	ACA1, PEA1	0	0.692372	2.2337	
BnaC08g19190D	purine permease 14	TGD1	0	0.862244	2.91769	
BnaC08g28200D	Transmembrane proteins 14C	0	0	1.00043	2.74495	
BnaA09g40900D	Mitochondrial substrate carrier family protein	EMB104, SHS1, EMB42, ATBT1	0	1.20211	2.60309	
BnaA08g18750D	autoinhibited Ca2+-ATPase 1	ACA1, PEA1	0	1.38528	3.46967	
BnaC03g00170D	unknown protein; FUNCTIONS IN: molecular_function unknown; INVOLVED IN: biological_process unknown; LOCATED IN: chloroplast, chloroplast envelope; EXPRESSED IN: 22 plant structures; EXPRESSED DURING: 13 growth stages; Has 60 Blast hits to 59 proteins in 31 species: Archae - 0; Bacteria - 20; Metazoa - 1; Fungi - 2; Plants - 33; Viruses - 0; Other Eukaryotes - 4 (source: NCBI BLink).	0	0	3.26164	0	
BnaA09g53430D	Uncharacterised protein family (UPF0114)	0	0	7.03878	11.0372	
BnaCnng41920D	Uncharacterised protein family (UPF0114)	0	0	8.0984	11.3124	
BnaA06g23190D	photosystem I reaction center subunit PSI-N, chloroplast, putative / PSI-	PSAN	0	-0.701947	-2.06273	chloroplast photosystem I & II

	N, putative (PSAN)					
BnaC06g07480D	photosystem I subunit G	PSAG	0	0	-2.18618	
BnaC03g50210D	photosystem I reaction center subunit PSI-N, chloroplast, putative / PSI-N, putative (PSAN)	PSAN	0	0	-2.05949	
BnaC04g51600D	photosystem I P subunit	PTAC8, TMP14, PSAP, PSI-P	0	0	-2.00493	
BnaA06g02370D	Photosystem II 5 kD protein	0	0	-0.746806	-2.61811	
BnaC06g04530D	0	0	0	0	-2.6051	
BnaA07g38700D	photosystem II BY	PSBY, YCF32	0	0	-2.17326	
BnaC08g46250D	photosystem II family protein	PSB27	0	0	-2.09896	
BnaA09g45770D	PsbQ-like 2	PQL1, PQL2	0	0	-2.08841	
BnaC06g26560D	photosystem II BY	PSBY, YCF32	0	0	-2.041	
BnaC08g44890D	photosystem II subunit P-1	PSBP-1, OEE2, PSII-P, OE23	0	0	-2.03301	
BnaA03g51200D	chloroplast sulfur E	EMB1374, CPSUFE, ATSUFE, SUFE1	-2.66825	0	-1.45599	chloroplast stroma
BnaC06g40610D	P-loop containing nucleoside triphosphate hydrolases superfamily protein	0	-2.58752	-1.99559	-2.50021	
BnaA09g24560D	phospholipid/glycerol acyltransferase family protein	ATS1, ACT1	-2.20309	0	-1.3514	
BnaA02g12840D	Ribulose bisphosphate carboxylase (small chain) family protein	0	-1.68707	-1.59445	-2.6807	
BnaC07g33500D	dihydrolipoyl dehydrogenases	0	-1.66233	0	-2.36792	
BnaC08g49440D	rubisco activase	#N/A	-1.00056	0	-2.20411	
BnaC08g17520D	D-3-phosphoglycerate dehydrogenase	PGDH	-0.834094	1.54729	4.31481	
BnaAnng03180D	dehydroquinate dehydratase, putative / shikimate dehydrogenase, putative	EMB3004, MEE32	-0.653006	0	2.67547	
BnaC03g23750D	cold regulated 15b	COR15B	0	-1.49517	-3.18146	
BnaA05g33810D	carbonic anhydrase 1	CA1	0	-1.09803	-2.05156	
BnaC01g21190D	chloroplast beta-amylase	CT-BMY, BAM3,	0	-0.98507	-2.38707	

		BMY8				
BnaA10g07790D	2 iron, 2 sulfur cluster binding	0	0	-0.952485	-2.16858	
BnaCnng27340D	2Fe-2S ferredoxin-like superfamily protein	FED A, ATFD2	0	-0.884174	-2.74939	
BnaC04g48100D	actin-11	ACT11	0	-0.874086	-2.21578	
BnaA09g33130D	alpha carbonic anhydrase 1	CAH1, ATACA1, ACA1	0	-0.867979	-2.13115	
BnaA01g17940D	chloroplast beta-amylase	CT-BMY, BAM3, BMY8	0	-0.846539	-2.4645	
BnaC09g22960D	0	FIB	0	-0.8433	-2.45783	
BnaA07g16660D	sedoheptulose-bisphosphatase	SBPASE	0	-0.7208	-2.17483	
BnaA06g38550D	Cupredoxin superfamily protein	DRT112, PETE2	0	-0.648941	-2.16194	
BnaA01g09640D	NAD(P)-binding Rossmann-fold superfamily protein	0	0	-0.648705	-2.00703	
BnaC05g36400D	high chlorophyll fluorescent 107	HCF107	0	-0.611845	-2.22546	
BnaC08g25700D	#N/A	#N/A	0	0	-10000	
BnaA10g04570D	#N/A	#N/A	0	0	-3.09479	
BnaC06g40420D	isopropylmalate dehydrogenase 2	ATIMD2, IMD2	0	0	-2.87536	
BnaC02g24220D	Uncharacterised BCR, YbaB family COG0718	0	0	0	-2.57402	
BnaA03g56650D	cold regulated 15b	COR15B	0	0	-2.51059	
BnaC03g56530D	Involved in response to salt stress. Knockout mutants are hypersensitive to salt stress.	0	0	0	-2.47252	
BnaA03g18710D	rubisco activase	RCA	0	0	-2.46454	
BnaC04g33570D	fructose-bisphosphate aldolase 1	FBA1	0	0	-2.45207	
BnaC01g21430D	GLU-ADT subunit B	GATB	0	0	-2.45047	
BnaC03g03950D	Plastid-lipid associated protein PAP / fibrillin family protein	0	0	0	-2.43563	
BnaC03g76960D	#N/A	#N/A	0	0	-2.43531	
BnaC04g34390D	Ribulose bisphosphate carboxylase (small chain) family protein	0	0	0	-2.38908	
BnaA03g04440D	magnesium-chelatase subunit chlH, chloroplast, putative / Mg-	GUN5, CCH, CHLH,	0	0	-2.33801	

	protoporphyrin IX chelatase, putative (CHLH)	CCH1, ABAR				
BnaC07g18140D	RAB GTPase homolog E1B	ATRAB8D, ATRABE1B, RABE1b	0	0	-2.24939	
BnaC08g13410D	elongation factor Ts family protein	emb2726	0	0	-2.22887	
BnaC08g07850D	phosphoribulokinase	PRK	0	0	-2.2244	
BnaA03g44710D	unknown protein; FUNCTIONS IN: molecular_function unknown; INVOLVED IN: biological_process unknown; LOCATED IN: chloroplast, chloroplast stroma; Has 30201 Blast hits to 17322 proteins in 780 species: Archae - 12; Bacteria - 1396; Metazoa - 17338; Fungi - 3422; Plants - 5037; Viruses - 0; Other Eukaryotes - 2996 (source: NCBI BLink).	0	0	0	-2.2068	
BnaC03g15660D	Dihydrodipicolinate reductase, bacterial/plant	crr1	0	0	-2.18986	
BnaA07g14420D	Ribulose bisphosphate carboxylase (small chain) family protein	0	0	0	-2.16228	
BnaC04g05700D	rubisco activase	RCA	0	0	-2.15523	
BnaC03g22220D	rubisco activase	RCA	0	0	-2.1465	
BnaCnng55860D	Ribulose bisphosphate carboxylase (small chain) family protein	0	0	0	-2.13117	
BnaC04g51070D	chlororespiratory reduction 6	CRR6	0	0	-2.09317	
BnaA08g07000D	phosphoribulokinase	PRK	0	0	-2.08365	
BnaC04g52490D	Plastid-lipid associated protein PAP / fibrillin family protein	0	0	0	-2.08195	
BnaA04g12130D	fructose-bisphosphate aldolase 1	FBA1	0	0	-2.07525	
BnaC08g41890D	CLP protease proteolytic subunit 6	CLPP6, NCLPP1, NCLPP6	0	0	-2.07098	
BnaC02g05810D	Heavy metal transport/detoxification superfamily protein	0	0	0	-2.05019	
BnaC08g44890D	photosystem II subunit P-1	PSBP-1, OEE2, PSII-P, OE23	0	0	-2.03301	
BnaA05g05840D	rubisco activase	RCA	0	0	-	

					2.03286	
BnaC08g35820D	fructose-bisphosphate aldolase 1	FBA1	0	0	-2.0124	
BnaC09g29820D	Tetratricopeptide repeat (TPR)-like superfamily protein	0	0	0	-2.00521	
BnaC04g30810D	Ribulose bisphosphate carboxylase (small chain) family protein	0	0	0	-2.00447	
BnaC05g25830D	chorismate synthase, putative / 5-enolpyruvylshikimate-3-phosphate phospholyase, putative	EMB1144	0	0	2.00562	
BnaA05g36080D	endoribonuclease L-PSP family protein	0	0	0	2.00844	
BnaCnng76000D	heat shock protein 60-2	HSP60-2	0	0	2.02866	
BnaA04g29220D	adenosine kinase	ADK, ATPADK1	0	0	2.03245	
BnaC03g15030D	NADH-dependent glutamate synthase 1	GLT1	0	0	2.03953	
BnaA01g31570D	sulfite reductase	SIR	0	0	2.04281	
BnaA03g35760D	endoribonuclease L-PSP family protein	0	0	0	2.04643	
BnaC03g03940D	actin 7	ACT7	0	0	2.0548	
BnaA08g11590D	Cystathionine beta-synthase (CBS) family protein	LEJ1, CDCP1	0	0	2.06659	
BnaC04g11280D	heat shock protein 60-2	HSP60-2	0	0	2.11023	
BnaA07g03650D	GLN phosphoribosyl pyrophosphate amidotransferase 1	ATASE, ATASE1, ASE1	0	0	2.11611	
BnaA07g25510D	cytosolic NADP+-dependent isocitrate dehydrogenase	cICDH	0	0	2.16874	
BnaC09g39920D	Cobalamin-independent synthase family protein	ATCIMS	0	0	2.19057	
BnaAnng01550D	DHFS-FPGS homolog B	ATDFB, DFB, FPGS1	0	0	2.19513	
BnaA06g14510D	catalase 3	CAT3, SEN2, ATCAT3	0	0	2.20682	
BnaC03g77890D	mitogen-activated protein kinase kinase 4	ATMKK4, MKK4, ATMEK4	0	0	2.21021	
BnaA08g01860D	mitogen-activated protein kinase kinase 4	ATMKK4, MKK4, ATMEK4	0	0	2.28148	
BnaC04g39340D	prephenate dehydratase 1	PD1, ADT3	0	0	2.32485	
BnaA03g10770D	TCP-1/cpn60 chaperonin family protein	0	0	0	2.34191	
BnaC08g28560D	N-acetyl-l-glutamate	NAGK	0	0	2.38685	

	kinase					
BnaC08g37250D	methylthioalkylmalate synthase-like 4	MAML-4, IPMS1	0	0	2.42369	
BnaC07g44730D	Cystathionine beta-synthase (CBS) family protein	LEJ1, CDCP1	0	0	2.44999	
BnaA10g20010D	aspartate kinase 1	AK-LYS1, AK1, AK	0	0	2.52003	
BnaC05g31670D	endoribonuclease L-PSP family protein	0	0	0	2.54274	
BnaC03g49870D	GTP cyclohydrolase II	ATGCH, GCH, ATRIBA1, RFD1	0	0	2.56881	
BnaC05g45470D	dehydroquinate dehydratase, putative / shikimate dehydrogenase, putative	EMB3004, MEE32	0	0	2.61588	
BnaC02g07610D	Cobalamin-independent synthase family protein	ATCIMS	0	0	2.61907	
BnaA03g50880D	Calcium-dependent lipid-binding (CaLB domain) family protein	LEJ1, CDCP1	0	0	2.62318	
BnaC02g12750D	HEAT SHOCK PROTEIN 81.4	Hsp81.4, AtHsp90.4	0	0	2.70992	
BnaC09g37840D	Chaperonin-like RbcX protein	0	0	0	2.71001	
BnaA08g25130D	arogenate dehydratase 1	ADT1	0	0	2.74245	
BnaA02g01540D	aspartate kinase 1	AK-LYS1, AK1, AK	0	0	2.91913	
BnaA06g23420D	GTP cyclohydrolase II	ATGCH, GCH, ATRIBA1, RFD1	0	0	3.00374	
BnaA02g35440D	HEAT SHOCK PROTEIN 81.4	Hsp81.4, AtHsp90.4	0	0	3.10948	
BnaCnng34620D	arogenate dehydratase 5	ADT5	0	0	3.13915	
BnaC04g00150D	glutathione S-transferase phi 8	ATGSTF8, ATGSTF5, GST6, GSTF8	0	0	3.23548	
BnaA04g04050D	glutathione reductase	GR, EMB2360, ATGR2	0	0	3.49463	
BnaC05g12400D	glyceraldehyde-3-phosphate dehydrogenase of plastid 2	GAPCP-2	0	0	3.60947	
BnaA05g00270D	glutathione S-transferase phi 8	ATGSTF8, ATGSTF5, GST6, GSTF8	0	0	3.82469	
BnaA02g01610D	Aldolase-type TIM barrel family protein	0	0	0	10000	

BnaA06g33410D	allene oxide cyclase 2	AOC2	0	0	10000	
BnaAnng25850D	cytosolic NADP+-dependent isocitrate dehydrogenase	cICDH	0	0	10000	
BnaC01g32570D	endoribonuclease L-PSP family protein	0	0	0	10000	
BnaC08g07340D	plastid ribosomal protein l11	PRPL11	0	0	10000	
BnaCnng41160D	#N/A	#N/A	0	0	10000	
BnaA03g55890D	actin 7	ACT7	0	0.659428	2.6655	
BnaAnng27440D	RNA 3'-terminal phosphate cyclase/enolpyruvate transferase, alpha/beta	0	0	0.670698	2.60332	
BnaC08g34140D	Cytosol aminopeptidase family protein	0	0	0.679291	2.65331	
BnaA10g22430D	pyrophosphorylase 6	AtPPa6, PPa6	0	0.706009	2.3756	
BnaA02g03770D	Cobalamin-independent synthase family protein	ATCIMS	0	0.717973	2.52291	
BnaC05g05550D	ascorbate peroxidase 1	APX1, MEE6, CS1, ATAPX1, ATAPX01	0	0.727124	2.1145	
BnaC02g04620D	aspartate kinase 1	AK-LYS1, AK1, AK	0	0.745571	3.22483	
BnaA10g25620D	sulfite reductase	SIR	0	0.750565	2.50072	
BnaCnng11100D	6-phosphogluconate dehydrogenase family protein	0	0	0.77291	2.45581	
BnaC08g03290D	chorismate synthase, putative / 5-enolpyruvylshikimate-3-phosphate phospholyase, putative	EMB1144	0	0.778565	3.11162	
BnaC03g08690D	Cobalamin-independent synthase family protein	ATCIMS	0	0.782733	2.30988	
BnaAnng04450D	stromal ascorbate peroxidase	SAPX	0	0.786295	2.65604	
BnaA03g13330D	Clp ATPase	ERD1, CLPD, SAG15	0	0.789527	2.65521	
BnaC09g39860D	tryptophan biosynthesis 1	TRP1, pat1	0	0.796022	3.51849	
BnaA06g04380D	ascorbate peroxidase 1	APX1, MEE6, CS1, ATAPX1, ATAPX01	0	0.82633	2.37944	
BnaC03g77030D	D-3-phosphoglycerate dehydrogenase	EDA9	0	0.827783	3.15565	
BnaC05g51080D	adenine phosphoribosyl transferase 1	APT1, ATAPT1	0	0.834817	3.49298	
BnaA10g16880D	Cobalamin-independent synthase family protein	ATCIMS	0	0.855224	2.83351	

BnaA03g00990D	Pyridine nucleotide-disulphide oxidoreductase family protein	ATMDAR2	0	0.866459	2.94879	
BnaA08g02980D	chorismate synthase, putative / 5-enolpyruvylshikimate-3-phosphate phospholyase, putative	EMB1144	0	0.883352	3.07464	
BnaC07g40410D	tryptophan synthase beta-subunit 2	TSB2	0	0.901223	3.71912	
BnaC09g46990D	pyrophosphorylase 6	AtPPa6, PPa6	0	0.90941	2.33068	
BnaC09g43800D	aspartate kinase 1	AK-LYS1, AK1, AK	0	0.940762	3.35772	
BnaC09g22760D	APS reductase 1	APR1, APR, PRH19, ATAPR1	0	0.963589	3.60185	
BnaC08g48460D	AMP-dependent synthetase and ligase family protein	0	0	0.96517	3.10114	
BnaC01g22950D	Pseudouridine synthase/archaeosine transglycosylase-like family protein	APS3	0	0.974406	3.50056	
BnaC09g09260D	homoserine kinase	HSK, DMR1	0	0.996883	2.69481	
BnaC03g18540D	heat shock protein 60-2	HSP60-2	0	1.01554	2.49631	
BnaC09g50680D	sulfite reductase	SIR	0	1.02392	4.22423	
BnaC09g36370D	arogenate dehydratase 5	ADT5	0	1.03963	3.78918	
BnaC09g50770D	ACT domain-containing protein	0	0	1.08194	3.06643	
BnaA03g36860D	ATP sulfurylase 1	APS1	0	1.12771	3.90757	
BnaA08g11320D	D-3-phosphoglycerate dehydrogenase	EDA9	0	1.1428	3.59083	
BnaC02g25850D	glyceraldehyde-3-phosphate dehydrogenase of plastid 2	GAPCP-2	0	1.14529	3.87023	
BnaC03g16140D	Clp ATPase	ERD1, CLPD, SAG15	0	1.15869	3.32844	
BnaA02g05780D	arogenate dehydratase 5	ADT5	0	1.15918	3.77769	
BnaC05g48310D	6-phosphogluconate dehydrogenase family protein	0	0	1.16911	3.86015	
BnaAnng26460D	Transketolase	0	0	1.33065	3.58287	
BnaA09g49190D	ascorbate peroxidase 1	APX1, MEE6, CS1, ATAPX1, ATAPX01	0	1.42417	3.37547	
BnaA09g20370D	APS reductase 1	APR1, APR, PRH19, ATAPR1	0	1.4948	4.40929	
BnaC04g56880D	RNA 3'-terminal	0	0	1.50504	4.4703	

	phosphate cyclase/enolpyruvate transferase, alpha/beta					
BnaA10g24820D	anthranilate synthase alpha subunit 1	ASA1, TRP5, AMT1, WEI2, JDL1	0	1.55855	4.37014	
BnaA05g33580D	6-phosphogluconate dehydrogenase family protein	0	0	1.56665	4.26022	
BnaA07g33590D	PDI-like 1-2	ATPDIL1-2, PDI6, ATPDI6, PDIL1-2	0	1.57296	3.48761	
BnaA10g13820D	arogenate dehydratase 5	ADT5	0	1.5799	4.17758	
BnaC03g44420D	Aldolase-type TIM barrel family protein	0	0	1.58668	4.4245	
BnaC08g43490D	ascorbate peroxidase 1	APX1, MEE6, CS1, ATAPX1, ATAPX01	0	1.60933	3.92717	
BnaC06g38200D	PDI-like 1-2	ATPDIL1-2, PDI6, ATPDI6, PDIL1-2	0	1.64356	3.40391	
BnaC03g25260D	RNA 3'-terminal phosphate cyclase/enolpyruvate transferase, alpha/beta	0	0	1.66893	4.18528	
BnaA03g48400D	tryptophan synthase beta-subunit 2	TSB2	0	1.70284	5.14686	
BnaA06g23120D	Inositol monophosphatase family protein	SAL1, ALX8, ATSAL1, HOS2, FRY1, RON1	0	1.71346	4.36682	
BnaC04g26180D	glutathione reductase	GR, EMB2360, ATGR2	0	1.73493	4.16842	
BnaA01g12900D	glutamate-cysteine ligase	GSH1	0	1.76417	4.2886	
BnaA05g15300D	mitogen-activated protein kinase kinase 4	ATMKK4, MKK4, ATMEK4	0	1.83205	3.58495	
BnaC09g06200D	Inositol monophosphatase family protein	SAL1, ALX8, ATSAL1, HOS2, FRY1, RON1	0	1.83832	4.27521	
BnaC03g01350D	Pyridine nucleotide-disulphide oxidoreductase family protein	ATMDAR2	0	1.87109	3.34448	
BnaC08g15080D	arogenate dehydratase 1	ADT1	0	1.88657	4.58686	

BnaC01g41470D	glutamate-cysteine ligase	GSH1	0	1.89602	4.34272	
BnaC03g53780D	arogenate dehydratase 4	ADT4	0	1.89666	5.20071	
BnaA06g16270D	AMP-dependent synthetase and ligase family protein	0	0	2.02831	4.63011	
BnaA03g57920D	Aldolase-type TIM barrel family protein	0	0	2.06248	5.09682	
BnaA07g20300D	glyceraldehyde-3-phosphate dehydrogenase of plastid 1	GAPCP-1	0	2.12702	2.06178	
BnaCnng10850D	endoribonuclease L-PSP family protein	0	0	2.14105	5.95212	
BnaC03g00160D	ferretin 1	ATFER1, FER1	0	2.15903	3.59517	
BnaA10g16850D	tryptophan biosynthesis 1	TRP1, pat1	0	2.26845	5.2648	
BnaA02g03850D	tryptophan biosynthesis 1	TRP1, pat1	0	2.34025	5.80901	
BnaA09g27900D	adenine phosphoribosyl transferase 1	APT1, ATAPT1	0	2.34551	5.08159	
BnaA03g14140D	glutathione S-transferase PHI 9	ATGSTF9, GLUTTR, ATGSTF7, GSTF9	0	2.38447	5.18796	
BnaA06g00880D	Chalcone-flavanone isomerase family protein	0	0	2.4172	0	
BnaA10g09090D	tryptophan synthase beta-subunit 1	TSB1, TRPB, TRP2, ATTSB1	0	2.48664	5.75702	
BnaC09g21610D	2-oxoacid dehydrogenases acyltransferase family protein	LTA2, PLE2	0	2.50945	-1.86908	
BnaA03g00260D	ferretin 1	ATFER1, FER1	0	2.55634	3.81068	
BnaA02g24400D	3-ketoacyl-acyl carrier protein synthase I	KASI, KAS1	0	2.61262	0	
BnaA08g22970D	D-3-phosphoglycerate dehydrogenase	PGDH	0	2.63966	5.49367	
BnaA05g16830D	ATP sulfurylase 1	APS1	0	2.64046	5.53	
BnaC06g34880D	enolase 1	ENO1	0	2.68934	4.53759	
BnaA09g34470D	tryptophan synthase alpha chain	TSA1, TRP3	0	2.72659	5.91159	
BnaC09g31260D	tryptophan synthase beta-subunit 1	TSB1, TRPB, TRP2, ATTSB1	0	2.78857	5.99151	
BnaA01g19120D	Pseudouridine synthase/archaeosine transglycosylase-like family protein	APS3	0	2.81296	5.99271	
BnaA07g31190D	enolase 1	ENO1	0	2.83255	5.20697	
BnaA09g51510D	pyruvate dehydrogenase E1 alpha	PDH-E1 ALPHA	0	2.93722	0	

BnaC03g05850D	Aldolase-type TIM barrel family protein	0	0	3.09531	5.37265	
BnaC08g25400D	tryptophan synthase alpha chain	TSA1, TRP3	0	3.17561	6.40882	
BnaC03g62400D	phosphoserine aminotransferase	PSAT	0	3.35271	6.43479	
BnaC09g49740D	anthranilate synthase alpha subunit 1	ASA1, TRP5, AMT1, WEI2, JDL1	0	3.37	6.97094	
BnaA08g14930D	phosphoserine aminotransferase	PSAT	0	3.48582	6.4199	
BnaA03g01690D	anthranilate synthase alpha subunit 1	ASA1, TRP5, AMT1, WEI2, JDL1	0	3.51698	6.7447	
BnaC05g08770D	arogenate dehydratase 1	ADT1	0	3.58027	6.35752	
BnaC06g26190D	lipoxygenase 2	LOX2, ATLOX2	0	3.68096	3.91346	
BnaC01g04190D	D-3-phosphoglycerate dehydrogenase	EDA9	0	3.97647	7.51259	
BnaA03g50990D	D-3-phosphoglycerate dehydrogenase	EDA9	0	4.15855	7.56796	
BnaA10g20180D	glucose-6-phosphate dehydrogenase 2	G6PD2	0	4.20887	7.11673	
BnaA07g24860D	lipoxygenase 2	LOX2, ATLOX2	0	5.30444	5.15502	
BnaC03g02240D	anthranilate synthase alpha subunit 1	ASA1, TRP5, AMT1, WEI2, JDL1	0	5.34951	3.38935	
BnaA01g02930D	D-3-phosphoglycerate dehydrogenase	EDA9	0	6.38008	9.90129	
BnaC07g44840D	D-3-phosphoglycerate dehydrogenase	EDA9	0	6.38165	9.83598	
BnaC03g07200D	Aldolase-type TIM barrel family protein	0	0	10000	0	
BnaA09g19550D	allene oxide cyclase 2	AOC2	0	10000	10000	
BnaC07g22910D	allene oxide cyclase 2	AOC2	0	10000	10000	
BnaC09g52570D	allene oxide cyclase 2	AOC2	0	10000	10000	
BnaC06g20420D	glutathione S-transferase TAU 19	ATGSTU19, GST8, GSTU19	0.600273	0.853688	3.28661	
BnaC04g41510D	glutathione S-transferase PHI 9	ATGSTF9, GLUTTR, ATGSTF7, GSTF9	0.66702	1.53344	4.23912	
BnaA07g20560D	glutathione S-transferase TAU 19	ATGSTU19, GST8, GSTU19	0.690858	1.14114	3.8589	
BnaC03g17110D	glutathione S-transferase PHI 9	ATGSTF9, GLUTTR, ATGSTF7,	0.735738	1.86618	4.66692	

		GSTF9				
BnaA04g17910D	glutathione S-transferase PHI 9	ATGSTF9, GLUTTR, ATGSTF7, GSTF9	0.852094	3.11788	6.48483	
BnaA03g04310D	Aldolase-type TIM barrel family protein	0	1.02951	3.20027	5.56171	
BnaA06g36560D	Pseudouridine synthase/archaeosine transglycosylase-like family protein	APS4	1.07653	0.806517	2.50388	
BnaC03g30880D	glutathione S-transferase PHI 2	ATGSTF2, ATPM24.1, ATPM24, GST2, GSTF2	2.15367	5.85971	8.3372	
BnaA03g26140D	glutathione S-transferase PHI 2	ATGSTF2, ATPM24.1, ATPM24, GST2, GSTF2	2.76625	5.15279	8.47369	
BnaCnng12430D	ribulose-bisphosphate carboxylases	RBCL	2.92099	0	3.29583	
BnaAnng01030D	ACT domain-containing protein	0	3.56437	2.54263	2.35609	
BnaC02g22900D	Pyridine nucleotide-disulphide oxidoreductase family protein	0	-1.72751	-1.88952	-2.59926	chloroplast thylakoid
BnaC04g06760D	lipid transfer protein 1	LP1, LTP1, ATLTP1	-0.766665	0	-2.14203	
BnaC09g22960D	0	FIB	0	-0.8433	-2.45783	
BnaCnng40790D	calcium sensing receptor	CaS	0	-0.831419	-2.04515	
BnaA06g23190D	photosystem I reaction center subunit PSI-N, chloroplast, putative / PSI-N, putative (PSAN)	PSAN	0	-0.701947	-2.06273	
BnaA06g38550D	Cupredoxin superfamily protein	DRT112, PETE2	0	-0.648941	-2.16194	
BnaA05g09380D	light-harvesting chlorophyll-protein complex II subunit B1	LHB1B1, LHCB1.4	0	0	-10000	
BnaA06g10660D	0	0	0	0	-10000	
BnaC01g05610D	#N/A	#N/A	0	0	-10000	
BnaA04g22080D	lipid transfer protein 1	LP1, LTP1, ATLTP1	0	0	-3.2449	
BnaC03g03350D	Protein of unknown function (DUF1118)	0	0	0	-2.68897	
BnaC04g33570D	fructose-bisphosphate aldolase 1	FBA1	0	0	-2.45207	
BnaC01g20550D	0	0	0	0	-2.34338	

BnaA09g22540D	light harvesting complex of photosystem II 5	LHCB5	0	0	-2.29183	
BnaA07g31590D	Pyridine nucleotide-disulphide oxidoreductase family protein	0	0	0	-2.2792	
BnaA06g15210D	unknown protein; Has 29 Blast hits to 29 proteins in 12 species: Archae - 0; Bacteria - 0; Metazoa - 0; Fungi - 2; Plants - 27; Viruses - 0; Other Eukaryotes - 0 (source: NCBI BLink).	0	0	0	-2.26103	
BnaC07g18140D	RAB GTPase homolog E1B	ATRAB8D, ATRABE1B, RABE1b	0	0	-2.24939	
BnaA07g07560D	chlorophyll A/B binding protein 1	CAB1, AB140, CAB140, LHCB1.3	0	0	-2.21754	
BnaC06g07480D	photosystem I subunit G	PSAG	0	0	-2.18618	
BnaC03g59670D	photosystem I subunit K	PSAK	0	0	-2.18291	
BnaA03g24350D	light harvesting complex of photosystem II 5	LHCB5	0	0	-2.17332	
BnaC06g35410D	Pyridine nucleotide-disulphide oxidoreductase family protein	0	0	0	-2.1691	
BnaA09g13710D	photosystem I light harvesting complex gene 3	LHCA3	0	0	-2.15324	
BnaC06g26580D	unknown protein; FUNCTIONS IN: molecular_function unknown; INVOLVED IN: biological_process unknown; LOCATED IN: chloroplast, chloroplast envelope; EXPRESSED IN: 22 plant structures; EXPRESSED DURING: 13 growth stages; Has 49 Blast hits to 49 proteins in 20 species: Archae - 0; Bacteria - 0; Metazoa - 0; Fungi - 0; Plants - 44; Viruses - 0; Other Eukaryotes - 5 (source: NCBI BLink).	0	0	0	-2.14383	
BnaA07g07570D	0	CAB1, AB140, CAB140, LHCB1.3	0	0	-2.11706	
BnaC08g46250D	photosystem II family protein	PSB27	0	0	-2.09896	

BnaA09g45770D	PsbQ-like 2	PQL1, PQL2	0	0	-2.08841	
BnaCnng31870D	photosystem I light harvesting complex gene 3	LHCA3	0	0	-2.08215	
BnaC04g52490D	Plastid-lipid associated protein PAP / fibrillin family protein	0	0	0	-2.08195	
BnaC07g37680D	PGR5-LIKE A	PGR5-LIKE A	0	0	-2.07929	
BnaA04g12130D	fructose-bisphosphate aldolase 1	FBA1	0	0	-2.07525	
BnaC08g41890D	CLP protease proteolytic subunit 6	CLPP6, NCLPP1, NCLPP6	0	0	-2.07098	
BnaC05g22880D	chlorophyll A/B binding protein 1	CAB1, AB140, CAB140, LHCB1.3	0	0	-2.06504	
BnaC03g50210D	photosystem I reaction center subunit PSI-N, chloroplast, putative / PSI-N, putative (PSAN)	PSAN	0	0	-2.05949	
BnaA09g00250D	thylakoid rhodanese-like	TROL	0	0	-2.05635	
BnaA09g26570D	chlorophyll A/B binding protein 1	CAB1, AB140, CAB140, LHCB1.3	0	0	-2.05566	
BnaC08g44890D	photosystem II subunit P-1	PSBP-1, OEE2, PSII-P, OE23	0	0	-2.03301	
BnaA02g09700D	light-harvesting chlorophyll B-binding protein 3	LHCB3, LHCB3*1	0	0	-2.03226	
BnaA08g23760D	light harvesting complex photosystem II subunit 6	LHCB6, CP24	0	0	-2.01437	
BnaC08g35820D	fructose-bisphosphate aldolase 1	FBA1	0	0	-2.0124	
BnaC09g29820D	Tetratricopeptide repeat (TPR)-like superfamily protein	0	0	0	-2.00521	
BnaC04g51600D	photosystem I P subunit	PTAC8, TMP14, PSAP, PSI-P	0	0	-2.00493	
BnaC08g28560D	N-acetyl-l-glutamate kinase	NAGK	0	0	2.38685	
BnaC03g60960D	photosystem II reaction center protein C	PSBC	0	0	3.70335	
BnaA04g17540D	thylakoid processing peptide	TPP	0	0.69564	2.04818	
BnaA02g23180D	allene oxide synthase	AOS, CYP74A, DDE2	0	1.43503	4.17412	
BnaC04g56710D	light harvesting complex photosystem II	LHCB4.3	0	1.87549	3.53763	

BnaC02g29610D	allene oxide synthase	AOS, CYP74A, DDE2	0	1.95554	4.70223	
BnaC09g21610D	2-oxoacid dehydrogenases acyltransferase family protein	LTA2, PLE2	0	2.50945	-1.86908	
BnaC02g13690D	thylakoidal ascorbate peroxidase	TAPX	0	2.87824	0	
BnaCnng04230D	photosystem I light harvesting complex gene 3	LHCA3	1.28468	2.20895	0	
BnaC09g26840D	#N/A	#N/A	1.53287	0	2.04154	
BnaCnng20740D	photosynthetic electron transfer D	PETD	2.05877	1.06414	2.70645	
BnaA06g19430D	photosystem II reaction center protein B	PSBB	2.09682	1.122	3.05219	
BnaC04g15570D	Photosystem I, PsaA/PsaB protein	PSAA	2.36198	1.24129	3.08799	
BnaC07g05360D	#N/A	#N/A	2.53198	1.51866	3.21439	
BnaA06g19410D	#N/A	#N/A	2.90608	0	3.26471	
BnaC09g27530D	Photosystem I, PsaA/PsaB protein	PSAB	3.10058	0	3.45785	
BnaC08g49440D	rubisco activase	#N/A	-1.00056	0	-2.20411	plastoglobule
BnaA02g03450D	PHYTOENE SYNTHASE	PSY	0	-0.87502	-2.15926	
BnaC09g22960D	0	FIB	0	-0.8433	-2.45783	
BnaC02g07120D	PHYTOENE SYNTHASE	PSY	0	-0.769363	-2.2793	
BnaA05g09380D	light-harvesting chlorophyll-protein complex II subunit B1	LHB1B1, LHCB1.4	0	0	-10000	
BnaA09g02120D	photosystem II light harvesting complex gene 2.3	LHCB2.4, LHCB2.3, LHCB2	0	0	-2.69229	
BnaC09g01520D	photosystem II light harvesting complex gene 2.3	LHCB2.4, LHCB2.3, LHCB2	0	0	-2.58305	
BnaC07g24660D	photosystem II light harvesting complex gene 2.3	LHCB2.4, LHCB2.3, LHCB2	0	0	-2.50369	
BnaA03g18710D	rubisco activase	RCA	0	0	-2.46454	
BnaC04g33570D	fructose-bisphosphate aldolase 1	FBA1	0	0	-2.45207	
BnaA09g22540D	light harvesting complex of photosystem II 5	LHCB5	0	0	-2.29183	
BnaC03g44110D	photosystem II light harvesting complex gene 2.1	LHCB2.1, LHCB2	0	0	-2.2892	
BnaA07g07560D	chlorophyll A/B binding protein 1	CAB1, AB140, CAB140, LHCB1.3	0	0	-2.21754	

BnaA03g24350D	light harvesting complex of photosystem II 5	LHCB5	0	0	-2.17332	
BnaA06g31910D	photosystem II light harvesting complex gene 2.3	LHCB2.4, LHCB2.3, LHCB2	0	0	-2.16026	
BnaC04g05700D	rubisco activase	RCA	0	0	-2.15523	
BnaA09g13710D	photosystem I light harvesting complex gene 3	LHCA3	0	0	-2.15324	
BnaC03g22220D	rubisco activase	RCA	0	0	-2.1465	
BnaA02g29010D	photosystem II light harvesting complex gene 2.3	LHCB2.4, LHCB2.3, LHCB2	0	0	-2.11876	
BnaA07g07570D	0	CAB1, AB140, CAB140, LHCB1.3	0	0	-2.11706	
BnaCnng31870D	photosystem I light harvesting complex gene 3	LHCA3	0	0	-2.08215	
BnaC04g52490D	Plastid-lipid associated protein PAP / fibrillin family protein	0	0	0	-2.08195	
BnaA04g12130D	fructose-bisphosphate aldolase 1	FBA1	0	0	-2.07525	
BnaC05g22880D	chlorophyll A/B binding protein 1	CAB1, AB140, CAB140, LHCB1.3	0	0	-2.06504	
BnaC02g37040D	photosystem II light harvesting complex gene 2.3	LHCB2.4, LHCB2.3, LHCB2	0	0	-2.06287	
BnaA09g26570D	chlorophyll A/B binding protein 1	CAB1, AB140, CAB140, LHCB1.3	0	0	-2.05566	
BnaA05g05840D	rubisco activase	RCA	0	0	-2.03286	
BnaA02g09700D	light-harvesting chlorophyll B-binding protein 3	LHCB3, LHCB3*1	0	0	-2.03226	
BnaA08g23760D	light harvesting complex photosystem II subunit 6	LHCB6, CP24	0	0	-2.01437	
BnaC08g35820D	fructose-bisphosphate aldolase 1	FBA1	0	0	-2.0124	
BnaC03g60960D	photosystem II reaction center protein C	PSBC	0	0	3.70335	
BnaA02g23180D	allene oxide synthase	AOS, CYP74A, DDE2	0	1.43503	4.17412	
BnaC04g56710D	light harvesting complex photosystem II	LHCB4.3	0	1.87549	3.53763	
BnaC02g29610D	allene oxide synthase	AOS, CYP74A, DDE2	0	1.95554	4.70223	

BnaC07g23920D	Esterase/lipase/thioesterase family protein	0	0.736714	1.96748	3.37545	
BnaCnng04230D	photosystem I light harvesting complex gene 3	LHCA3	1.28468	2.20895	0	
BnaA06g19430D	photosystem II reaction center protein B	PSBB	2.09682	1.122	3.05219	
BnaC04g15570D	Photosystem I, PsaA/PsaB protein	PSAA	2.36198	1.24129	3.08799	
BnaCnng12430D	ribulose-bisphosphate carboxylases	RBCL	2.92099	0	3.29583	
BnaC09g27530D	Photosystem I, PsaA/PsaB protein	PSAB	3.10058	0	3.45785	
BnaC01g18730D	translocon at the inner envelope membrane of chloroplasts 110	ATTIC110, TIC110	-2.70131	0	0	protein import into chloroplast stroma
BnaC01g26850D	0	0	0	0	2.21961	
BnaA06g19290D	Chloroplast Ycf2;ATPase, AAA type, core	YCF2.2	0	0	2.7881	
BnaCnng04000D	unknown protein; FUNCTIONS IN: molecular_function unknown; INVOLVED IN: biological_process unknown; LOCATED IN: chloroplast, chloroplast envelope; EXPRESSED IN: 22 plant structures; EXPRESSED DURING: 13 growth stages; Has 60 Blast hits to 59 proteins in 31 species: Archae - 0; Bacteria - 20; Metazoa - 1; Fungi - 2; Plants - 33; Viruses - 0; Other Eukaryotes - 4 (source: NCBI BLink).	0	0	0	10000	
BnaC03g00170D	unknown protein; FUNCTIONS IN: molecular_function unknown; INVOLVED IN: biological_process unknown; LOCATED IN: chloroplast, chloroplast envelope; EXPRESSED IN: 22 plant structures; EXPRESSED DURING: 13 growth stages; Has 60 Blast hits to 59 proteins in 31 species: Archae - 0; Bacteria - 20; Metazoa - 1; Fungi - 2; Plants - 33; Viruses - 0; Other Eukaryotes - 4 (source: NCBI BLink).	0	0	3.26164	0	

BnaC09g22960D	0	FIB	0	-0.8433	-2.45783	thylakoid lumen
BnaA06g38550D	Cupredoxin superfamily protein	DRT112, PETE2	0	-0.648941	-2.16194	
BnaC01g05610D	#N/A	#N/A	0	0	-10000	
BnaC04g33570D	fructose-bisphosphate aldolase 1	FBA1	0	0	-2.45207	
BnaA07g32780D	Photosystem II reaction center PsbP family protein	0	0	0	-2.22829	
BnaA04g12130D	fructose-bisphosphate aldolase 1	FBA1	0	0	-2.07525	
BnaC08g44890D	photosystem II subunit P-1	PSBP-1, OEE2, PSII-P, OE23	0	0	-2.03301	
BnaC08g35820D	fructose-bisphosphate aldolase 1	FBA1	0	0	-2.0124	
BnaC09g29820D	Tetratricopeptide repeat (TPR)-like superfamily protein	0	0	0	-2.00521	
BnaA07g28860D	inorganic carbon transport protein-related	CRR23	-0.74948	0	-2.45813	thylakoid membrane
BnaA05g09380D	light-harvesting chlorophyll-protein complex II subunit B1	LHB1B1, LHCB1.4	0	0	-10000	
BnaC06g31900D	inorganic carbon transport protein-related	CRR23	0	0	-2.50608	
BnaAnng19090D	Pheophorbide a oxygenase family protein with Rieske [2Fe-2S] domain	CH1, ATCAO, CAO	0	0	-2.21313	